NTNU

Norwegian University of
Science and Technology

Correlation Between Electroluminescence and Partial Discharges in Silicone Rubber Used for High Voltage AC Subsea Connectors

Øystein Midttveit

Master of Science in Electric Power Engineering
Submission date: June 2018
Supervisor: Frank Mauseth, IEL
Co-supervisor: Sverre Hvidsten, SINTEF Energy Research

Norwegian University of Science and Technology
Department of Electric Power Engineering

Problem Description

The demands towards future oil and gas production include increased recovery and long step-outs. Subsea processing is considered as one of the main issues in achieving these goals. To enable the next generation subsea boosting and processing facilities, high power electrical connectors are strongly needed and considered one of the most critical components. The project work is part of a four year research project on subsea connectors run by SINTEF Energy Research and NTNU in cooperation with national and foreign industry companies.

Electrical tree growth is a precursor to electrical breakdown in high voltage insulation materials. The project work will mainly be experimental, where the main purpose is to test and use a new experimental set-up for studying the correlation between electroluminescence and partial discharge pattern in silicone rubber samples. This should be done by the use of a needle-plane gap. By extracting the needle partly, a needle-tip shaped void should be made in order to examine the partial discharges and electroluminescence occurring in air cavities. A proper molding and testing procedure should be made.

Compared to other known insulation materials as cross-linked polyethylene (XLPE) and polyethylene (PE), few studies has been performed on silicone rubber. In order for manufacturers of high voltage cables and accessories to meet the future requirements, more research must be done on the material.

Preface

This is a master thesis written at the Norwegian University of Science and Technology (NTNU) in Trondheim. It is part of the Electrical Power Engineering study - a two year masters program. The thesis as part of a larger, ongoing project called ”SUBCONN”. It is a collaboration between SINTEF Energy Research AS, industrial companies and the Norwegain Research Council.

I would like to thank both my supervisors; Frank Mauseth at NTNU and Sverre Hvidsten at SINTEF Energy Research AS for good guidance when needed, discussions and consulting. I would also like to thank Emre Kantar for good guidance and communication throughout this thesis and Hans Helmer Sæternes for teaching me how to mold the silicone rubber samples and otherwise help when needed.

Sammendrag

Prosessering og behandling av olje forekommer i stor grad på platformer eller på land, i nærheten av oljebrønner. I nærmeste framtid vil denne virksomheten bli flyttet ned til havbunnen, flere titalls kilometer vekk fra nærmeste platform og på dypere havnivå. Denne virksomheten trenger strøm for å kunne driftes. Strømforsyning fra platform eller land kobles på store konnektorer på havbunnen. Silikon har gode elektriske og mekaniske egenskaper, er bøyelig og avstøter vann. Materialet er derfor godt egenet som isolasjonmateriale i konnektorer.

Dersom det foreligger feil ved støping av silikonet kan det forekomme delutladninger. Disse delutladningene framskynder aldringsprosessen av materialet og kan på sikt føre til at konnektoren havarerer.

Denne oppgaven sammenligner delutladningsmønster og lysutsendelse i silikongummiprøver med forhåndsdefinert hulrom. Totalt seks prøver har blitt testet; tre prøver med forhåndsdefinert sprekk i overflaten på hulrom og tre prøver hvor overflaten på hulrommet er intakt. Det har også blitt utarbeidet en prosedyre for å støpe prøvene samt en optimal test-prosedyre for prøvene.

Det har blitt funnet et klart mønster i hvordan delutladningene forekommer i forhold til hvordan lysutsendelsene opptrår. Jo hyere energi i utladningene, desto sterkere lys blir observert i hulrommet. Delutladninger initieres for spenninger lavere enn 1 kV for samtlige prøver. Elektrisk trevekst oppstår for alle prøver med forhåndsdefinert sprekk, mens det ikke oppstår for prøvene uten i det aktuelle spenningsområdet. Samtlige prøver var tydelig degradert som følge av delutladninger.

Abstract

Processing of oil and gas has been performed on topside installations close to the wells. In the future, wells will be further away from the infrastructure and more processing will be performed on the seabed. This will require more electrical power on subsea installations in deep waters and far away from the platforms and shore.

Large power cables are connected in subsea connectors at the subsea installations. Because of its good electrical abilities, flexibility and water repelling, silicone rubber is a good candidate as insulation material in these subsea connectors. As the industry looks towards deeper sea-levels and more challenging terrain, studies and research must be conducted on the materials to be used in order to estimate operation-time. Life time of the power system is crucial for the complete subsea processing plant and long term properties of the insulation materials must be known.

This study aims to find a correlation between partial discharges and electroluminescence in a pre-made cavity in silicone rubber. In total six samples have been tested; three samples with a pre-made crack in the surface wall of a cavity and three samples with a smooth surface wall in the cavity. A molding procedure in addition to a test-procedure of the samples has been found.

It has been found a clear correlation between partial discharges and electroluminescence in a pre-made cavity. If the dissipated energy is high, the emitted light is accordingly high, independent of the peak magnitude of a partial discharge. Partial discharges occur for voltages below 1 kV for all samples. Electrical tree growth was observed to occur at a lower voltage level in samples with a pre-made crack in the surface wall of the cavity. No electrical tree growth was seen in the three samples with a smooth cavity surface wall. All samples showed sign of degradation in the tip of the surface cavity.

Table of Contents

List of Tables

List of Figures

Abbreviations

PD	=	Partial discharge
SiR	=	Silicone Rubber
HV	=	High voltage
LV	=	Low voltage
PDIV	=	Partial discharge inception voltage
PDEV	=	Partial discharge extinction voltage
XLPE	=	Cross-linked polyethylene
PE	=	Polyethylene
p	=	Pressure [atm]
d	=	Distance [mm]

Chapter 1

Introduction

1.1 Background

Processing of oil and gas has been performed on topside installations close to the wells. In the future, wells will be further away from the infrastructure and more processing will be performed on the seabed. This will require more electrical power on subsea installations in deeper waters and far away from the platforms or shore. It is expected that the high power demand will require equipment with higher voltage rating, above 36 kV. This will also apply to subsea cables and electrical connectors. Very few connectors and penetrators have voltage rating above 36 kV today. Silicone is considered to be an interesting insulation material for subsea equipment with higher voltage ratings.

1.2 Subsea power equipment

Some of the main subsea equipment in subsea power systems are listed below:

- Subsea pumps and compressors.
  - Subsea pumps have been on the seabed for some tens of years. Power rating is increasing, current technology is in the range 3-4 MW. Typical voltage rating on subsea motors is 6.6 kV. In recent years, subsea gas compressors have also been installed with power rating up to 12 MW.
- Subsea transformers
  - Subsea transformers are used to transform from transmission voltage level to motor voltage level. Subsea transformers are oil-filled.

- Templates
  - Also known as ”Big Yellow Thing”. The template acts as the vessel for any other subsea component. Depending on the topology of the sea bed, the template can be installed with or without suction anchors. Examples of components placed on a template:
    * Engines/pumps/drives.
    * Separators and compressors.
- Power umbilical/cable.
  - To be able to energize and control the subsea equipment, large cables or umbilicals are installed from the topside installation to the subsea station. The content of an umbilical varies on each individual project but typically comprises power cables, chemical tubes, optical fibre cables etc. With longer distances and higher power in future applications, the voltage level is expected to increase. Typical power applications today have a maximum voltage rating of 6-12 kV. In the future, voltage ratings are expected to be above 36 kV.
- Subsea connectors and penetrators
  - The power cables/umbilicals are terminated in subsea connectors. Subsea connectors allow connection and disconnection of equipment on the seabed. This is required for installation and maintenance/repair. Penetrators are mounted in the walls of the subsea equipment as power feed-throughs, for instance in transformers and motors. Connectors and penetrators are quite complex components and are considered very critical in the power system. Quality in the termination work, risk for partial discharge and risk for leakages make the connectors a very critical component. As the voltage level increases this interface becomes even more critical.

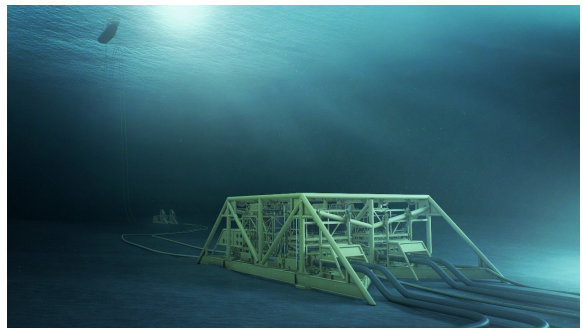

Figure 1.1: A template with umbilicals connected at subsea connectors.[1]

1.3 Subsea challenges

A higher subsea power demand with more subsea loads introduce several challenges:

- Deeper water levels means greater hydraulic pressure on components.
- Larger mechanical stresses.
- Longer step-outs means higher voltage and current level.
- High number of electrical drives and loads.
- High power demand.

In order for manufacturers to create and produce subsea equipment within the specified requirements, more knowledge on how different materials behave under challenging stress levels is needed.

1.3.1 Subsea connectors

Subsea connectors are as mentioned quite complex components. They are normally oil-filled. Silicone is used in some connectors, both as insulation material and also in other internal components.

Figure 1.2 shows a typical connection sequence between a ”plug” and a ”socket” in a subsea connector. The exposed conductor pin is pushed into the socket, which is inside an oil-filled chamber (yellow). Water intrusion is very critical and will lead to failure.

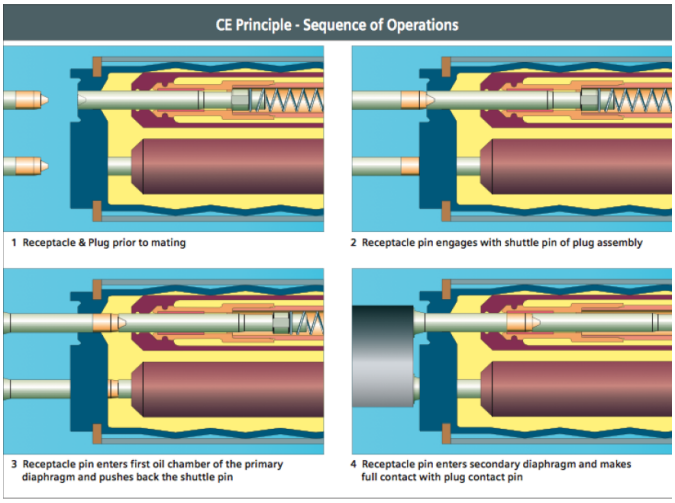

Figure 1.2: Cable termination. [2]

1.4 Scope of work

As mentioned above, silicone rubber is used in subsea connectors, very often surrounded by insulating oil. In this thesis, silicone rubber submerged in oil will be tested. The oil used is Midel 7131, a synthetic ester. Both ”dry” and saturated samples will be used. A ”dry” sample is not saturated with Midel 7131; It is used as it after molding. When the power system have been in use for some time this oil will diffuse into the silicone rubber material. If the subsea power system is in its start phase, the oil will not have diffused into the silicone. If an unwanted impurity is introduced in the insulating material (in this thesis: silicone rubber) during manufacturing, this could lead to two different fault scenarios:

1. Aging mechanism occurring in oil saturated insulation.

2. Aging mechanism occurring in unsaturated insulation.

This thesis aims to examine aspects of both; Aging mechanism occurring in saturated and unsaturated insulation by the means of studying emitted light photons and partial discharge patterns. Pressure is also an external parameter, but this is not included in these tests.

When manufacturing cables or when assembling connectors, small cavities may be introduced in the insulation itself or in interfaces between different materials. As will be explained in the theory chapter, these cavities contributes to a higher internal electrical field and partial discharges are likely to occur. With time, this will cause the entire cable/-connector to fail and replacements must be made.

In order to test the aging mechanism occurring due to partial discharges in cavities in silicone rubber, test samples has been made. By the use of a needle-plane gap method, with a pre-made cavity at the needle-tip end, silicone rubber samples was molded as indicated in Figure: 1.3. For measurements, see Appendix B.

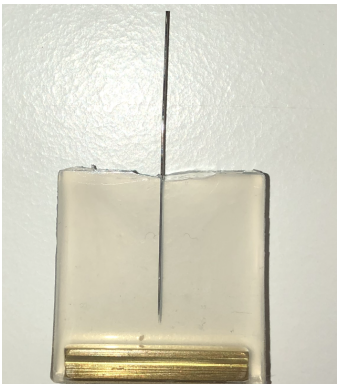

(a) Silicone rubber sample

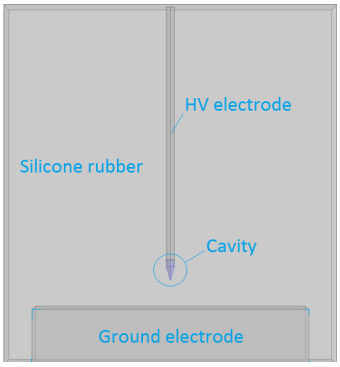

(b) Silicone rubber sample model

Figure 1.3: Silicone rubber sample. Actual and computer-modeled.

The samples will be submerged in Midel 7131 and tested at various high voltage levels by the means of a step-test. The examined area is the cavity area indicated in Figure: 1.3b and an electrical tree, if this occurs.

1.5 Previous work

This master theses is part of larger, ongoing project called ”SUBCONN”. It is a collaboration between SINTEF Energy Research AS, industrial oil companies and the Norwegian Research Council. The main workpakages consist of many different subparts leaving room for multiple masters and Ph.d theses to be prepared on the subject.

The project develops around the insulation material used in subsea connectors. In the past, much attention has been given to the insulation materials XLPE, PE and epoxy resin in terms of research. Because of its many good qualities such as electrical withstand strength and flexibility, silicone rubber is considered to be a good insulation material in subsea connectors, but not much research has been conducted on the material.

This master theses builds upon the findings done in the pre-study prior to this theses [3] in addition to the results found by Ingvild Spurkeland [4] and Miguel Soto Martinez [5]. The objective in Spurkeland and Martinezs theses was to describe how partial discharges in silicone rubber behaves by varying the hydrostatic pressure. Test were performed on identical silicone rubber samples (without a pre-made cavity) used in this thesis, with and without a pre-grown electrical tree. In addition tests were performed on silicone samples saturated with Midel 7131 and ”dry” samples.

1.5.1 Findings in previous thesis and pre-study

From all three theses it can be read that the partial discharge inception voltage (PDIV) for dry samples with a pre-grown tree (no cavity) is in the range of 3-4 kV. From Ingvilds theses it could also be read that saturated samples had a higher PDIV than ”dry” samples because of the Midel 7131 changing the silicone rubber samples’ electrical abilities when diffused into the polymer.

Silicone rubber test platform

In the pre-study the main goal was to verify the method used for capturing electroluminescence by use of a highly complex charge coupled device camera (CCD-camera). This camera was placed above the silicone rubber sample, pointing downwards. To be able to easily switch between the silicone rubber samples after a test was conducted, a special test platform was created. It had certain qualities:

- The platform should have a higher PDIV than the expected PDIV for the silicone rubber sample. The platform was tested to withstand at least 20 kV. No partial discharges was seen at this voltage level.
- The platform makes it easy to change between the silicone rubber samples between each experiment without disassemble the whole set-up.

- When changing the silicone rubber sample and placing a new one, the focus point of the camera remains in tact at the needle point.
- The platform is easy to disassemble in order to make room for another ongoing test.

All the specifications were met during the pre-study and the test platform will be used throughout this master theses. It is illustrated in Figure: 1.4 and 1.5 on the following page.

From the test conducted on the silicone rubber samples in the pre-study, it was found that to be able to capture the emitted photons during partial discharge, the magnitude of the partial discharge should be at least 20 pC. If the magnitude is less, the camera will not be able to capture the light.

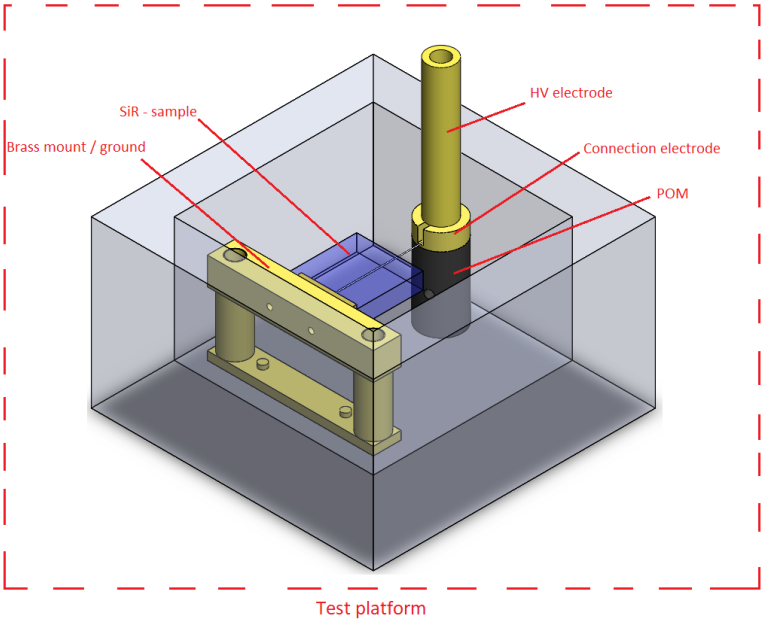

Figure 1.4: Modeled test platform with named parts.

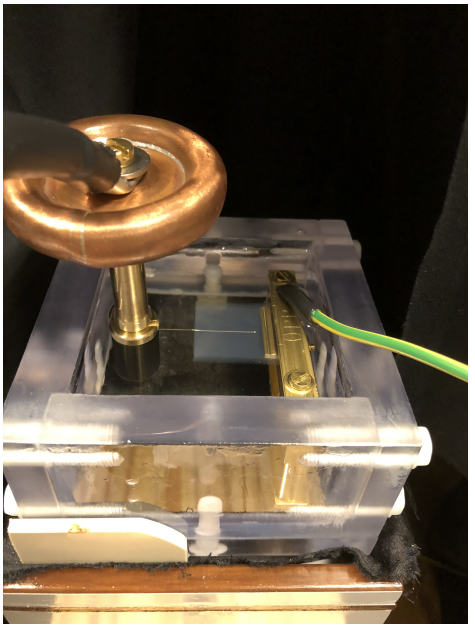

Figure 1.5: Test platform with SiR sample installed.

1.5.2 Goal of project

The main goal of this master theses is to find a correlation between electroluminescence and partial discharge patterns in a needle shaped void, with and without a pre-made crack, in silicone rubber samples.This is done by the use of a charge coupled camera and the Omicron MP600 measurement system. How the partial discharges deteriorate the surface of the silicone rubber is also of interest.

It is not possible for the camera to capture all the light emitted from PD activity. The camera can only ”see” one side of the test set-up. Some photons will be absorbed in the Midel 7131 and some photons will have a trajectory outside the camera lens and some towards the back end. The photons observed and studied will hence not be from all possible angles of the sample.

1.5.3 Hypothesis

This theses develops around previous findings done in the pre-study, Spurkelands theses and Martinez' theses. The primary object is to determine a correlation between light emitted and PD pattern in a pre-made cavity in a silicone rubber sample both with and without a pre-made crack. Tests will be conducted with silicone rubber samples tested as is after molding and Midel 7131 saturated silicone rubber samples.

- The partial discharges will initiate from the needle-tip as the local electrical field is high at this point. Given the Pachens curve, the partial discharge inception voltage will be lower than in a silicone rubber sample without a cavity as the cavity consist of air.
- Electroluminescence will be detected as before by the charge coupled camera.
- It shall be investigated if there is a difference in initiation of tree growth between samples with and without pre-made cracks. It is expected that initiation of tree growth happens at lower voltages in samples with a pre-made crack.
- The light emitted intensity will be dependent on the energy dissipated in the cavity.

In order to conduct sufficient experiments, pre-testings will be done on silicone rubber samples to determine a test procedure. It is expected that the procedure will vary for each type of sample.

Chapter 2

Theory

2.1 Silicone rubber

Silicone rubber is a polymer often used as insulation material in electrical equipment. The chemical structure of silicone rubber differs from eg. cross-linked polyethylene (XLPE) and polyethylene (PE) with a main chemical chain consisting of Si-O bonds as to the carbon based chain in XLPE and PE. This can be seen by Figure: 2.1. The silicone rubber used in this thesis is a two component silicone. It consist of ELASTOSIL A and ELASTOSIL B. (Appendix A)

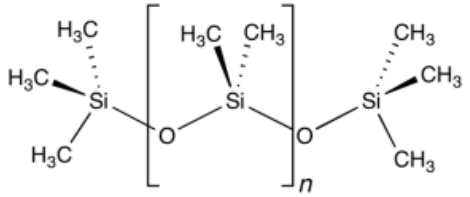

Figure 2.1: Chemical structure of silicone rubber [6]

Compared to the common carbon (C-C) bonds found in XLPE and PE, the Si-O binding has a higher binding energy which makes it more resistant to heat and a better electrical insulation. With its helical molecules structure it also makes the silicone rubber elastic and compressible. One of its many good qualities is the water repelling. This comes as a result of the methyl groups on the outside of the chemical structure, which are free to move.[7]

When silicone rubber is deteriorated by partial discharges it does not release much carbon. This is in great contrast to other electrical insulation materials used today (XLPE, PE etc.). Studies show that the carbon present in the silicone reacts with oxygen forming gasses in tubular channels (electrical trees). [8] It follows that these tubular channels are non-conductive. What materials are combined when deteriorating ELASTOSIL A/B

silicone rubber is not known. Tianyu et. Al. investigated the material properties of the silicone rubber "*Dow Corning Sylgard 184 Silicone Elastomer*" when a pre-made void existed in the silicone. The results indicated that the carbon present in the outer groups of the silicone reacted with the gas in the cavity, leaving graphitic carbon in the deteriorated areas in the cavity. [9]

2.2 Partial discharge

2.2.1 General partial discharge theory

While manufacturing cables or other insulation parts, it is very important to avoid contamination or voids in the insulation material. A contamination or gas in the void usually has smaller permittivity than the solid insulation and when exposed to an electric field the risk for small "sparkovers" inside the contamination/void is high. These sparkovers are the result of the electric field at the contamination site exceeding the withstand strength (kV/mm) of the particle. An avalanche of electrons will hit the surface walls of the cavity and deteriorate it and the surrounding insulation. This event is called partial discharge (PD) and leads to electrical treeing. After some time the branches of the tree will cross the entire insulation and reach ground potential; Breakdown is certain to follow. [10, p. 212]

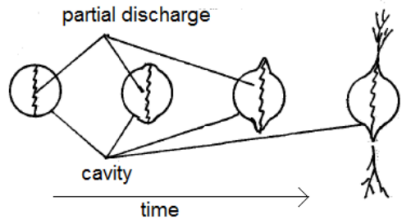

Figure 2.2: Partial discharge development [10, p. 224]

2.2.2 Detection of partial discharges

There are numerous ways of detecting partial discharges in insulation. A common way is to use a measuring circuit with the test object (T.O) in parallel with a coupling capacitor as can be seen in Figure: 2.3.

When a partial discharge occurs inside the T.O, the voltage across the T.O will drop. The coupling capacitor will "recharge" the T.O with a charge equal to the voltage drop until they both are at the same electric potential. This charge is referred to as the apparent charge as it is impossible to measure the exact charge drop in the T.O. This apparent charge causes a current to flow through the measurement impedance. A voltage drop is measured at the impedance, correlating to the apparent charge, and the charge is displayed on the user

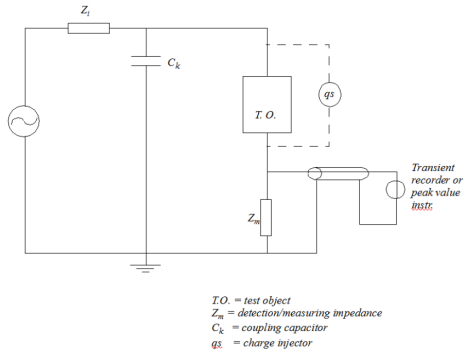

Figure 2.3: Partial discharge detection circuit [10, p. 221]

interface. Before a test is conducted, a known charge is injected over the capacitance to calibrate the measurement equipment. The measurement equipment used in this thesis is Omicron MP600.

2.2.3 Partial discharge in voids

There are different types of contamination that can occur in solid insulation. Small gas particles can be trapped inside the insulation when manufacturing, but it can also be introduced at a later point due to partial discharges deteriorating the solid insulation to gas.

The PD activity will deteriorate the walls of the cavity. When this happens, the solid material is converted to gas. The pressure in the void will increase. This effect was studied by Illias et. al[11]. It was found that in a round void cavity, the temperature increased as a result of a single discharge. The temperature increased mostly in the centre of the void. The pressure increased, and before the second PD occurred the conditions in the void had changed. As is explained by the Pachen's curve later on, an increase in pressure leads to a higher inception voltage. After some time, it is expected that this increased pressure will cause the gas to diffuse into the surrounding insulation material.

2.2.4 Partial discharge numbers increasing with increasing voltage

Once the applied voltage reaches a certain value, a partial discharge occurs. This voltage level is defined as the partial discharge inception voltage (PDIV). When increasing the applied voltage further, the number of discharges increases. It is shown that the partial discharge repetition rate is proportional to the applied frequency, and also the applied peak voltage. [12]

$$n_{AC} \propto f_{AC} \frac{\hat{V}_{AC}}{V_{PDIV,AC}} \tag{2.1}$$

Where:
n_{AC} = Repetition rate of partial discharges [1/s]
f_{AC} = Frequency of applied voltage [Hz]
$\hat{V}_{AC}$ = Peak of applied sinusoidal voltage [V]
$V_{PDIV,AC}$ = Partial discharge inception voltage [V]

2.2.5 Partial discharge / breakdown in dielectric liquids

D. André studied partial discharges and breakdown in dielectric liquids.[13] No matter the the nature of the liquid, it is found that all types have a certain conductivity. How high the conductivity is depends on the level of impurities contained in the liquid and the liquids ability to cleanse itself; e.g: Midel 7131 is highly capable of containing water without changing its dialectic strength abilities.[14]

2.2.6 Energy release in partial discharge

The relation between voltage and energy is given by Equation: 2.2. This equation can be used to estimate the energy in the partial discharges, given that the voltage is known.

$$E = V * Q \tag{2.2}$$

Where:
E = Energy released in Joules [J]
V = Voltage potential difference [V]
Q = Charge [C]

In a needle-plate configuration it is difficult to measure the exact voltage at the discharge place. With the Omicron MP600 system, the voltage across the test sample will be measured with a voltage divider circuit in series with the coupling capacitor(ref Figure: 2.3).

By using the measured apparent charge and the voltage across the terminals of the silicone rubber sample, it is possible to measure the energy "fed into" the sample. The Omicron MP600 measure the voltage every $48\,\mu s$ in addition to measuring the time and magnitude of the partial discharge. By using Equation: 2.3 the energy fed into the sample can be calculated. This approach was used by Schurch et al.[15]

$$E_{tot} = \sum v_i c_i \tag{2.3}$$

Where:
E_{tot} = Total energy fed into sample [J]
v_i = Voltage at sample terminals when partial discharge occurs [V]
c_i = Magnitude of partial discharge [C]

This method does not give the exact value of dissipated energy inside a cavity during a partial discharge. Figure: 2.4 shows two voltage curves; one over the entire test sample and one over the cavity where partial discharges occur. As can be seen, once the inception voltage (U_{s0}) is reached at t_1, the voltage over the cavity drops to a remanent voltage (U_{r0}). After the voltage drop, the voltage increases again (sinusoidally) until the inception voltage is reached again and the same procedure occurs.

By using Equation: 2.3 as described, the charge size would be multiplied with the voltage across the entire sample. It is unclear how large error is introduced by using Equation: 2.3. It is clear that the actual energy released inside the cavity is lower than given by the equation.

Dissipated energy proportional to apparent charge

It can be shown that the energy dissipated in a partial discharge is [10, p. 220]:

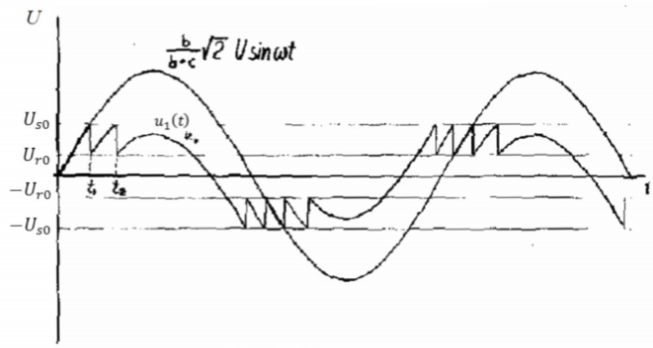

Figure 2.4: Applied voltage on sample and voltage curve across cavity. [10, p. 217]

$$\Delta W = \sqrt{2} U_e q_a \tag{2.4}$$

Where:
ΔW = Energy in the circuit before partial discharge minus energy after patital discharge [J]

U_e = Extinction voltage. The voltage at which partial discharges no longer occurs (after first occurring) [V]

q_a = Apparent charge.[C]

In this thesis it is not possible to measure the extinction voltage due to the high numbers of discharges in addition to the difficulty in measuring the extinction voltage. As the energy dissipated in the void is proportional to the apparent charge, it would, by summing every apparent charge measured, give an indication of how much energy that is dissipated in the cavity during the discharges. T

Energy released from a discharge

The energy dissipated during a partial discharge converts to multiple energy sources [16]:

- Mechanical waves.
- Chemical processes.
- Light emission / Electroluminescence.
- Heat.
- Current in external circuit.
- Electromagnetic radiation.

In this thesis the main objective revolves around the detection of light emitted during a partial discharge; this is the only energy form discussed.

Electroluminescence

An atom consist of multiple orbital levels where the electrons fluctuates. When an atom is exposed to an electrical field it can, if strong enough, excite the electron out of its orbital level to a higher energy state. When the electron ”jumps back” to its original energy level it releases energy; a photon. [17] This effect is illustrated in Figure: 2.5 and referred to as electroluminescence.

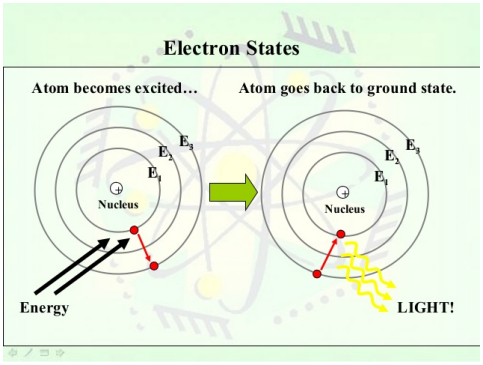

Figure 2.5: Excited and grounded atom.[18]

To fully understand how electrical trees behave in insulation materials it is crucial to understand how the electrons and charge carriers behave. By using high sensitive cameras, it is possible to detect emitted photons from partial discharges in polymers. [3][19]

Pachen's curve

Pachen's law says: "*The sparkover voltage in a homogeneous field is a function of the product p*d only (at a given temperature).*" [10, p. 63].

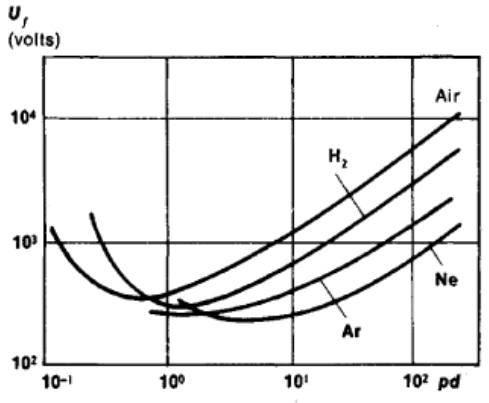

Figure 2.6: Pachens curve for various gases[20]

As can be seen in 2.6, if the distance "d" is constant, the voltage needed to get a sparkover (PD) when decreasing the pressure is reduced when travelling from the right on the graph to the left. This is because a free electron would make fewer gas-molecule collisions and hence maintain its energy (enough energy to create new ionizing collisions). When travelling from the graphs minimum point to the left, while keeping the distance "d" constant, it can be seen that the sparkover voltage increases. This is because the mean free path of the electron increases, and an ionizing collision is no longer certain. [10, p. 64]

Breakdown strength in air

As can be seen in [10, p. 18], the dielectric strength of air is 3 kV/mm. If the applied electrical field in an electrode surrounded with air is higher than this, partial discharges occurs.

2.3 Townsend discharges

For low pressure gases in narrow spaces (p*d <5 atm mm), Townsend discharges is used to describe the breakdown mechanism. A Townsend discharge is an electron avalanche moving from the cathode towards the anode. When a gas is submitted to an electric field, a free electron is accelerated towards the anode. If the electron has sufficient velocity/energy, a collision with a gas particle will cause ionization and release a new electron. These two electrons will continue the process and an avalanche is achieved. It is governed by two ionization coefficients, three if the gas involved is an electronegative gas:

- α. Townsend first ionization coefficient. This is the probability that an accelerated electron will give an ionization collision per unit length.
- γ. Townsend second ionization coefficient. The probability that one electron is released from the cathode for each generated positive ion.
- η. Townsends third coefficient. The probability that one electron is captured by an electronegative atom. Electronegative gases such as SF_6 lack electrons, making it possible to absorb any free electrons, increasing the breakdown voltage of the gas.

For this process to occur, a free electron needs to be present in the field area. This electron could be introduced due to light or cosmic radiation. When ionizing collisions are occurring during a Townsend discharge, photons are emitted. This can be seen as light filling the available space.[10, p. 56] [21]

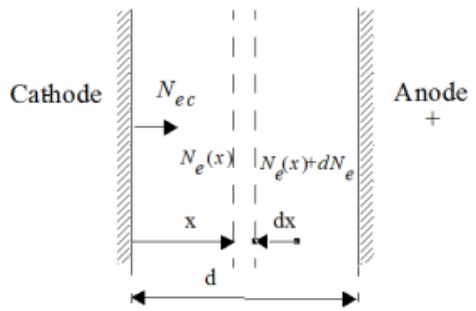

Figure 2.7: Illustration of number of electrons calculation.[10, p. 56]

2.4 Streamers

For higher pressures or distances between the electrodes ($>$5 atm mm), Townsend discharges can no longer explain the occurring breakdown event. For a critical electron length, the electron avalanche becomes unstable and the number of electrons calculated at the tip av the avalanche is greater than $5 * 10^8$ electrons.[10, p. 65] What differs Townsend discharges and streamer discharges is the speed of the breakdown, shape, temperature and pressure/distance. The streamer mechanism is much faster, has higher temperature and the shape is bright channels with clear branches. [21]

2.5 Electrical tree

Electrical trees is a known aging mechanism of insulation materials. When partial discharges deteriorate the surrounding insulation, small hollow tubular channels are formed. The number of channels formed is a stochastic phenomenon.[10] The conductivity of these channels is highly dependant of the deteriorated material. When one of these channels bridges between the high voltage electrode and ground, electrical breakdown will occur.

The initiation of the tree is caused by many small rapid partial discharges at the tip of the high voltage electrode, contamination or cavity. When the surrounding insulation material is deteriorated the solid is converted to gas. The continuous growth of the tree channels is caused by partial discharges occurring in gas. The chemical composition of the gas is depending on the solid insulation material. PE and XLPEs chemical structure is highly carbon based [22], making the tubular channels highly carbonated and thus very conductive. A conductive tree channel will push the electrical field forward to the channel and where the partial discharges will continue to bombard the surface of the cavity wall.

Figure 2.8: Electrical tree.[23]

2.5.1 Tree growth in silicone rubber

As mentioned above, the chemical composition of the silicone rubber is Si-O bonds. Compared to other known insulation materials such as PE and XLPE the carbonation level in the tree channels is very low.[24] This gives a low conductivity in the tubular channels and the electrical field is not as high at the tree channel end. As a result, the voltage level after tree initiation in silicone rubber must be increased in order for the tubular channels to grow further.

Having less carbon, the electrical tree structure is white and difficult to spot under a microscope.[25]

2.5.2 Tree growth stages

Electrical tree growth can be divided in three stages. The first stage is called the initiation phase. As partial discharges is bombarding the surface of the insulation, tree branches starts forming. The tree length will increase fast.

If the applied voltage is kept constant, the growth of the electrical tree will decrease. As mentioned, when partial discharges deteriorate the solid insulation it will transform to gas. Further growth of the electrical tree is depending on the composition of these gases in addition to the applied pressure (Pachens curve). This phase is called the stagnation phase.

When the time or voltage applied is high enough breakdown will follow.

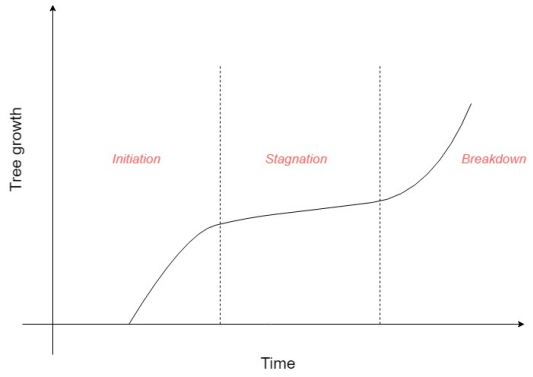

Figure 2.9: Electrical tree growth phases.

Electric tree modelling

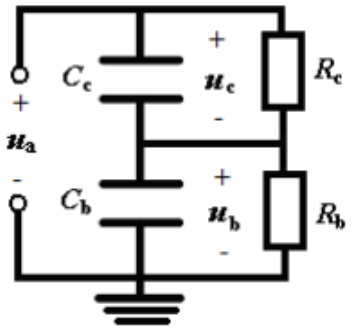

Figure 2.10: Circuit model of electrical tree [26]

Figure: 2.10 illustrates how an electrical tree is modeled in an electrical circuit. Once

the insulation material is deteriorated the deteriorated area is converted to gas (u_c). The remaining healthy insulation still acts as a capacitor until the tree channels bridges the electrodes (u_b).

2.6 Diffusion

When two different substances are mixed in a gas/gas, gas/liquid, liquid/liquid or liquid/-solid combination, its called diffusion. Gases will always mix, but when it comes to the other combinations its dependant on the substances' solubility (how much of one substance can mix with the other substance). The more solid the substance, the longer time to diffusion reaches equilibrium (ref Figure: 2.11).

On a molecule level, solid insulation consist of holes, incorrectly placed molecules etc. When a solid material is placed in a liquid container the molecules of the liquid will, dependant on the solubility, use these imperfections and hence diffusion takes place. At a higher temperature the molecules move faster and the diffusion process will accelerate.[27]

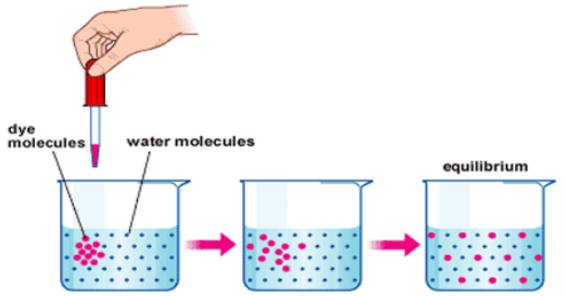

Figure 2.11: Diffusion process of liquids. From start to equilibrium. [28]

2.6.1 Diffusion in silicone rubber

In this thesis the diffusion process builds upon findings done by Rune Gravaune [29]. When saturating the silicone rubber, the method of "Mass uptake measurement" is used to determine the saturation level. Prior to submerging the silicone rubber samples in Midel 7131, the weight of each sample is measured. When submerged in the synthetic ester, the ester will diffuse into the silicone, increasing its weight. When the sample is saturated the weight will remain unchanged.

As mentioned, a higher temperature will accelerate the diffusion process, making more room for the ester to fill and reduce the saturation time. When the temperature drops, the SiR molecules will slow down. The sample is now over-saturated and the some of the ester taking the silicone rubber molecules ”place” will be pushed out. This effect is illustrated in Figure: 2.12.

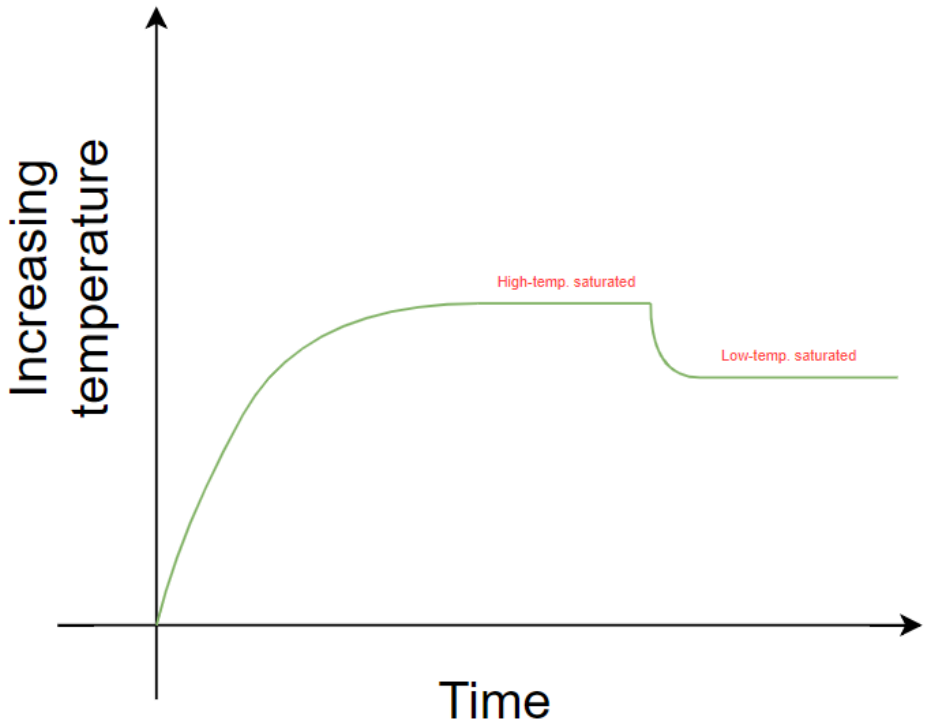

Figure 2.12: Illustrative time/temperature saturation graph.

Chapter 3

Silicone rubber samples

The silicone rubber used in the experiment is a two component silicone (ELASTOSIL A/ ELASTOSIL B). Its properties can be found in Appendix: A. Initially the two components are stored in a fridge, separated from each other. As one of them consist of a hardening component it will change its properties once blended. As mentioned in the Theory chapter, impurities can greatly reduce the withstand strength of insulation materials once present. To avoid introducing impurities when mixing the silicone rubber, the work was done in a clean environment. The workdesk used was cleaned using isopropanol and the mixing of the two silicone components was conducted under a suction fan.

The procedure for making the silicone rubber samples, with cavities and pre-made cracks, are presented in the following sections:

3.1 Preparation of needles and ground electrode

The needles used in the samples are used to achieve a high local electrical field in the void. The needle used is normally used for acupuncture. To make sure the electrical field was sufficient enough to create partial discharges, a tip radius was set to $2\,\mu\mathrm{m} \pm 1$.

In order to measure the radius of the tip, a highly sensitive digital microscope was used. The measurement technique is illustrated in Figure: 3.1 . If any needled had imperfections, asymmetry or they were out of tolerance they were set aside not to be used in the silicone rubber samples.

The ground electrodes used is the same ground electrodes as used during the pre-study paper. Before molding, the ground electrode was polished and washed with isopropanol.

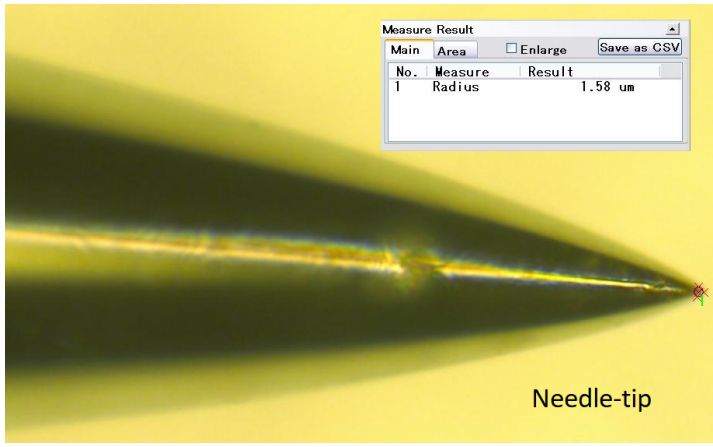

Figure 3.1: Measurements of needle-tip radius.

3.2 Casting mold

The casting mold used to make the samples is the same casting mold as used in the pre-study.[3] It consists of four parts, correlating with Figure: 3.2a:

1. **Iron plate.** The iron plate is used to provide force and equalize the pressure on the plexiglass while vulcanizing the silicone rubber.
2. **Bottom plate.** The bottom plate was the main vessel for the casting mold containing the silicone rubber sample during the entire vulcanization process. The casting mold is placed on top of the bottom plate and under the plexiglas.
3. **Casting mold.** Figure 3.2a shows a disassembled casting mold. This is the vessel for the electrode (needle) and the silicone rubber when assembled.
4. **Plexiglas.** The plexiglas is used to ensure a smooth surface on the silicone rubber while vulcanizing. As plexiglas is see-through it provides possibilities when placing the needle 2 mm above the ground electrode. The placement of the needle must be done while the entire casting mold (Figure: 3.2 is assembled. This is only present for the first part of the vulcanization (One hour at 100°C) as it would be deformed if kept in higher temperatures.

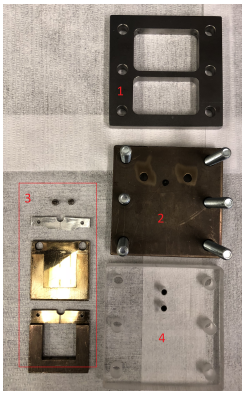

(a) Casting mold parts

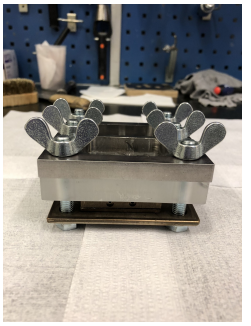

(b) Fully assembled casting mold

Figure 3.2: Casting mold

3.3 Molding of samples

The procedure for preparing the silicone is the same as in the pre-study.[3]

3.3.1 Preparation of silicone

The silicone consist of two parts; ELASTOSIL A / ELASTOSIL B. When mixing the two a ratio of 1:1 has been used, in accordance with the data sheet (Appendix: A).

After a ratio of 1:1 was achieved (typically with a total weight of 70g, 35g each) the mixture was blended by hand before but in a mechanical blender in a vacuum chamber. Here it was blended for a minimum of 30 minutes. Since the mixture was exposed to air after this process it is uncertain if the use of vacuum is necessary for extracting unwanted air bobbles.

After a minimum of 30 minutes of blending in the vacuum chamber, the mixture was extracted into a plastic syringe. A plastic syringe is easy to handle when extracting the silicone in the molding shape. The syringe was then placed back into the vacuum chamber with the tip pointing upwards for a minimum of two hours. The purpose of doing this is to extract unwanted air bubbles introduced in the silicone during the mixture process. It also makes the molding process quicker as the silicone is air free and no additional waiting is required.

After the vacuuming period, the syringe was placed in the fridge over night. This ensured a air-free silicone mixture in addition to slowing down the curing process.

If kept in the fridge for more than three days, the transparency of the silicone could be reduced. This could potentially make it difficult to observe electroluminescence during experiments.

3.3.2 Molding process

Before molding, the molding cast, ground electrode and electrode(needle) was cleaned using isopropanol and pressurized air before assembled as indicated in Figure: 3.3. This was done to ensure an impurity-free surface of the parts.

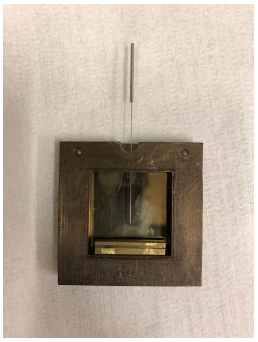

Figure 3.3: Molding cast assembled with needle- and ground electrode.

Silicone rubber was extracted from the plastic syringe kept in the fridge and put on the bottom plate of the molding cast. The plexiglas was put on top followed by the iron plate. The parts were screwed with six screws to ensure equalized pressure along the entire casting mold to make a smooth surface of the silicone rubber sample. This process could introduce small air cavities in the silicone. To remove these, the fully assembled casting mold was put in the fridge. The time in the fridge was highly dependent on the size and numbers of cavities. When no cavities were seen, the needle electrode was placed 2 mm apart from the ground electrode using a highly sensitive digital microscope. This placement procedure could introduce some air cavities at the top of the sample, but these would go away during the first part of vulcanization as the polymer is expanding when introduced to heat. The fully assembled casting mold was put in the oven at $100°C$ for one hour.

After the first vulcanization process the iron plate and plexiglas was removed. As the sample is done with its first vulcanization process the viscosity of the silicone has increased some, but it is still flexible. By the use of a leatherman and a digital microscope, the electrode was extracted 1 mm further away from the ground electrode leaving a hollow room in the sample with the shape of the electrode. This is shown in Figure: 3.4. The sample was put back in the oven for the second hardening process. It was kept here for four hours to fully vulcanize it.

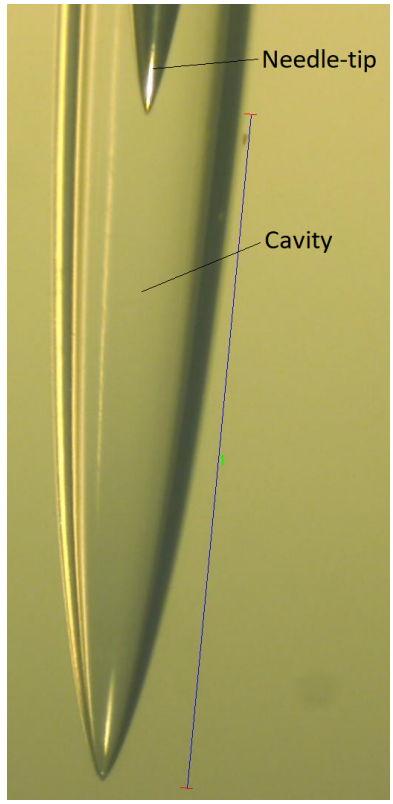

Figure 3.4: Illustration of needle-shaped cavity in the silicone rubber samples.

To make a crack in this cavity the extraction of the needle was done after the second vulcanization process.

3.4 Midel-saturated samples

In order to saturate the samples with Midel 7131, it was necessary to know the saturating procedure. As the material and size of the samples is the same as both Spurkeland and Martinez's, the same procedure were used. The samples were kept in Midel for 60°C for 10 days, following 13 days in room temperature. A new container for the samples during saturation was made. A platform of teflon with a handle made it easy to lower and hoist the silicone rubber samples in the Midel 7131. This is indicated in Figure: 3.5.

Figure 3.5: Container for samples during saturation.

3.4.1 Saturated samples made wrong

After the saturation period, it became clear that the silicone rubber samples never should have been completely submerged in Midel 7131 as indicated in Figure: 3.5. By doing this the oil could diffuse into the cavity by penetrating the sample via the surface between high voltage electrode and silicone rubber. If the samples only were partly submerged as shown in Figure: 3.6, the oil would have diffused through the silicone rubber into the surface of the cavity, never penetrating it because of its internal pressure. This is a realistic approach and also the motivation for testing saturated samples with a cavity.

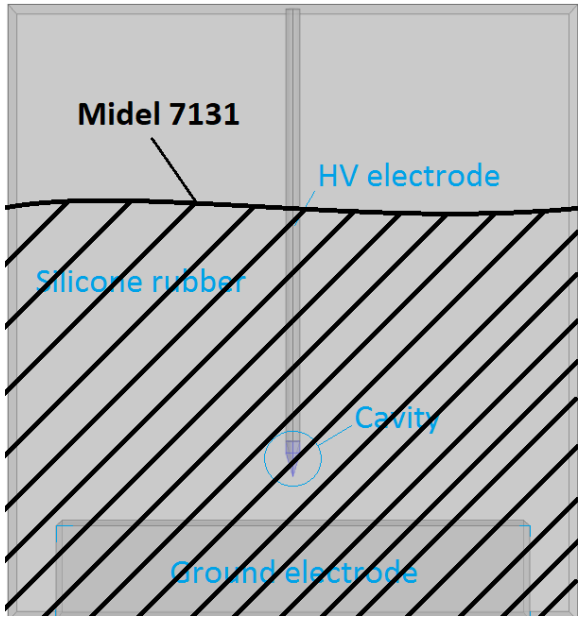

Figure 3.6: Indication of correct Midel 7131 level during saturation.

If the saturated samples should have been tested, new samples had to be made and saturated. Because of limited time, this was not done and hence no saturated samples were tested in this thesis.

3.5 Failed attempt at making cavities in silicone rubber samples

Some challenges were experienced when attempting to establish a method for making samples with cavities. One of the challenges was related to ensuring a sealed interface between the cavity and the surrounding oil (avoid leakage into cavity along the needle). This section describes how this challenge was approached by use of silicone rubber glue. The procedure of making the silicone rubber is the same.

3.5.1 Silicone rubber as glue

The first pre-made cavities in the silicone rubber sample were made after the second hardening process (ref subsection 3.3.2 on page 31) was done. A leatherman was used to extract the electrode (needle) 1 mm further away from the electrode.

It was believed that the loosening of the needle would make room for the Midel 7131 to penetrate into the cavity at the top intersection between the electrode and the silicone rubber. After the needle was placed 1 mm further away from the ground electrode, unhardened silicone rubber (from the syringe) was glued on top in order to "seal" this intersection. As this process could introduce air bubbles it was left in the fridge for a minimum of three days. As this intersection area is of little interest while examining the emitted light during partial discharges it did not matter if the transparency in the silicone rubber became reduced. The samples was then fully vulcanized for four hours at $200°C$. This method was performed on a total of eight silicone rubber samples, all samples being unsaturated and with a needle tip radius of $\sim 2\,\mu m$.

The new-glued intersection of the silicone rubber samples were submerged in Midel 7131 to break the refraction index of the light and examined by a highly sensitive microscope. Figure: 3.7 shows the result for a sample. This picture is also representative for the seven other samples this method was conducted on. For reasons not known, the small cavities was introduced during the gluing-process had not disappeared during its time in the fridge - as it did while in the plastic syringe. The cavity would not be penetrated with Midel 7131 during measurements, but partial discharges occurring in these cavities would interfere with the wanted results; partial discharges occurring in the cavity.

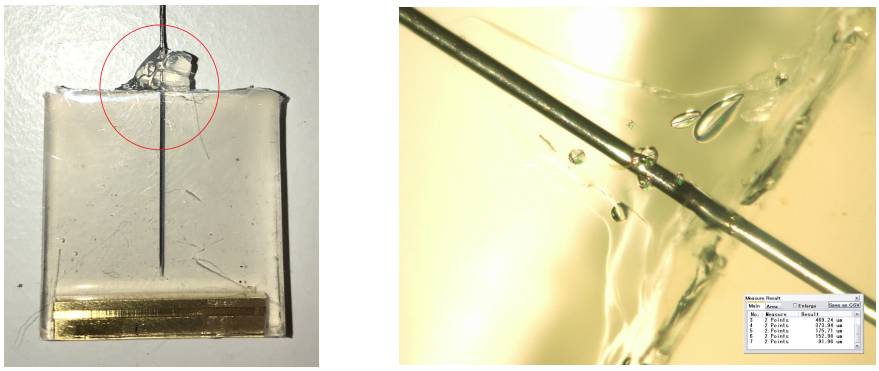

(a) **(b)**

Figure 3.7: Air cavities at interface between electrode and silicone rubber.

Cancel the electrical field in the cavities

The making of silicone rubber samples is a time consuming process. In order to produce two samples, making the silicone rubber from scratch, two to three days is required depending on how quickly the air cavities disappear while in the casting mold. As the air trapped in the intersection area, as indicated in previous subsection, revolved all eight samples it was decided to figure out a solution to the cavity problem.

A solution was to equalize the field inside the cavities. This was done by placing the intersection area inside an electrode at the same voltage potential as the needle electrode inside, as indicated in Figure: 3.8. The new electrode had a ”ring” form covering the entire circumference of the air filled cavities. The theory was that if there were no voltage potential difference between the two electrodes, the electric field between them would cancel out and no partial discharges would occur.

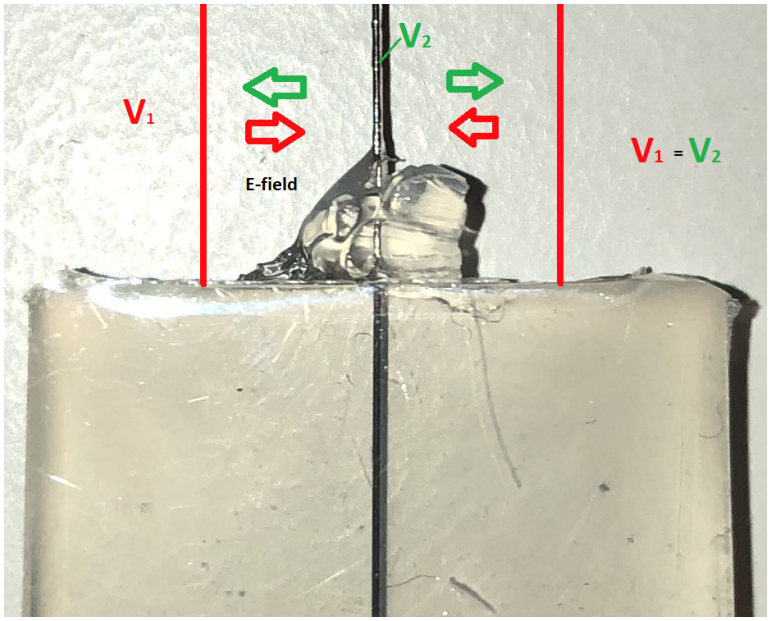

Figure 3.8: Electrode at same voltage potential as the needle. The fields will cancel each other out.

The workshop produced the ring electrode, making it long enough to reach the connection electrode (ref Figure: 1.4 on page 8). This is indicated in Figure: 3.9. As the ring is just a bit longer than the distance between the silicone rubber and the connection electrode, some pressure had to be added in order to get it in the right place. As the silicone is elastic this was no problem.

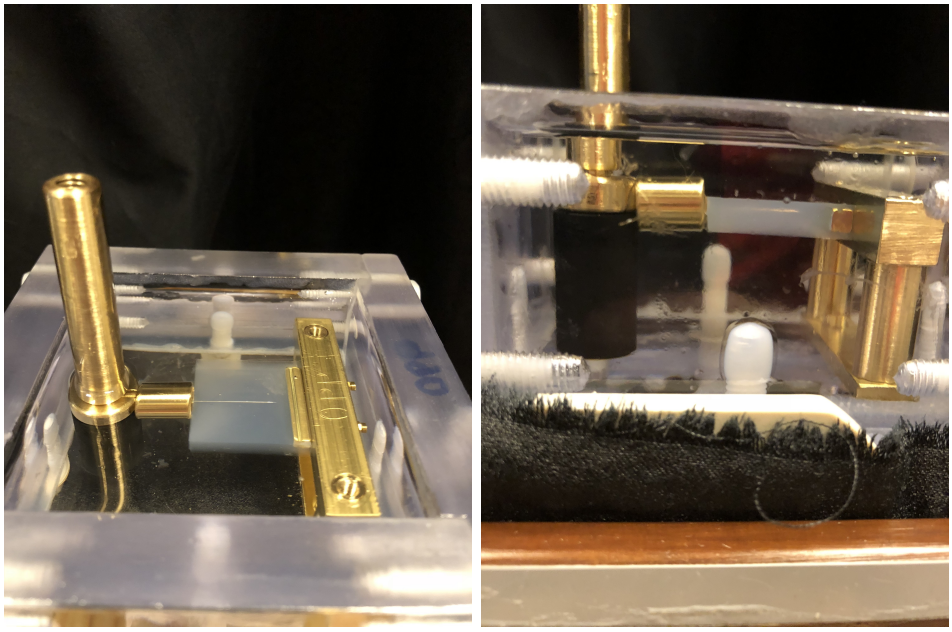

(a) Top view **(b)** Side view

Figure 3.9: Ring electrode covering the air cavities at the top of the sample

When testing the solution it became clear that unwanted partial discharges still occurred in the sample without being able to see it on the CCD camera. This indicated that the partial discharges happened elsewhere on the sample, not knowing where. It may be that this solution could have worked, but when considering this being a time based thesis it was decided to figure out another solution.

Removing the silicone filled with air cavities

A different solution was to remove the applied ”glue” in the intersection area with a scalpel and use it as is (same as using the sample as is after molding it from scratch). Without knowing if this would make the Midel 7131 penetrate into the cavity, a sample was submerged in the ester, with success; no midel penetrated the cavity. This could be because of capillary forces between the silicone rubber and the needle electrode, but also because of the pressure inside the cavity could will be higher than that of the midel (it is not submerged much). This made it possible to use the eight samples already created.

When testing this solution with the CCD camera and Omicron MP600 measurement system, partial discharges and electroluminescence was detected. This was the molding procedure chosen, and the same as described in subsection 3.3.2 on page 31.

Chapter 4

Test equipment/procedure

4.1 Electrical circuit

The electrical circuit used in the experiments is shown in Figure: 4.1.

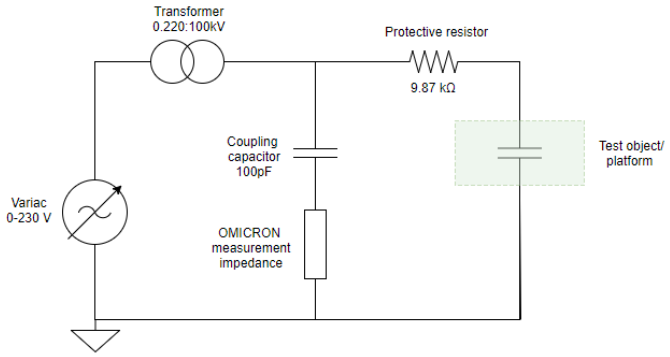

Figure 4.1: Electrical circuit

Variac: The variable power source of the circuit. Placed outside the high voltage test cell.

Transformer: Transforms the power with a ratio of 0.22:100 kV. Placed inside the high voltage test cell.

Coupling capacitor: The coupling capacitor in the circuit. Provides the apparent charge when a PD occurs.

OMICRON: The PD measuring system.

Protective resistor: If a breakdown occurs the protective resistor will reduce the fault

current and protect the measuring equipment.

Test object: The test object is the platform illustrated in Figure: 1.4 on page 8 containing the silicone rubber samples.

4.2 Omicron MPD 600

To detect partial discharges in the system, a special made analysis system is used called Omicron MP600. It gives a live overview of the applied voltage in addition to detect both the size and numbers of the partial discharges. The user interface is illustrated in Figure: 4.2. As can be seen, the interface also indicates where on the voltage phase the partial discharge is happening.

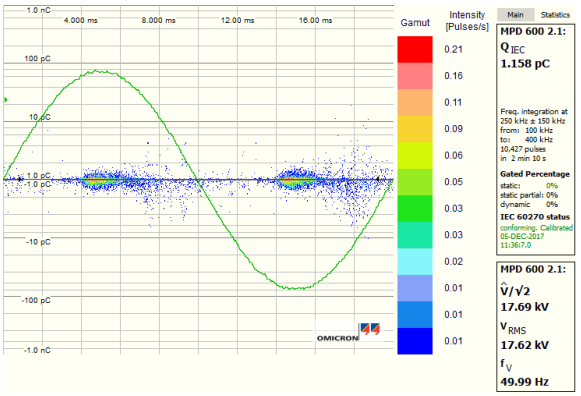

Figure 4.2: Interface of OMICRON system

The Omicron MP600 also have the ability to replay recorded streams and turning the files into readable MATLAB files. It is possible to record files of the voltage curve during the experiment, size and time of partial discharge and where on the voltage phase the discharge is occurring.

Different types of partial discharge patterns

Different types of defects gives different types of partial discharges patterns in the Omicron system:

Void cavity: Figure: 4.3 illustrates pattern of the partial discharges occurring in a void cavity. As can be seen, the partial discharges takes place when the voltage applied is positively and negatively increasing, following the voltage curve.

Corona: Figure: 4.4a illustrates pattern of partial discharges occurring due to corona. The PD pattern of the corona is highlighted with red circles. Corona typically happens when the applied voltage is at its peak or at the zero crossing point.

Noise: Figure: 4.4b illustrates pattern of partial discharges occurring when the system experiences noise. There is no symmetry in the pattern, only stochastic generated noise along the entire voltage curve.

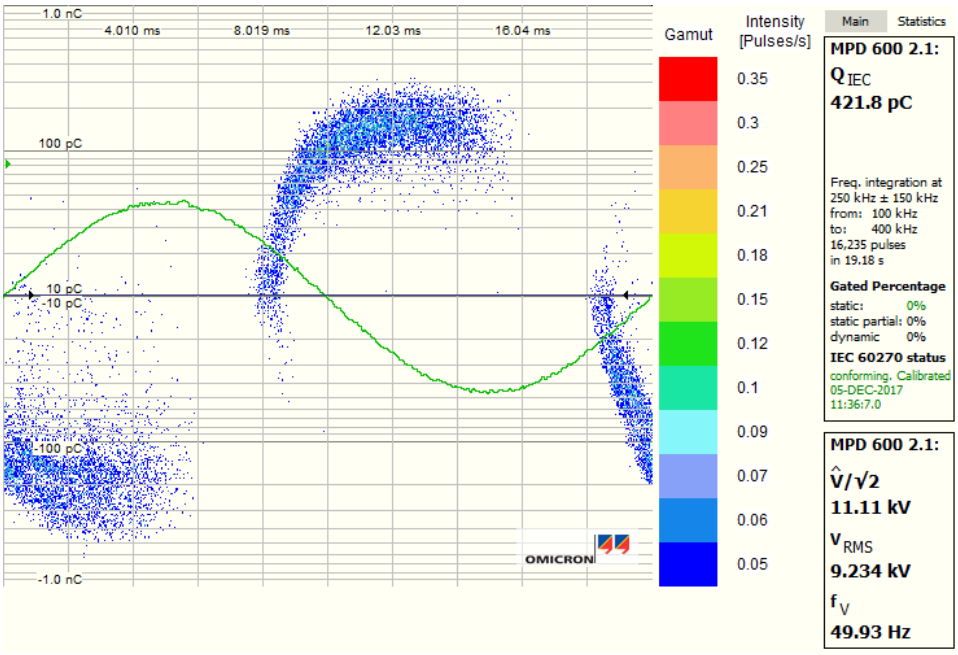

Figure 4.3: Partial discharge pattern of a void cavity in OMICRON

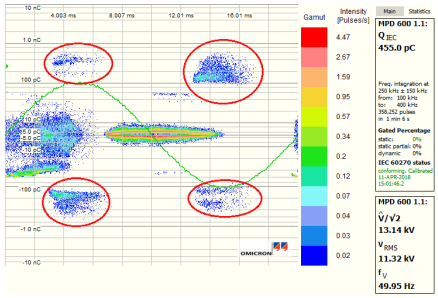

(a) Partial discharge pattern of corona in OMICRON

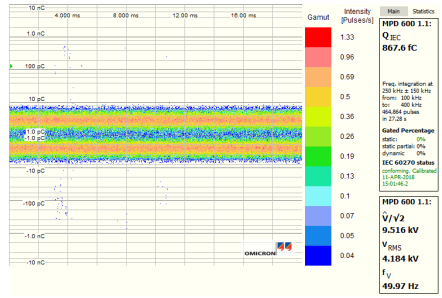

(b) Partial discharge pattern of noise in OMICRON

Figure 4.4: Casting mold

4.2.1 Replay modus

As mentioned, Omicron MP600 has a replay function which enables the user to analyze the experiment at a later time. When doing so, it is possible to choose at what time the replay should start and for how long. The Omicron replay function also has a build in timeline which displays the applied voltage and the partial discharge magnitude. This is illustrated in Figure: 4.5. The red graph indicates the voltage level, with its value given in the left y-axis, whereas the blue indicates the partial discharge magnitude given in pC with its value on the right y-graph.

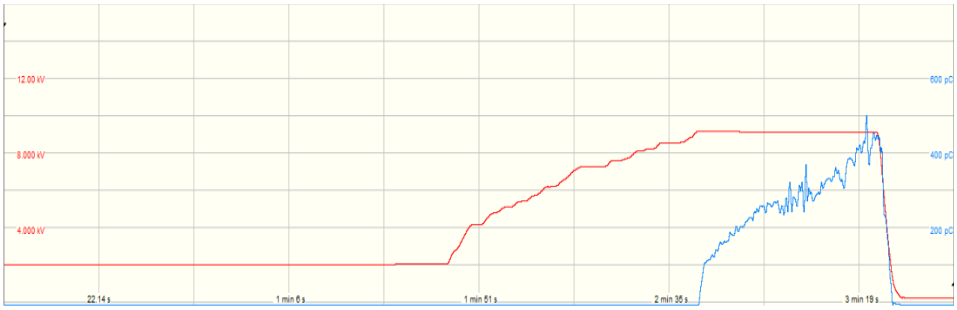

Figure 4.5: Omicron MP600 voltage and partial discharge curve.

4.3 Charge coupled camera, Photometrics QuantEM:512SC

To be able to capture the movement of the electrons, and also be able to control the electrical tree growth if it were to happen, a highly complex charge coupled camera was used.

The camera captures the light occurring in the lens and coverts the light into electrons with a given charge. The magnitude of the light corresponds to a certain charge magnitude which corresponds to a colour displayed on the user interface.

A partial discharge does not send out much light. Because of this, other light sources such as outdoor sun-light, houselights etc. will make it difficult for the camera to detect the light emitted from the electrons in the silicone rubber sample during partial discharges unless the environment is completely dark. In order to minimize external light sources interfering with this, all experiments were done in a dark room (the lights in the room were turned off). In addition, the test object was covered in a black curtain as indicated in Figure: 4.6.

As was done in the pre-study; When capturing photos, the shutter time of the camera was set to 12 seconds. This was done to make sure enough light was exposed to the lens in the CCD camera in order to get a good enough picture. When conducting experiments the photos were captured using a ”stream” function, capturing pictures every 12th seconds for a given time period (or for a given number of pictures).

When the stream acquisition is started simultaneously with the Omicron MP600 system, it is possible to relate the occurring partial discharge for each 12 seconds with its related picture.

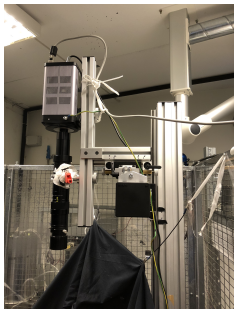

(a) CCD camera

(b) Open curtain

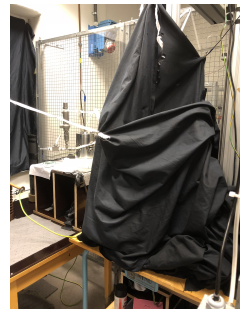

(c) Closed curtain

Figure 4.6: Pictures indicating camera and how the curtain is covered around the test object

4.3.1 MetaMorph software

The software used to control the camera is the MetaMorph software. It provides numbers of different ways to capture and manipulate the given picture and to change the CCD camera settings. This is also where the shutter time is set. When a picture or stream is acquired it is possible to view in different ways. This theses will focus on the pictures taken in monochrome light and pseudo-color light. Monochrome presents pictures using black and white colours while pseudo-color uses the entire colour spectre where red is high intensity light emitted and blue is low intensity light emitted. Figure: 4.7 indicates the same picture of an electrical tree displayed in both monochrome and pseudo-colour light. These pictures are from the pre-study. [3]

(a) Monochrome light.

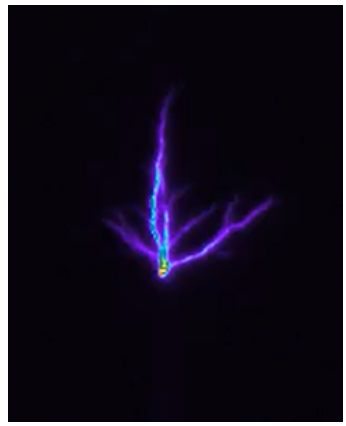

(b) Pseud-colour light

Figure 4.7: Same picture of an electrical tree displayed using monochrome- and pseudo-colour light

4.4 COMSOL Multiphysics model

Two COMSOL Multiphysics models have been created; one silicone rubber model without the pre-made cavity and one model including the pre-made cavity. The model without the cavity is created to have a reference to how much the electrical field will change by introducing the cavity. COMSOL Multiphysics is a FEM tool; finite element method. A finite element method divides the figure in a grid with a given number of nodes. When simulating, calculations are done at each node.

How the models have been created is presented in the two next subsections. Both models have been made using a 2D-axisymmetric model with stationary electrostatics. A 2D-axisymmetric simulation is drawn in 2D, but given the axisymmetry, it is modeled as a 3D figure with corresponding results. This shortens down the simulation period and makes the mesh (number of nodes) more accurate. A relative permittivity of 2.3 has been used for the silicone rubber, while the built in characteristics material data have been used for the electrodes (aluminum) and cavity(air).

4.4.1 Model without cavity

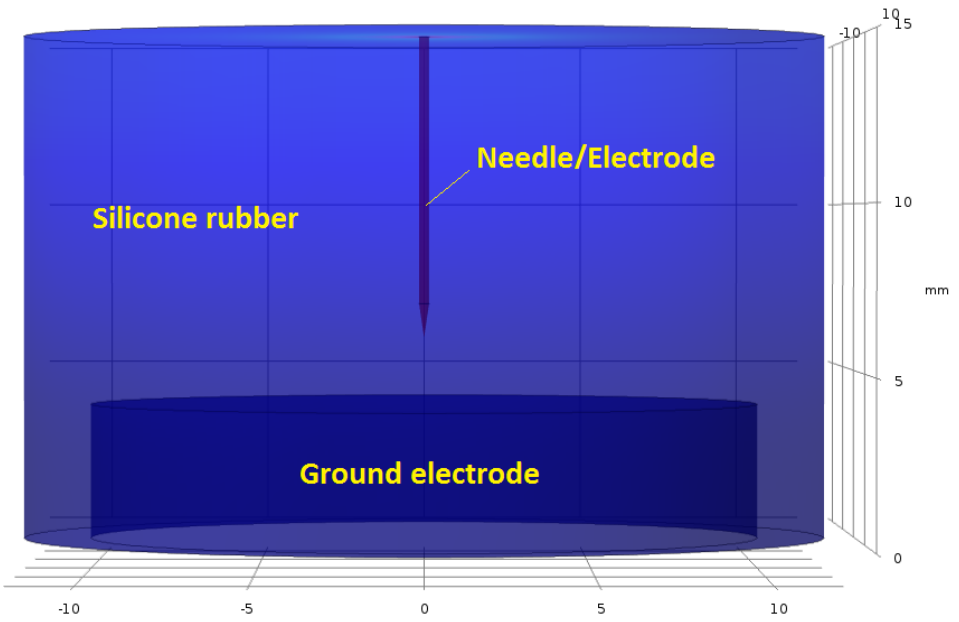

Figure 4.8: 3D-view of silicone rubber sample without cavity

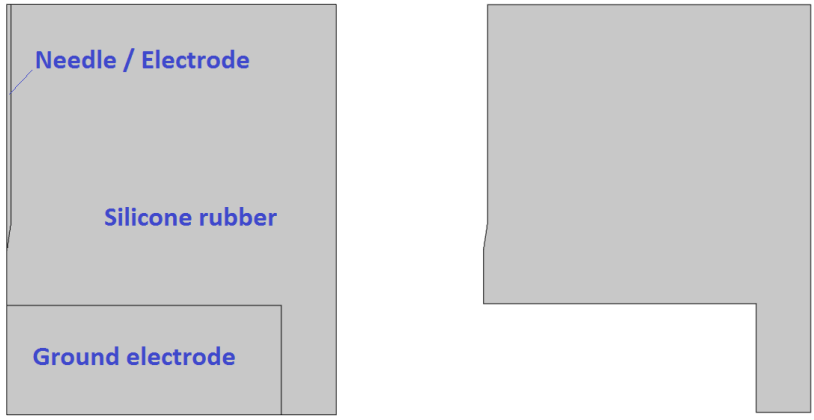

(a) 2D-view before partition. **(b)** 2D-view after partition.

Figure 4.9: 2D-view of silicone rubber sample without cavity

Figure: 4.9 illustrates how the silicone rubber sample is modeled in 2D. As can be seen, only half of the silicone rubber sample is drawn due to the axial symmetry. To increase the mesh accuracy further, both the ground electrode and the high voltage electrode (needle) have been cut out from the drawing, replaced by boundary conditions as indicated in Figure: 4.10.

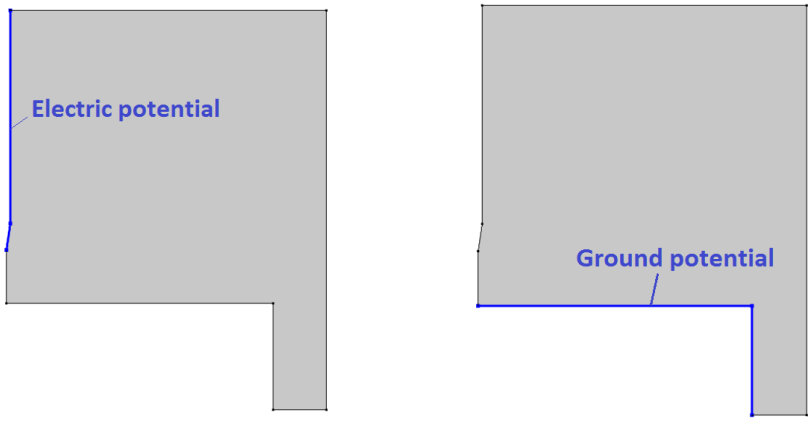

(a) Indication of placement of electrical potential. **(b)** Indication of ground potential.

Figure 4.10: Electrostatic placements on 2D-model without cavity.

4.4.2 Model with cavity

A COMSOL Multiphysics model of the geometry has been made in order to study the electrical field inside the cavity. By doing so it is possible to calculate a theoretical value of the number of electrons in an avalanche and therefore also determine if number of electrons is critical.

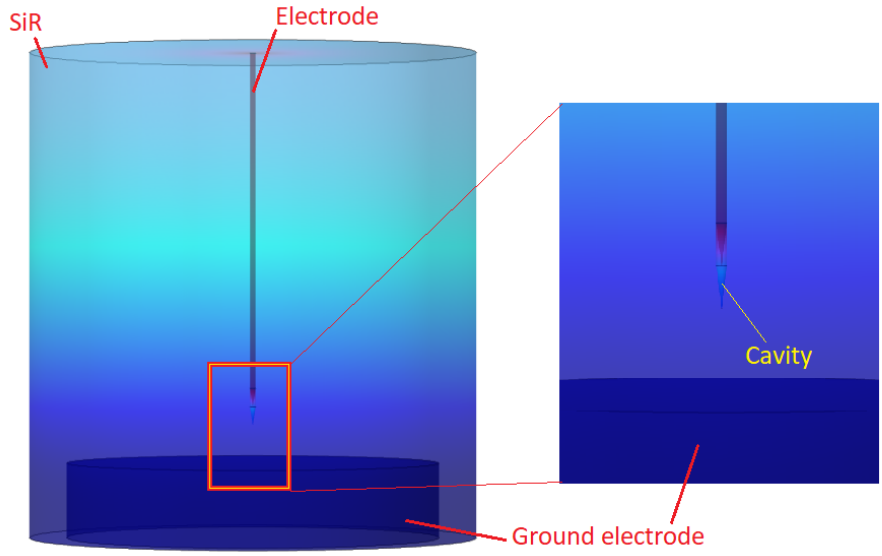

Figure 4.11: 3D-view of COMSOL modeled silicone rubber sample with pre-made cavity.

Figure: 4.11 gives a 3D-view of the COMSOL model for the reader to better understand the nature and shape of the silicone rubber sample model. The result have been studied using the 2D as shown in Figure: 4.12.

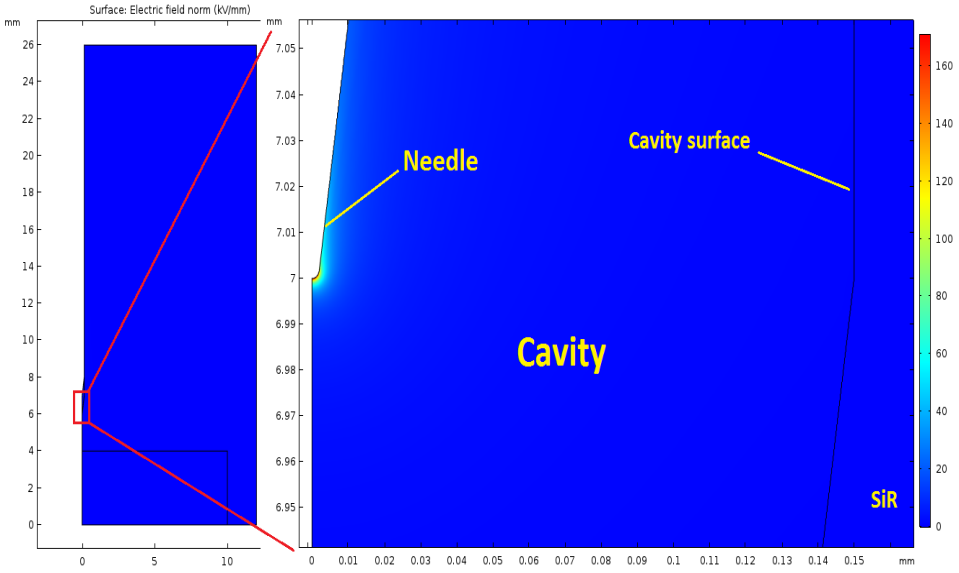

Figure 4.12: 2D-view of model with cavity.

4.5 Finding testing procedure

Testing of silicone rubber samples with a pre-made cavity had never been done before. How the partial discharges would deteriorate the surface wall of the cavity was uncertain; it was not known for how long and what voltage level needed to be applied in order to produce electrical treeing in the samples. To be able to determine the right test procedure, pre-testings had to be conducted.

4.5.1 First testing unsaturated sample

One silicone rubber sample was tested. No test procedure was established at this stage as it was not certain what would happen. It was seen from the Omicron MP600 software that partial discharges happened momentarily after reaching 2 kV. The partial discharges magnitude was in the order of 150 pC for some time and later dropped to about 100 pC. As can be seen from Figure: 4.13 the partial discharge was most stable at 6 kV. The voltage was gradually increased for 25 minutes until reaching 9-10 kV. An electrical tree begun growing while the partial discharge magnitude increased some. It was also observed that the number of partial discharges increased rapidly with increasing voltage (as expected), but the discharge magnitude remained unchanged.

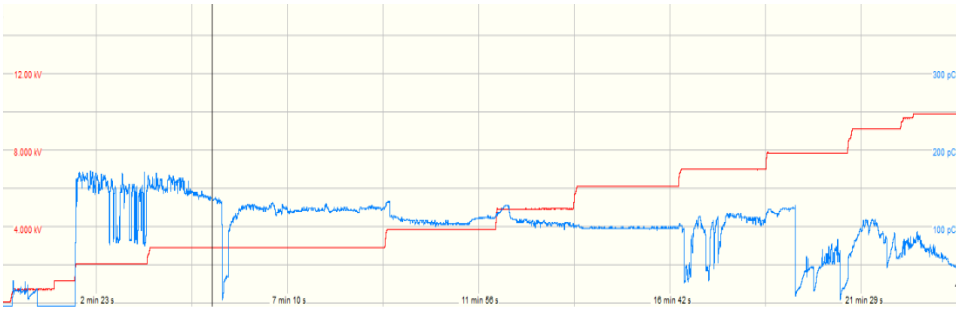

Figure 4.13: First testing unsaturated sample.

From this results, a testing procedure was formed:

1. Start recording of Omicron MP600 and photo-stream from CCD camera simultaneously.
    - Select suitable names of files and storage place before starting.
2. Turn voltage level up to 6 kV.
    - Keep at 6 kV until electrical tree is observed to grow one third of the distance to ground electrode.
3. Turn down voltage level before turning the variac off.
4. Stop recording of Omicron and CCD camera.

4.5.2 Second testing unsaturated sample

With the test procedure established above, a sample was tested. The partial discharge results are given in Figure: 4.14.

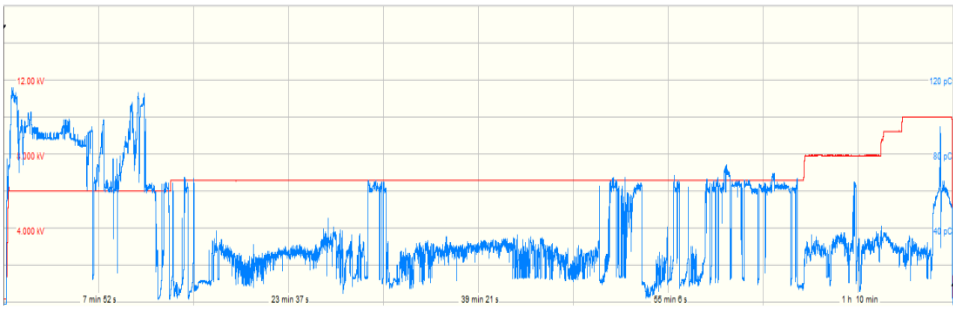

Figure 4.14: Second testing unsaturated sample.

As in the first testing, the partial discharge immediately raised to 100 pC. Different from the first test is the drop in discharge magnitude. After reaching 100 pC, the magnitude decreases to 40 pC with some random spikes, for the same voltage level. This would mean that the total energy dissipated in the void is quickly reduced while the time to make an electrical tree is increased. As can be seen in Figure: 4.14 the voltage is increased at the end. Before increasing the voltage, no electrical tree was observed. Using the sample to map when the tree would initiate the voltage level was increased. As a result, the electrical tree was detected when the voltage level was about 10 kV.

It was decided to change the test procedure voltage level to 8 kV as this would increase the energy released in the void.

4.5.3 Third testing unsaturated samples

The second test procedure was conducted on a total of three unsaturated silicone rubber samples. The results are given in the Figures:

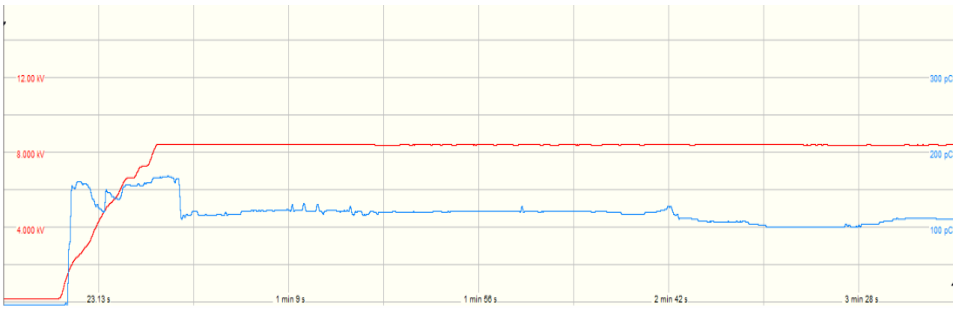

Figure 4.15: Third test 1

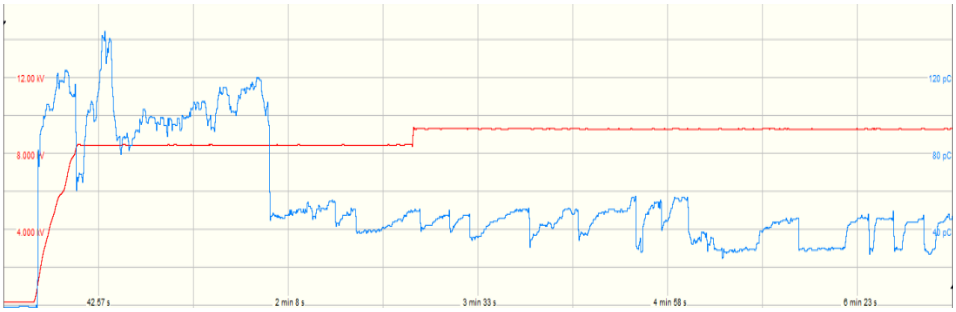

Figure 4.16: Third test 2

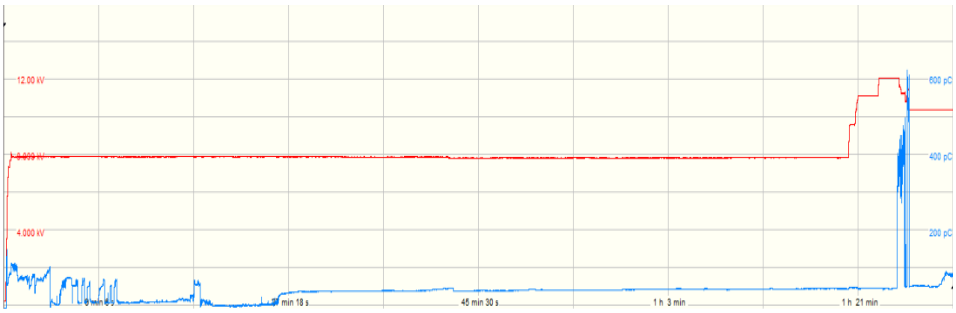

Figure 4.17: Third test 3

As observed in the two previous samples, the partial discharge magnitude quickly rises to 100 pC + before decreasing again. In addition to the partial discharge behaviour, the photo stream taken by the CCD camera was examined. It was found that different light events could occur early in the process, while raising the voltage.

A new test procedure was found, and its also the one used and discussed in the Results and Discussion chapter:

Step-test

1. Start recording of Omicron MP600 and photo-stream from CCD camera simultaneously.
    - Select suitable names of files and storage place before starting.
    - A limitation when acquiring a photo stream is the number of photos needed. If the test period is expected to last for several hours and the shutter time of the CCD camera is low, an external hard disk should be used as it demands much memory from the computer.
    - A shutter time of 12 seconds gives one picture each twelfth second. A test lasting for six hours would need the photo-stream to last 1800 pictures.
2. Turn voltage level to 2 kV.
    - Increase the voltage level by 1 kV / 30 min.
    - Keep increasing until an electrical tree has grown for 1 mm (half the distance from the cavity to the ground electrode).
3. Turn voltage level down.
4. If possible, let one more photo be acquired by the CCD camera before turning the recording of the OMICRON and photo-stream off.

Chapter 5

Results and discussion

5.1 Noise measurement of platform

Two noise tests were performed on the setup; one noise test before conducting tests, and one after. The noise test was run with the platform connected to high voltage, but without the silicone rubber sample, as indicated in Figure: 5.1

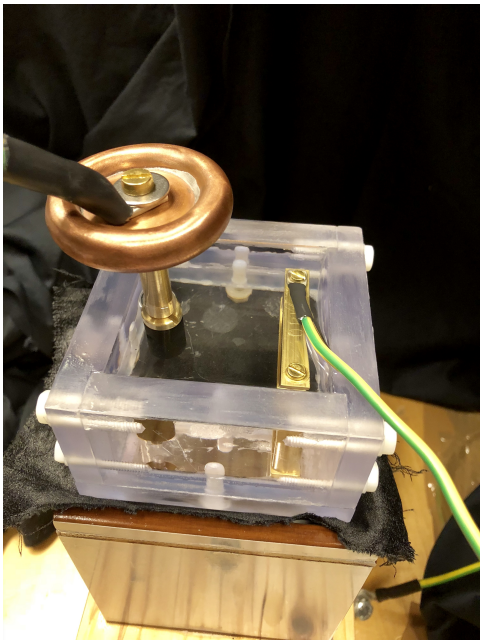

Figure 5.1: Platform connected to high voltage during noise test.

5.1.1 First noise test - conducted before testing

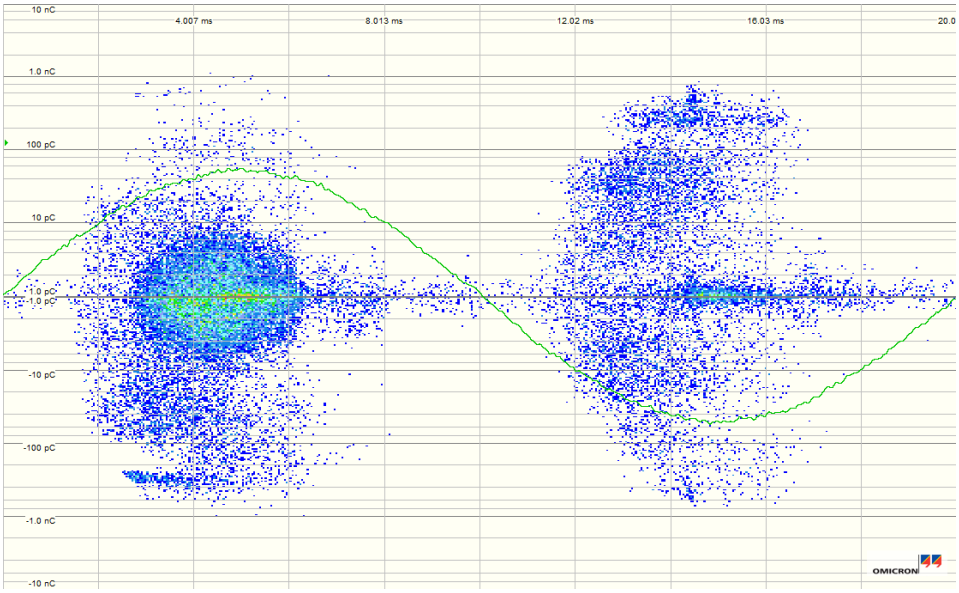

Figure 5.2: First noise test Omicron MP600 discharge pattern.

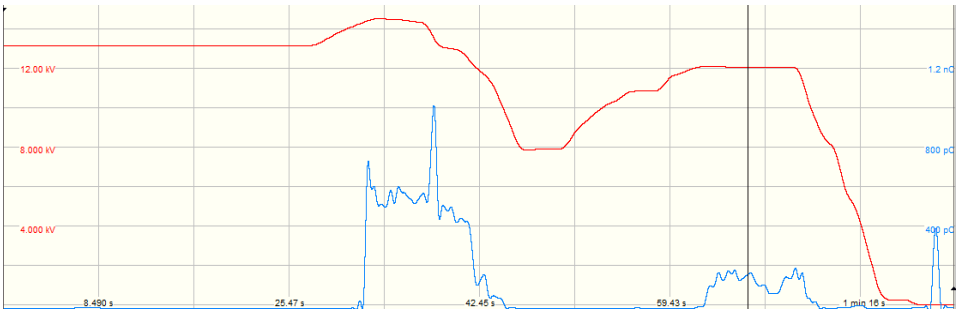

Figure 5.3: First test Omicron MP600 voltage and partial discharge curves.

5.1.2 Second noise test - conducted after testing

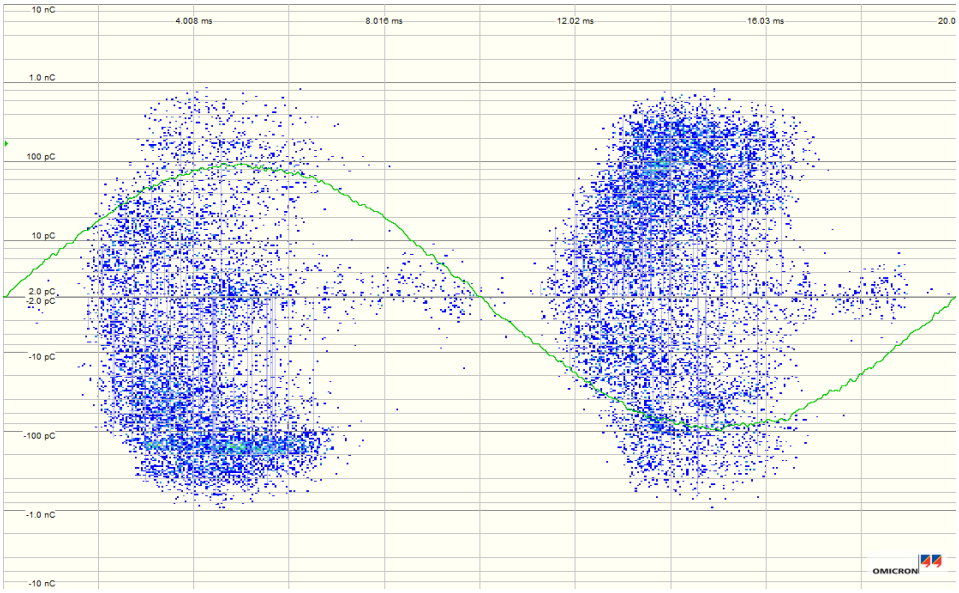

Figure 5.4: Second noise test Omicron MP600 discharge pattern.

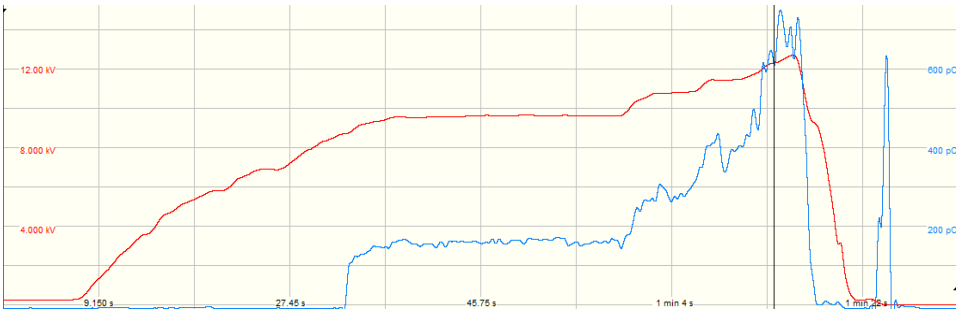

Figure 5.5: Second test Omicron MP600 voltage and partial discharge curves.

5.1.3 Noise band at 12 kV

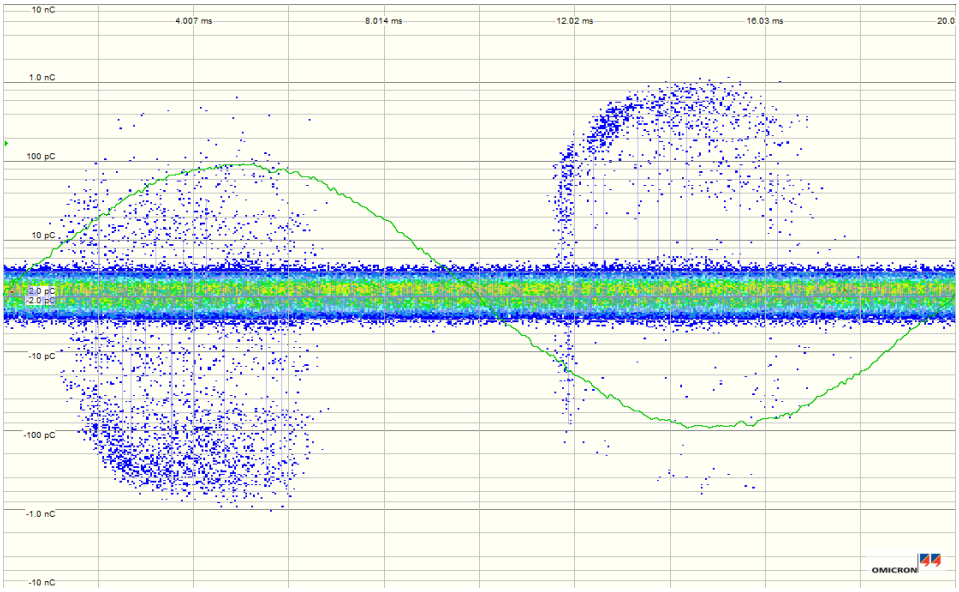

Figure 5.6: Noise band occurring around 12kV.

5.1.4 Noise tests comparison

As can be seen in Figure: 5.2 and 5.3 it looks like there are void discharges occurring some place in the setup. Multiple trouble-shootings were conducted both with and without supervisor, but the source of partial discharges was not to be found. It was concluded that the source of the discharges could come from other units in the circuit, e.g the transformer. At that time these parts could not be tested.

Figure: 5.3 gives an indication of the applied voltage and when the partial discharges occurred during the first noise test. As can be seen, the discharges did not occur before some time after reaching 12 kV. At the time, considering not being able to locate the cavity, it was considered acceptable to start testing. Starting the step test at 2 kV, electrical tree was thought to appear before reaching 12 kV. The small radius tip gives a high field, leading to partial discharges almost immediately after turning on the voltage - starting deteriorating the cavity surface.

The second noise test was performed just after test measurements of the samples was conducted. The discharge pattern remains the same as it did before testing, but as can be seen in Figure: 5.5 the discharges occurred at a lower voltage level. It is not clear why this happens, but given the variation in voltage level, this must be considered when interpreting the data from the sample measurements.

When the voltage reached a value greater than 12 kV, a noise band reaching from $\pm$ 10 pC appeared. The reason for this was not found, though it might be caused by another unit connected in the circuit or the grid. Figure: 5.6 illustrates this noise band.

5.2 COMSOL results. Electrical field at needle tip and cavity surface

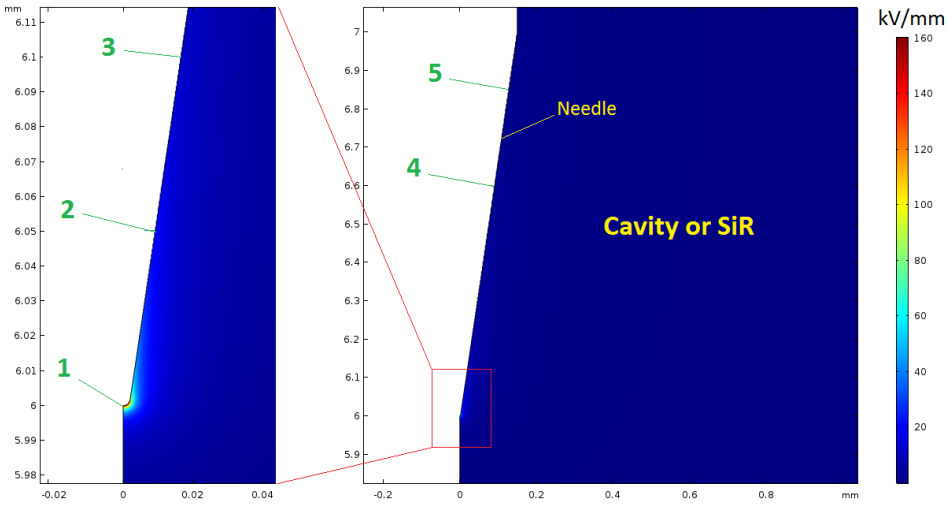

Figure 5.7: Points at where electrical field is measured in COMSOL.

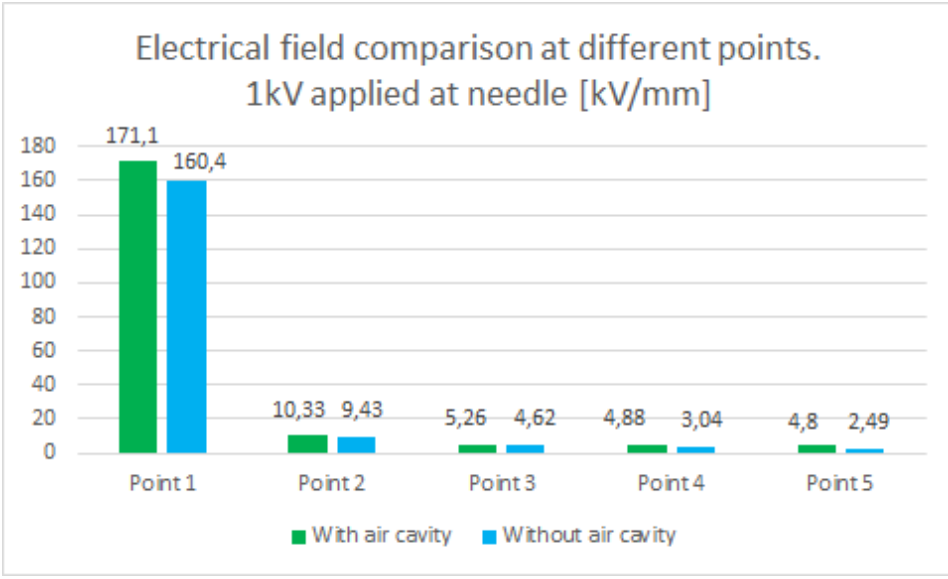

Figure 5.8: Electrical field at points indicated in Figure 5.7 for model with and without air cavity.

As can be seen from the results, the electrical field is high at the needle-tip compared with the rest of the needle. It can also be seen that the electrical field at point 5, further up the needle, is almost 5 kV/mm for the sample with an air cavity. This is higher than the dielectric strength of air, making partial discharges possible.

5.3 Samples

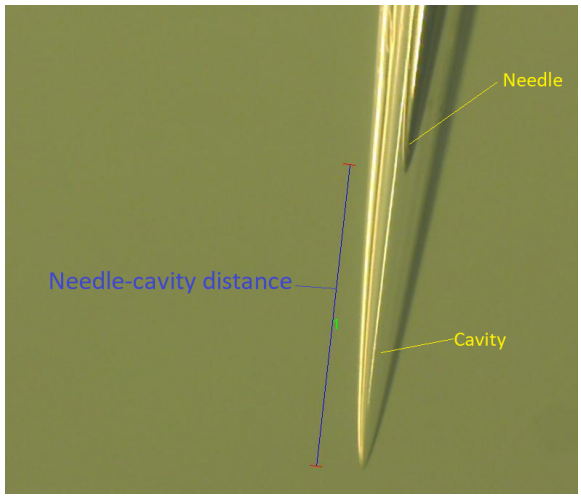

Figure 5.9: Microscope view of needle and cavity.

Figure: 5.9 shows how the measurements of the distance between needle tip and cavity tip was done. Before conducting high voltage testing, this distance was measured using a digital microscope. Figure: 5.10 shows how the CCD camera images of the needle and the cavity is presented on the computer screen.

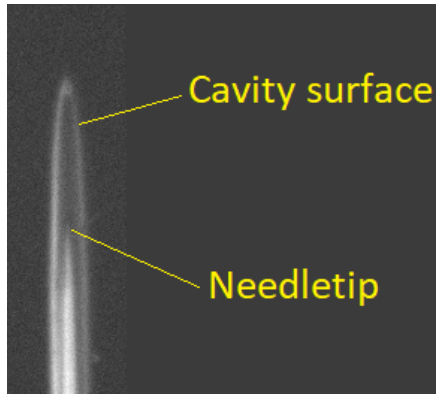

Figure 5.10: Needle and cavity as seen by the CCD camera.

5.3.1 Test samples

Samples containing a pre-made crack

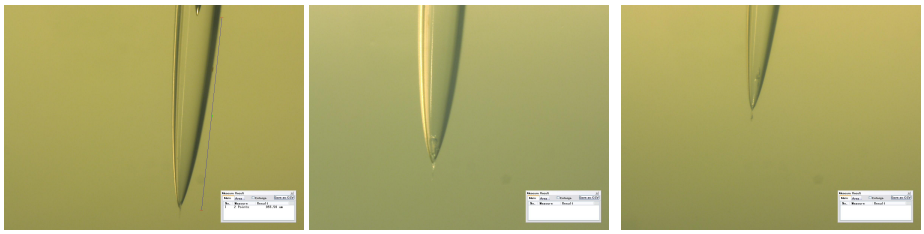

(a) Sample 1 **(b)** Sample 2 **(c)** Sample 3

Figure 5.11: Samples containing a pre-made crack

Samples without cracks

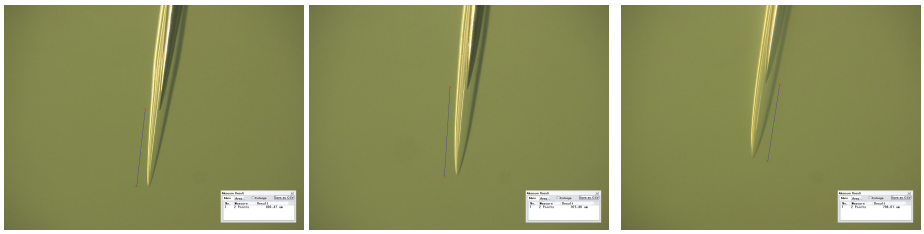

(a) Sample 4 **(b)** Sample 5 **(c)** Sample 6

Figure 5.12: Samples without pre-made cracks

Table 5.1: Needle tip radius and needle-cavity distance.

#Sample	Needle tip radius[μm]	Needle-cavity distance[μm]
1	2,35	955
2	2,01	1033
3	1,79	1012
4	1,76	803
5	2,38	915
6	1,99	797

5.3.2 Events observed during measurements

For all three samples with cracks (sample 1,2 and 3), four different events was observed. The samples without a crack, did not have a tree-initiation or a visible tree-growth. Only three of these events where seen for these samples during experiments and processing of data.

1. Light in whole cavity.
    - During partial discharge measurements, partial discharges ”filled” the complete cavity with light.
2. Light at needle tip.
    - Light at the needle tip was the event seen most during measurements for every sample. Just at the tip of the needle, light was observed in a cluster ball. The light occurred around the needle tip and seemed to vary in intensity with the number of partial discharges occurring.
3. Light alongside needle.
    - Discharges occurring further up the needle, between the needle and the isolation, could be observed multiple times. The photons emitted from this area did not appear as bright as the partial discharges occurring at the needle tip, but they were still possible to detect.
4. Electric tree growth.
    - This observation was made for the samples with pre-made crack only. Immediately after turning voltage on, partial discharges were detected; Void discharges was observed for some time by the Omicron MP600 system. If looking closely at the interface between air and insulation at this instant, small tubular channels could be observed on the pictures. This was interpreted to be an electric tree initiation. With increasing voltage and increasing deterioration at the crack point, electrical tree-growth could be observed.

Figures with belonging Omicron MP600 partial discharge measurements are given in section 5.5 on page 72 and in Appendix: C.

5.4 Voltage-time event graphs

Following is an illustration of when the events occurred as seen visually on the CCD camera stream. It must be taken into consideration that events might occur on the backside of the needle; photons emitted from here would not hit the CCD camera lens.

The samples were tested in the order 1,6,2,3,4 and 5, but are presented in a chronological order here. A power outage occurring at Gløshaugen while testing sample 4 made the CCD camera shut down and the photo-stream was lost. Because of a computer error, the Omicron MP600 measurements belonging to sample 6 was lost as well. Having the CCD camera stream it was still possible to observe the occurring events for this sample.

5.4.1 Sample 1

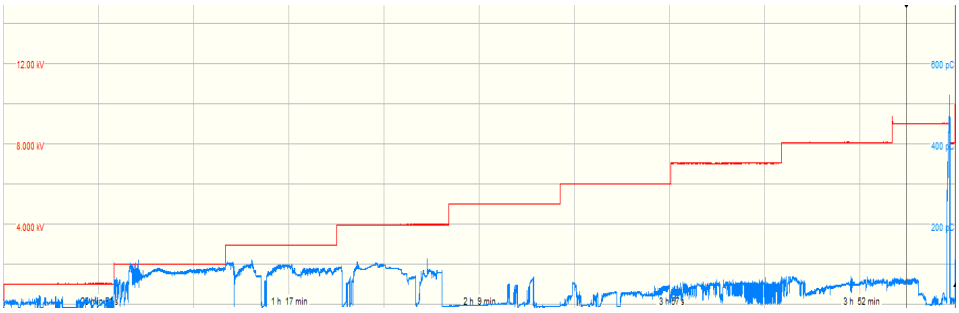

Figure 5.13: Sample 1. Omicron voltage and PD measurements.

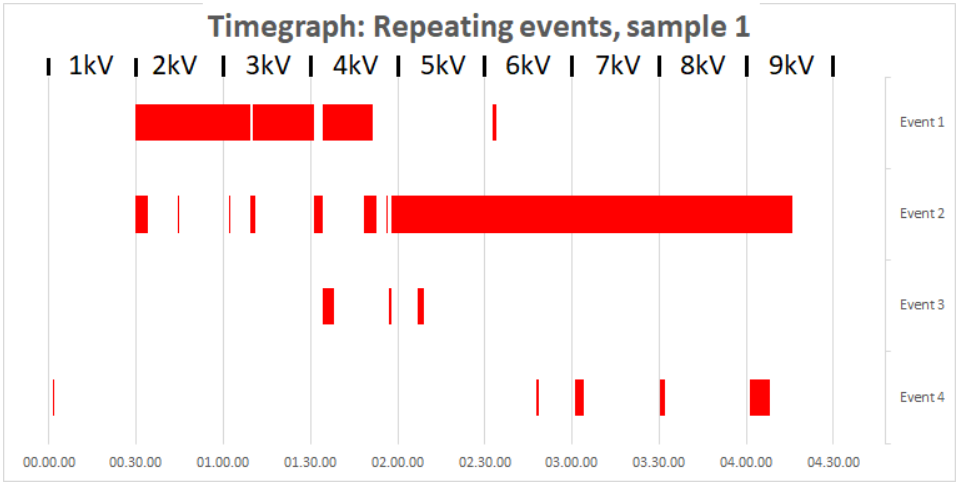

Figure 5.14: Repeating events time-graph: Sample 1

The experiments on the first sample were performed with a camera focus point that was not optimal. This was revealed later, when the focus point was improved. This means that the pictures for sample 1 have been hard to read an interpret.

As the figures illustrates, tree initiation is believed to be seen very early in the process followed by some light in the whole cavity and intervals of light emitted from the needle-tip. Light emission from the needle-tip appeared on and off up until reaching 5 kV before being present for the rest of the measurement. The light emitted from the tip increased as the voltage increased. As explained in the theory chapter, partial discharges increases in numbers when increasing the voltage level. This correlates to the visual observation made with more intense light emitted when increasing the voltage; more ionization collisions occurs due to the higher voltage.

It was possible to see the electrical tree growth, but due to a limitation on the CCD camera stream at the time, the experiment ended before further growth could be seen.

5.4.2 Sample 2

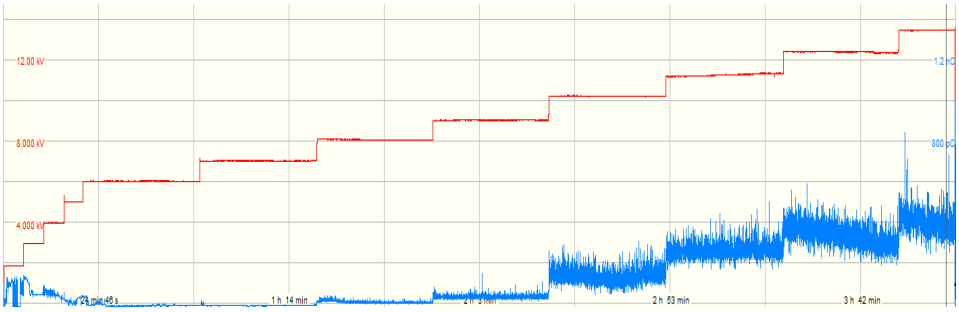

Figure 5.15: Sample 2. Omicron voltage and PD measurements.

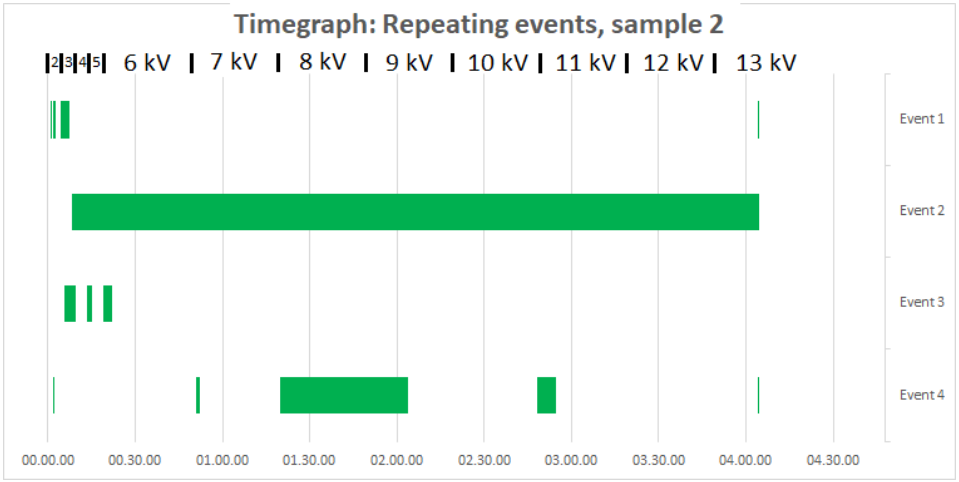

Figure 5.16: Repeating events time-graph: Sample 2

After testing sample 1 and 6 (one with a pre-made crack and one without), it was clear that a higher voltage level was needed in order obtain electrical tree growth. The testing procedure was therefore cut in steps of 5 minutes from 2 to 6 kV. Starting from 2 kV the voltage was increased 1kV/5min to 6 kV. When reaching 6 kV the test procedure was followed as normal.

As can be seen from Figures: 5.15 and 5.16 the electrical tree was believed to be initiated early on. All three events occurred at voltages below 5 kV. Light emitted from the needle-tip lasted throughout the measurement period once it had occurred.

This sample was pushed to electrical breakdown which occurred at 13 kV. The electrical tree had been observed to grow further around 8 and 10 kV, but not having much carbon

makes the channels less conductive; more voltage, or deteriorating time, is needed to further grow the tree. Once the breakdown phase had initiated, it happened in less than 12 seconds. This made it impossible to act for the voltage operator. One picture was obtained before breakdown. At this picture, intense light from the cavity, needle-tip and electrical tree could be observed.

5.4.3 Sample 3

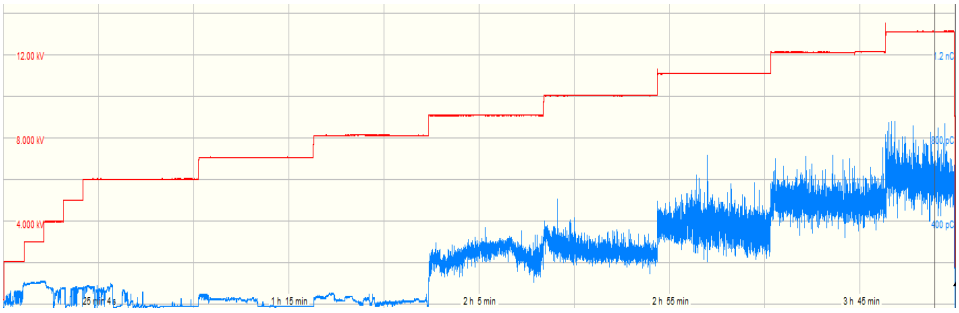

Figure 5.17: Sample 3. Omicron voltage and PD measurements.

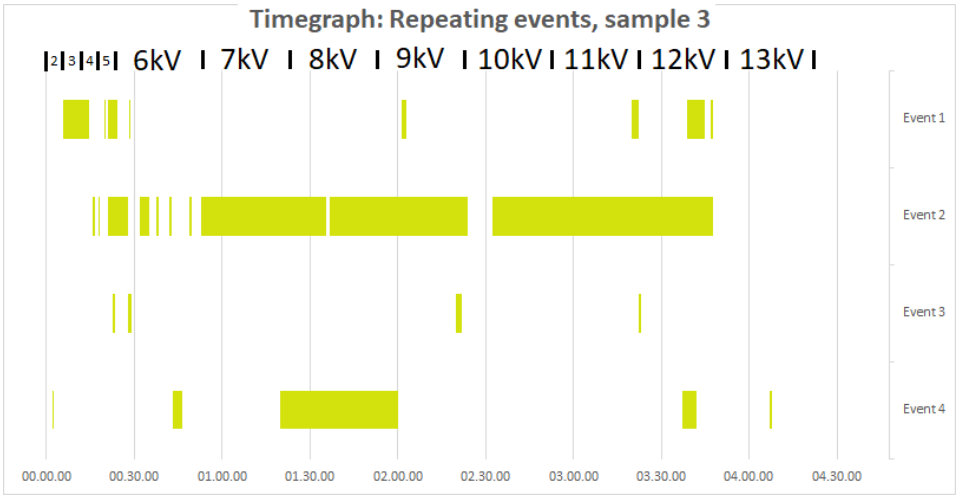

Figure 5.18: Repeating events time-graph: Sample 3

From Figures: 5.17 and 5.18 it can be seen that light in the whole cavity is observed to happen early on, but then only appears after some time. Light emitted from the needle-tip can be seen almost throughout the experiment. As in sample 1 and 2, the electrical tree appears to be initiated early followed by a demand of higher voltage in order to grow further. The experiment was terminated once the tree started growing again at 13 kV to prevent electrical breakdown.

5.4.4 Sample 5

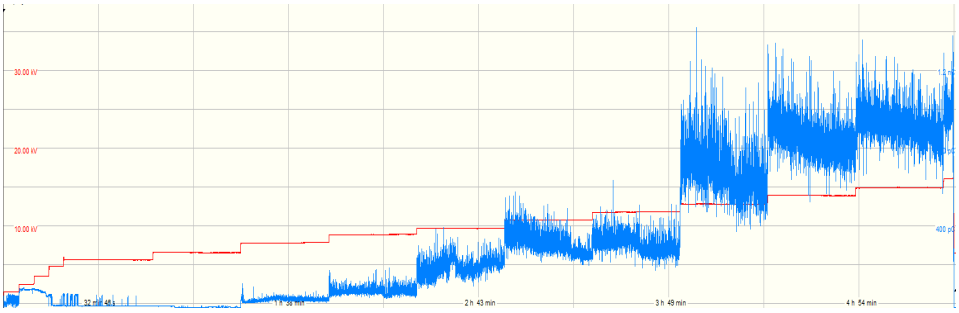

Figure 5.19: Sample 5. Omicron voltage and PD measurements.

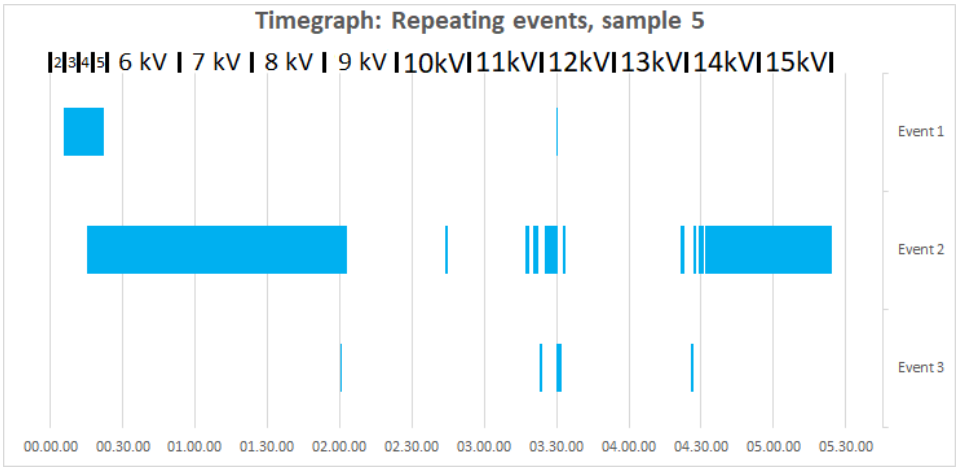

Figure 5.20: Repeating events time-graph: Sample 5

Not having a pre-made crack makes it harder to produce an electrical tree as the void does not contain any field enhancement points. These points must be made from deteriorating the cavity surface by partial discharge. An electrical tree initiation or growth was not seen throughout the experiment. The light pattern was resembling that of the other samples.

5.4.5 Sample 6

Because of a computer error, the Omicron MP600 measurements to sample 6 was lost, and can therefore not be examined. The time-based graphs for the repeated events could be examined as the CCD-camera stream was in tact.

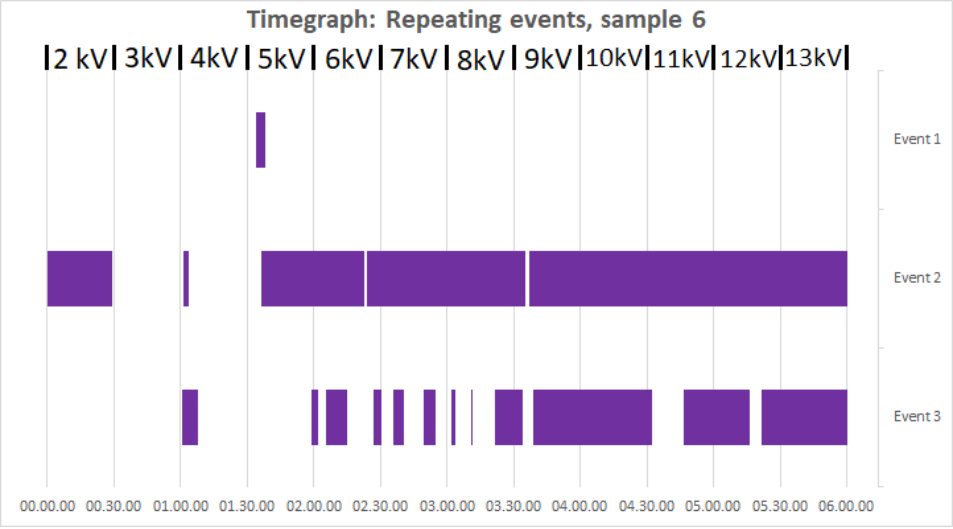

Figure 5.21: Repeating events time-graph: Sample 6

Sample 1 and 6 were tested using the same procedure (same increase in voltage vs time). Having no pre-made crack the only events to be observed was light emitted in the whole cavity, needle-tip and alongside the needle. As in the previous samples, light emitted from the needle-tip was present almost the entire duration of the experiment.

The needle-tip is a sharp point making the electrical field is high in this area. This can be seen from the COMSOL solutions. This contributes to the great numbers of discharges, and explains why the light emitted here is present in all samples regardless of the pre-made crack or not.

5.5 Typical events

In the next sections, the typical events are illustrated by pictures obtained from the CCD camera and their belonging partial discharge measurements. Each picture taken represents 12 seconds as this is the exposure time of the camera. Each Omicron MP600 measurement represents the partial discharges occurring during these 12 seconds. For every sample the noise level is set to $\pm$ 1 pC, filtering out all the partial discharges happening in this interval.

Only pictures and PD plots for sample 2 are represented here as they are representative for the rest of the samples. Sample 1 and sample 6 were tested with a different focus point on the camera making them harder to interpret. At the time, this focus point was thought to be the best, but after finding the focus point while in a dark room, better pictures were obtained. The best pictures are hence for sample 2. In addition, the quality of the pictures tend to vary some, even with a good focus point. The data for the other three samples are attached in Appendix C.

As mentioned, a computer error erased the partial discharge pattern for sample 6 while a power outage occurring at Gløshaugen during measurements of sample 4 erased the pictures taken by the CCD camera.

5.5.1 Light in whole cavity

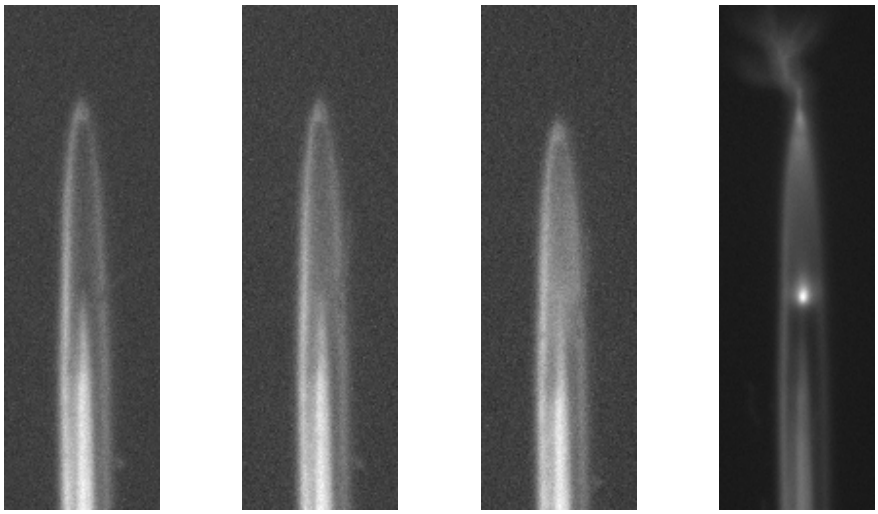

(a) <1kV **(b)** 2 kV **(c)** 3k V **(d)** 13 kV

Figure 5.22: (a) Reference picture: No PD occurring. (b)(c)(d) Different intensity of light occurring in the cavity: Sample 2

Figure: 5.22b with belonging partial discharge pattern. 2kV.

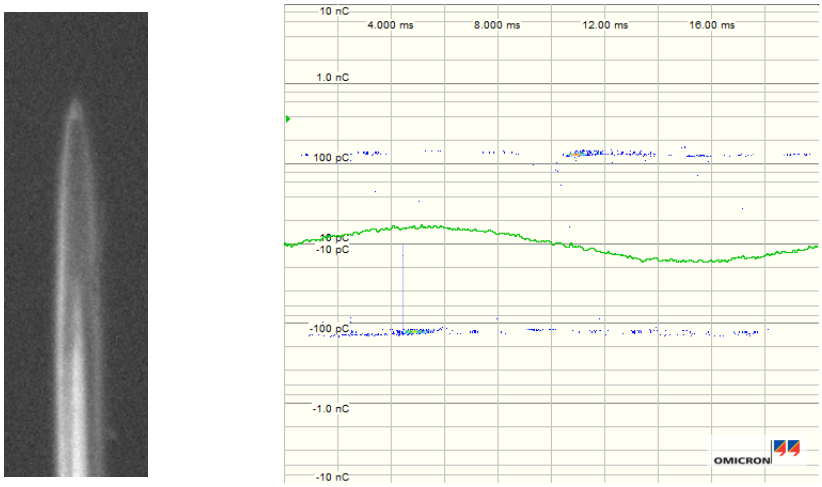

Figure 5.23: CCD-camera picture with belonging Omicron measurement for 12 seconds at 2 kV: Sample 2

Figure: 5.22c with belonging partial discharge pattern. 3kV.

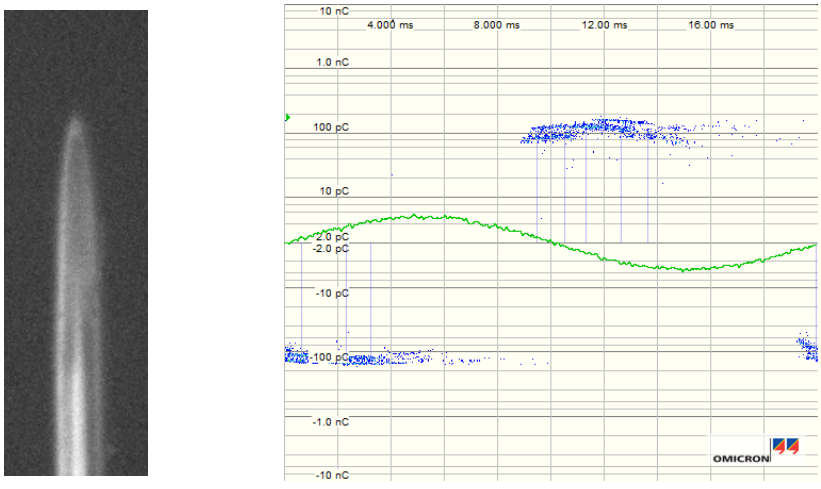

Figure 5.24: CCD-camera picture with belonging Omicron measurement for 12 seconds at 3 kV: Sample 2

Figure: 5.22d with belonging partial discharge pattern. 13 kV.

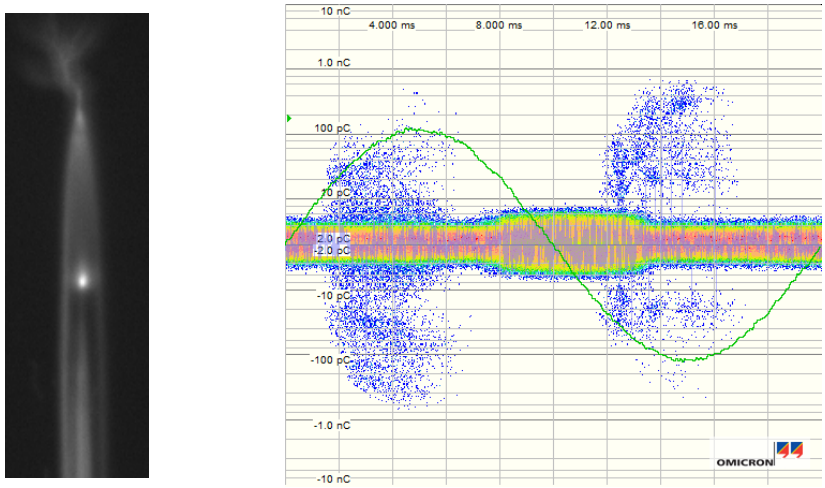

Figure 5.25: CCD-camera picture with belonging Omicron measurement for 12 seconds at 13 kV: Sample 2

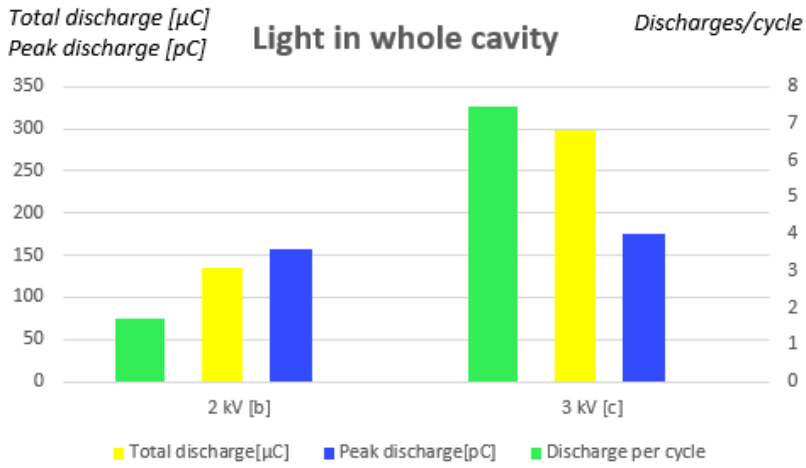

Figure 5.26: Bargraph: Total discharge, peak discharge and discharges/cycle for Event 1: Light in whole cavity.

Because of the noise level occurring at 13 kV it is impossible to calculate the total discharge, peak discharge and number of discharges per cycle for Figure: 5.25. A solution might have been to measure the noise level at the same voltage level and subtract the achieved values here from the test measurements. This has been difficult in this thesis as it requires the noise test to have a minimum of 12 seconds steps at each voltage level (should be exact in order to minimize the differences). As indicated in section 5.1.4 on page 58, the voltage at which the noise occurs varies, making it exposed to errors.

Figure: 5.23 shows the discharges occurring at 2kV for 12 seconds for sample 2. As the voltage is low, not many discharges occurs. The magnitude of each discharge is in the order of 100 pC, and the pattern is resembling to that of a cavity discharge. This is more visible in Figure: 5.24 where the voltage level has been increased to 3 kV. As expected, the increase of voltage increases the number of discharges. The light emitted during these 12 seconds at 3 kV is higher than that of the discharges occurring at 2 kV. This is also clear for Figure: 5.25, but the Omicron MP600 measurements are difficult to obtain.

When comparing these results with the other samples (Appendix C), resembling patterns can be seen for lower voltage levels. Once the voltage has reached a value higher than 3-4 kV the pattern changes. The magnitude of the partial discharges appears constant (pluss minus 10 pC) from $350°$-$60°$ and $150°$-$260°$, only varying some. It can be difficult to separate the cavity discharge pattern from other discharges occurring at the same time. This is shown in Figures: 5.27 and 5.28.

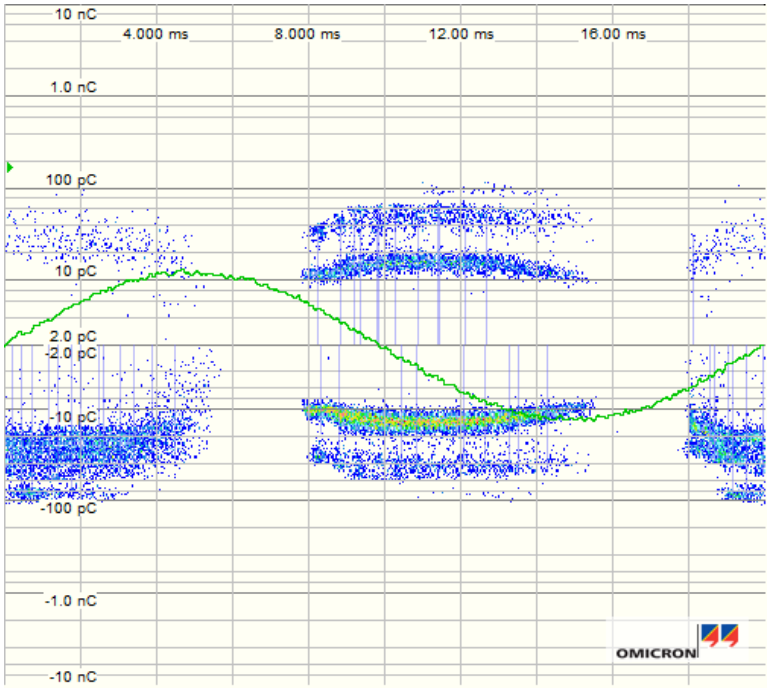

Figure 5.27: OMICRON measurements from sample 3 while light occurring in whole cavity at 6 kV.

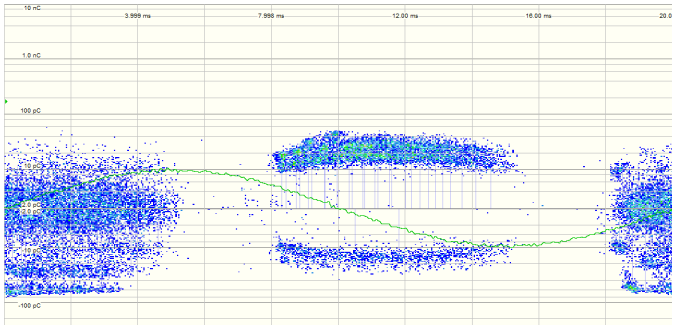

Figure 5.28: OMICRON measurements from sample 5 while light occurring in whole cavity at 5 kV

5.5.2 Light at needle-tip

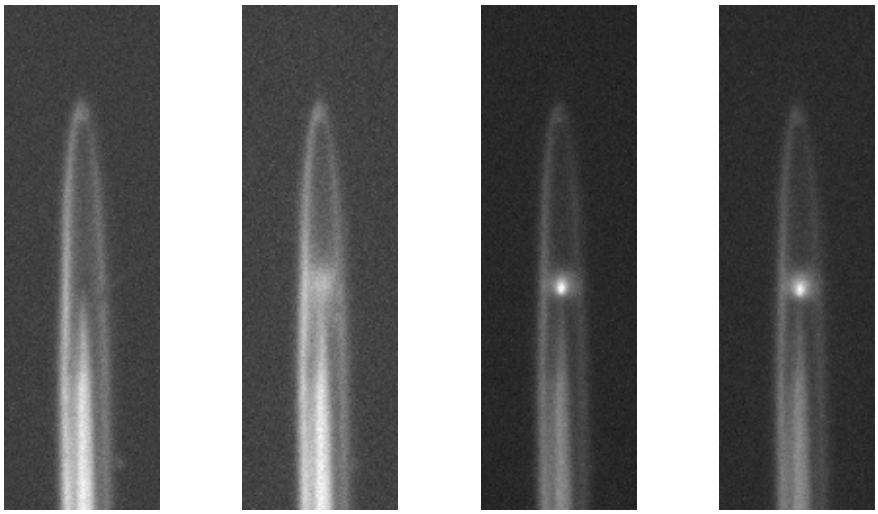

(a) <1kV **(b)** 4 kV **(c)** 6 kV **(d)** 7 kV

Figure 5.29: (a) Reference picture: No PD occurring. (b)(c)(d) Different intensity of light occurring at the needle-tip: Sample 2.

Figure: 5.29b with belonging partial discharge pattern. 4 kV.

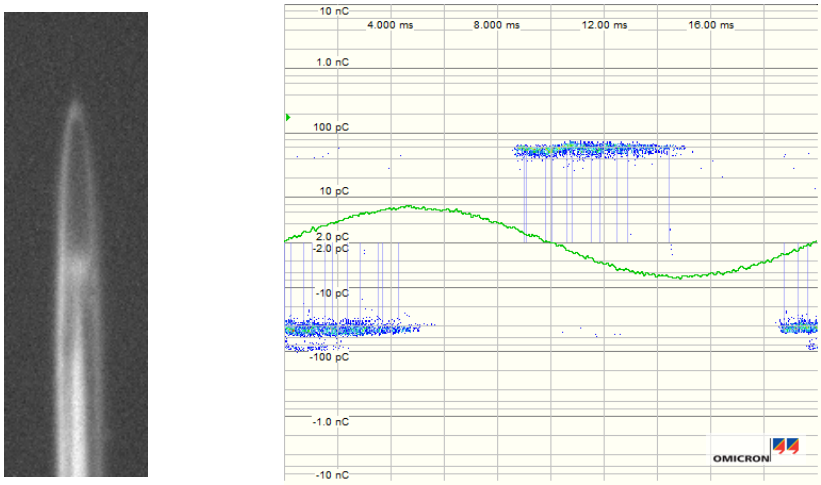

Figure 5.30: CCD-camera picture with belonging Omicron measurement for 12 seconds at 4 kV: Sample 2

Figure: 5.29c with belonging partial discharge pattern. 6 kV.

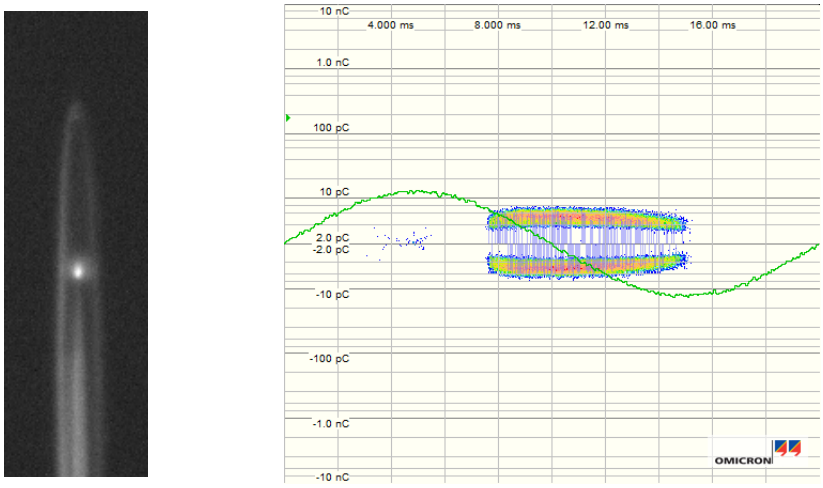

Figure 5.31: CCD-camera picture with belonging Omicron measurement for 12 seconds at 6 kV: Sample 2

Figure: 5.29d with belonging partial discharge pattern. 7 kV.

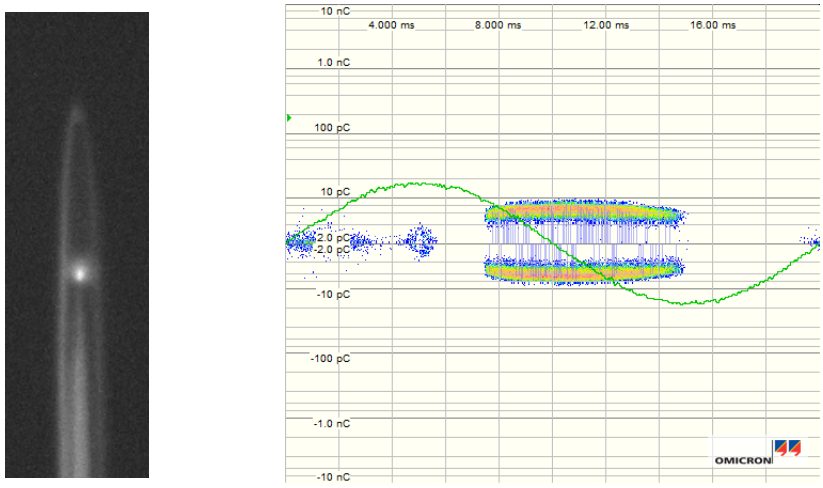

Figure 5.32: CCD-camera picture with belonging Omicron measurement for 12 seconds at 7 kV: Sample 2

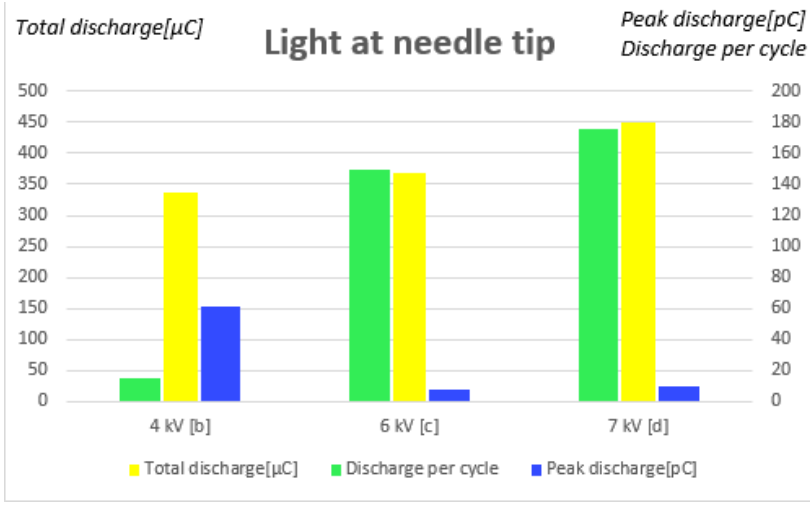

Figure 5.33: Bargraph: Total discharge, peak discharge and discharges/cycle for Event 2: Light at needle-tip. Sample 2

As can be seen from Figures: 5.29-5.33 the more energy dissipated in the cavity along with a high number of discharges, the more light is emitted. From the bar graph it can be seen that the peak magnitude of the partial discharges occurring at 4 kV is higher than the partial discharges happening at 6-and 7 kV, but the number of discharges/cycle increases with voltage. If an electron accelerated in the field at 6 and 7 kV has sufficient energy to ionize the molecules in the cavity, photons will be emitted from every electron collision. When the number of discharges is high, with sufficient energy, photons will be emitted regardless of the discharge magnitude.

Comparing with other samples given in the appendix, the results are the same; the higher energy dissipated in the cavity, the more light is emitted. As discussed previously, once the voltage level reaches higher than 3-4 kV the pattern changes.

5.5.3 Light alongside needle

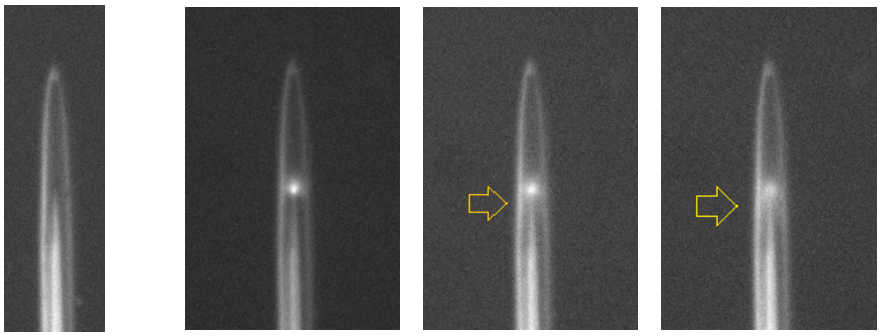

(a) <1 kV **(b)** 5 kV **(c)** 5 kV **(d)** 5 kV

Figure 5.34: (a) Reference picture: No PD occurring. (b) Picture taken before light alongside needle occurs. (c) Taken when light alongside occurs. (d) Taken during light alongside needle.

Figure: 5.34b with belonging partial discharge pattern. 5 kV. Before slot light occurs.

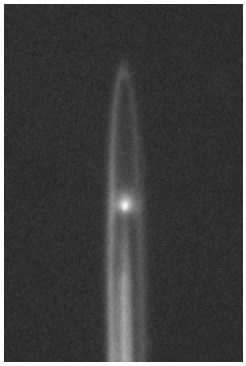

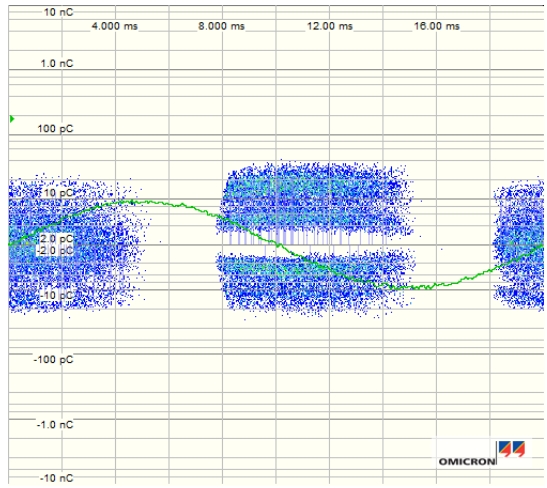

Figure 5.35: CCD-camera picture with belonging Omicron measurement for 12 seconds at 5 kV: Sample 2

Figure: 5.34c with belonging partial discharge pattern. 5 kV. Slot light occurs.

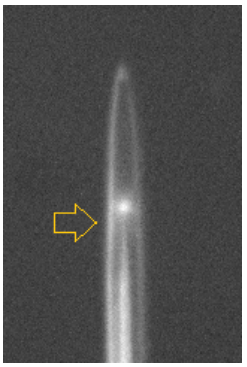

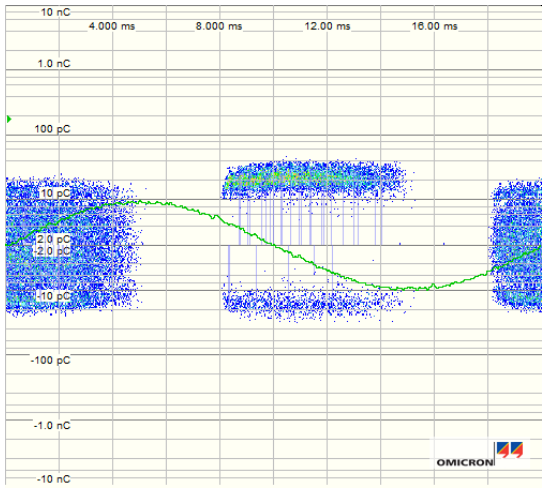

Figure 5.36: CCD-camera picture with belonging Omicron measurement for 12 seconds at 5 kV: Sample 2

Figure: 5.34d with belonging partial discharge pattern. 5 kV. During slot light.

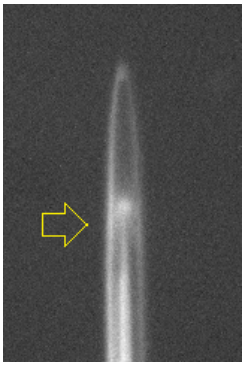

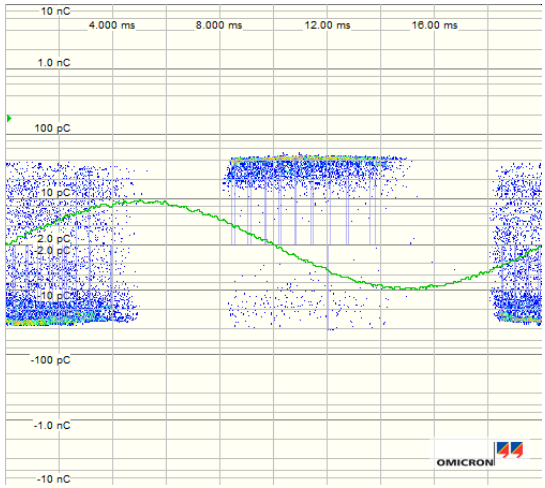

Figure 5.37: CCD-camera picture with belonging Omicron measurement for 12 seconds at 5 kV: Sample 2

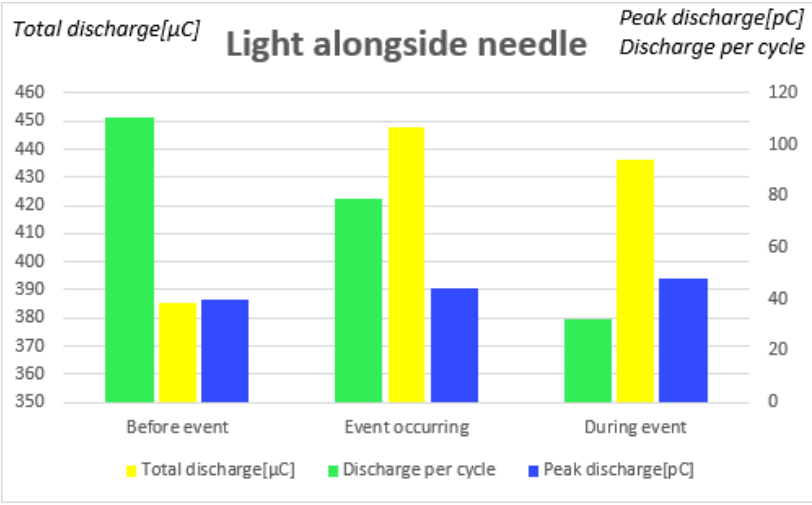

Figure 5.38: Bargraph: Total discharge, peak discharge and discharges/cycle for Event 3: Light alongside needle.

The detection of the light emitted from the side of the needle is difficult to present with just a few pictures, and best interpreted while looking at the camera stream obtained from the CCD camera. In this event the light is observed to be emitted alongside the needle going almost perpendicular out to the cavity surface wall.

Because of the difficulty in determining when this is happening it is difficult to discuss. From the samples it can be seen that the amount of energy dissipated in the cavity remains almost the same, but the number of discharges decreases and the peak magnitude increases. Fewer ionization collisions could mean fewer photons emitted. From some samples it can also be seen that the number of of negative discharges decreases as the event endures.

As calculated in the COMSOL Multiphysics calculations, partial discharges might occur at the beginning of the cavity, alongside the needle. As mentioned in the theory chapter, the dielectric strength for air is 3 kV/mm. The COMSOL calculations were done with 1 kV applied, and the electrical field at the beginning of the cavity was about 5 kV/mm. The applied voltage for Figures: 5.35-5.37 is 5 kV, making the field five times higher. Partial discharge in this area is therefore a possibility.

5.6 Tree growth

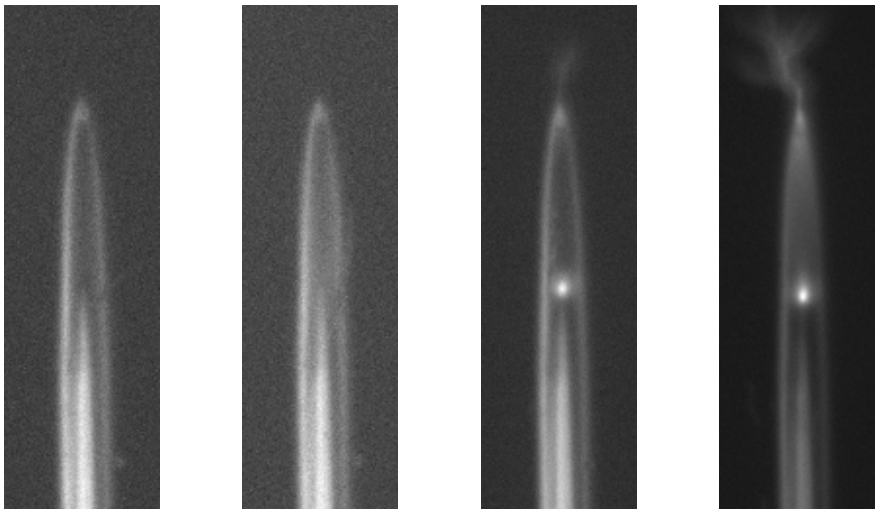

(a) <1 kV **(b)** 2 kV **(c)** 9 kV **(d)** 13 kV

Figure 5.39: (a) Reference picture: No PD occurring. (b)(c)(d) Different growth stages of the electrical tree.

Figure: 5.39b with belonging partial discharge pattern. 2 kV.

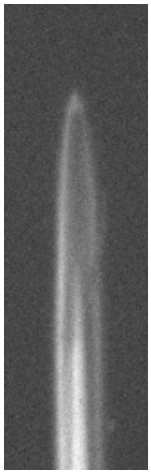

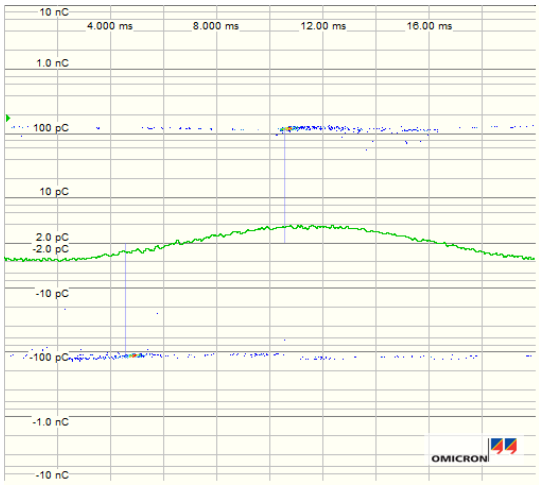

Figure 5.40: CCD-camera picture with belonging Omicron measurement for 12 seconds at 2 kV: Sample 2

Figure: 5.39c with belonging partial discharge pattern. 9 kV.

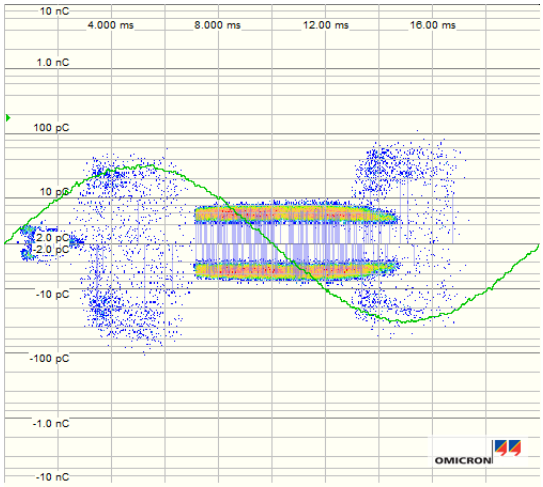

Figure 5.41: CCD-camera picture with belonging Omicron measurement for 12 seconds at 9 kV: Sample 2

Figure: 5.39d with belonging partial discharge pattern. 13 kV.

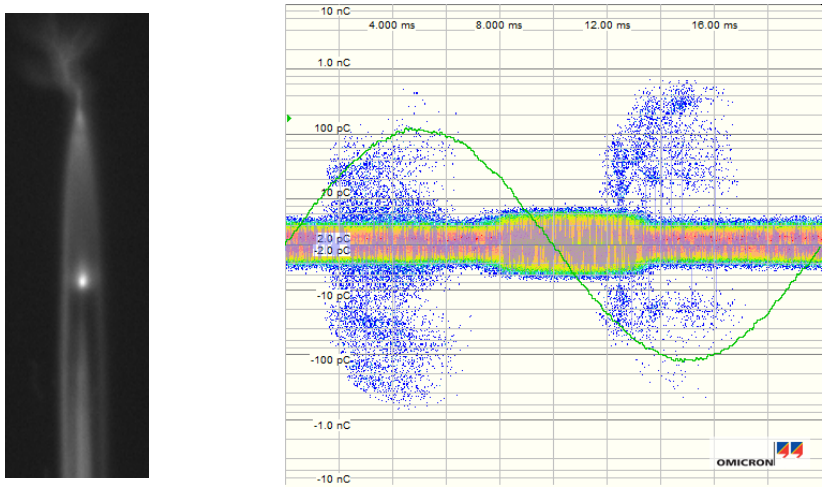

Figure 5.42: CCD-camera picture with belonging Omicron measurement for 12 seconds at 13 kV: Sample 2

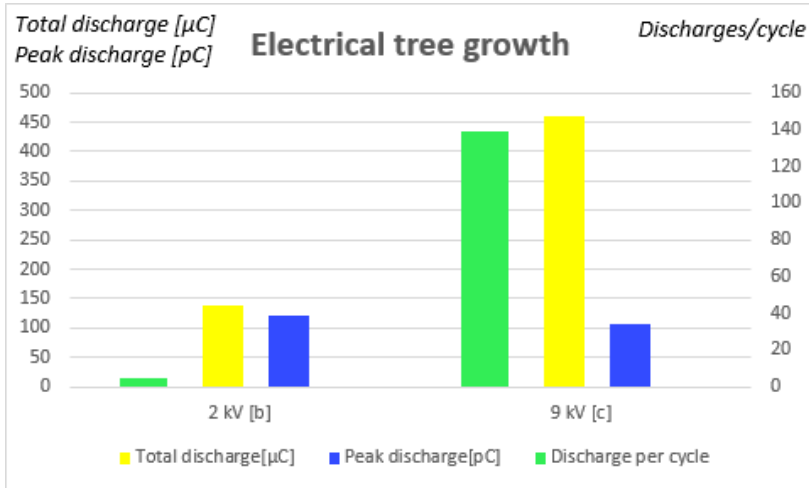

Figure 5.43: Bargraph: Total discharge, peak discharge and discharges/cycle for Event 4: Electrical tree growth.

As can be seen from Figures: 5.39-5.43 the electrical tree initiation is believed to happen early in the measurement process. Figure: 5.40 shows the discharge pattern for 12 seconds at 2 kV where the electrical tree is believed to be initiated. As with the other samples containing a crack, the discharge pattern is resembling to that of a cavity during the first 2 minutes. Once the tree is initiated, and since silicone rubber contains little carbon, a higher voltage level is demanded to increase the growth rate.

On figure: 5.41 it is possible to see further growth of the electrical tree. The voltage level is 9 kV making the dissipated energy that much higher. The Omicron MP600 discharge pattern shows the same constant magnitude ”band” as previously mentioned once above 3-4 kV. In addition, cavity discharges can be seen. It is likely that this is the discharges occurring in other parts of the electrical circuit as mentioned in the noise section on page 5.1.

No discharges can be seen in the whole cavity, making it likely that the discharges hits the cavity surface and travel along in the field direction accumulating at the tip end deteriorating here.

5.7 Cavities after testing

The samples were studied in a microscope after testing. The pictures are enlarges in the range of x 300-500.

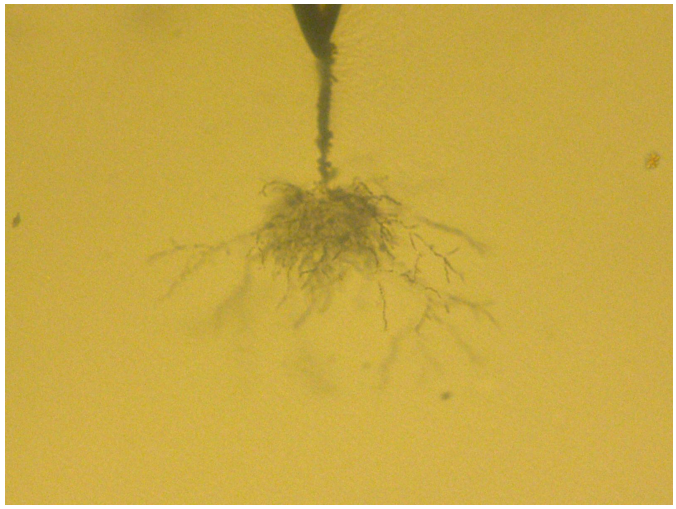

Figure 5.44: Electrical tree grown at the cavity tip in sample 1

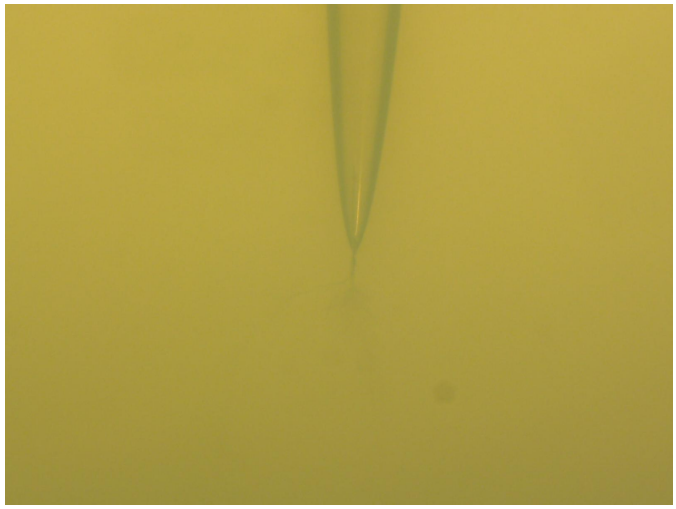

Figure 5.45: Electrical tree grown at the cavity tip in sample 3

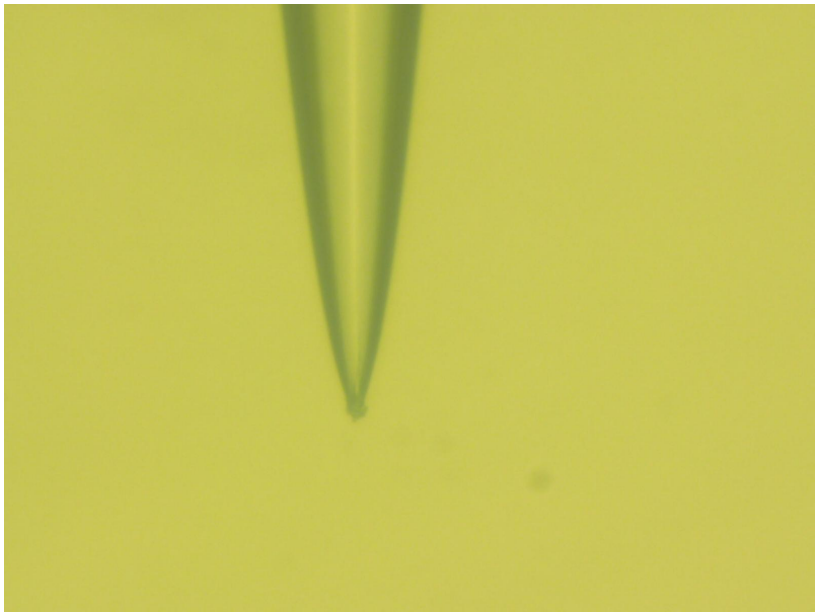

Figure 5.46: Deteriorating of the cavity tip in sample 4

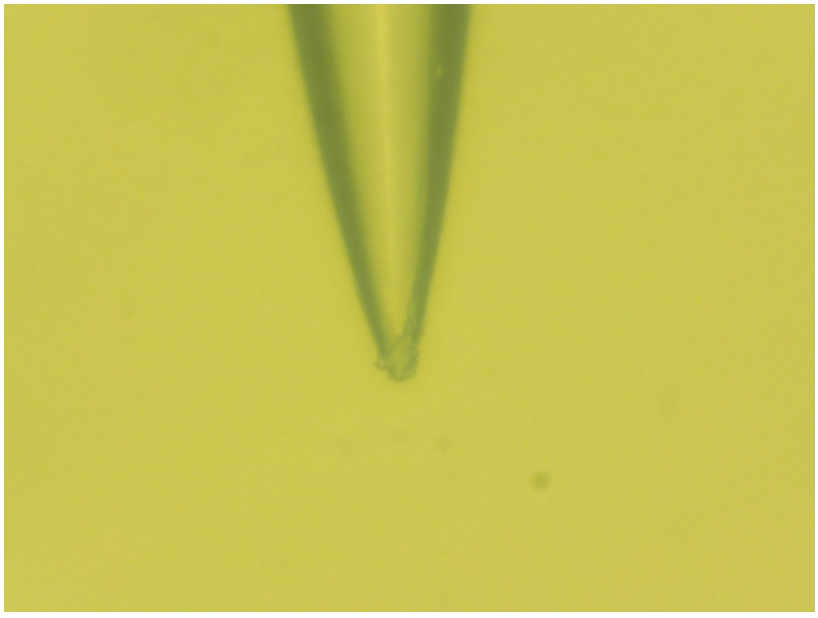

Figure 5.47: Deteriorating of cavity tip of sample 5

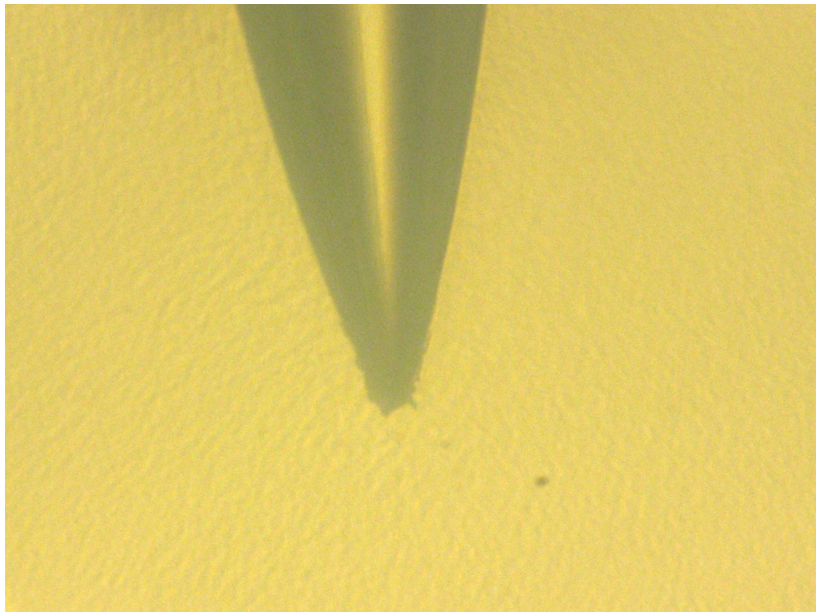

Figure 5.48: Deteriorating of cavity tip of sample 6

As can be seen from the pictures no electrical tree was initiated in the samples without premade cracks, but partial discharges have deteriorated the tip surface of the cavity. With time, the electrical field would be greatly enlarged at this position and an electrical tree growth would be initiated.

Even though not being able to see the partial discharge or correlating the pictures obtained when testing sample 4, the test was ended at 20 kV. This was done in order to protect other equipment from failing or partial discharges/breakdown to occur other places in the circuit. As can be seen from Figure: 5.46 it is likely that the electrical tree, when initiated, would have a very fast growth rate. Sample 2 had a breakdown when tested. The breakdown occurred at 13 kV and happened during seconds. Having a high exposure time on the camera makes it difficult to act in such a case, leaving the operator blind for some time between each picture.

Chapter 6

Conclusion

In this theses a correlation between the partial discharge pattern occurring in a silicone rubber sample, both with and without a pre-made crack, and the light emitted has been examined.

Silicone rubber samples have successfully been molded, with and without a pre-made cavity. A molding procedure has been found for both types.

It has been found that partial discharges occurs almost instantaneously after switching on voltage. The intensity of the light is depending on the dissipated energy during partial discharges. Small magnitudes of partial discharges were often found to have the highest light intensity due to the high numbers of discharges. By examining the samples after testing it was found that the cavity surface tip was deteriorated; the samples containing a pre-made crack had electrical tree growth or electrical breakdown while the samples without a pre-made crack had visible deteriorating cavity tip. It is likely that electrical treeing soon would appear in these samples as well.

Chapter 7

Recommended further work

7.1 Detect partial discharge noise source

To better correlate the partial discharges pattern to the pictures obtained by the CCD camera test should me made in order to locate the origin of the partial discharge source interfering the measurements at 6 and 12 kV.

7.2 Investigation of cavity surface

Finding a better approach to calculate the energy dissipated in the cavity would make room for further investigations. If it is possible to measure the roughness of the cavity surface before and after a test is conducted, how much (volume) dissipated silicone rubber per joule could be determined.

In addition to the surface investigations, longer aging test should be done on silicone rubber samples without a pre-made crack in order to determine when electrical tree is initiated. As can be seen from Figures: 5.44-5.48 the cavity surface is deteriorated at the cavity tip, but the voltage in these experiments is increased rapidly. By doing so, it would also be possible to determine how much energy it takes to start an electrical tree growth.

7.3 Introduction of pressure

Introducing pressure would make the test more realistic as to how the environment around the silicone rubber will be in actual subsea applications. At sea level the pressure is higher, given by the water debt. Having a cavity and increased pressure it is likely that the PDIV is increased as can be seen from the Pachen's curve.

7.4 Change camera conditions

To achieve better pictures the camera should be lowered in order to get an enlargement of the cavity. A new focus point has to be found for this new position. In this theses the best focus point was found having all lights in the room switched off, making it as dark as possible.

To achieve even better pictures, the setup should be conducted in a complete dark room with the user interface on the outside.

Bibliography

[1] *Getting to the bottom of it*, 2016. [Online]. Available: http://www.npd.no/en/Publications/Norwegian-Continental-Shelf/No-2-2016/Quantum-leap/.

[2] *Spectron*, 2015. [Online]. Available: https://w3.siemens.com/markets/global/en/oil-gas/PublishingImages/applications/subsea/products/SpecTRON.pdf.

[3] Ø. Midttveit, *Test of partial discharges and electroluminescence in silicone rubber at atmospheric pressure.* Master theses, 2017.

[4] I. Spurkeland, *Elektrisk trevekst og partielle utladninger i silikongummi for hvac konnektorer*, Master theses, 2016.

[5] M. S. Martinez, *Electrical treeing in insulation materials for high voltage ac subsea connectors under high hydrostatic pressures*, Master theses, 2017.

[6] *Silicone rubber*, 2017. [Online]. Available: https://albrightsilicone.com/siliconerubber/.

[7] *Characteristic properties of silicone rubber compounds*, 2016. [Online]. Available: https://www.shinetsusilicone-global.com/catalog/pdf/rubber_e.pdf.

[8] B. X. Du, Z. L. Ma, and Y. Gao, "Phenomena and mechanism of electrical tree in silicone rubber," in *2009 IEEE 9th International Conference on the Properties and Applications of Dielectric Materials*, Jul. 2009, pp. 37–40. DOI: 10.1109/ICPADM.2009.5252511.

[9] T. Bai and P. L. Lewin, "Degradation behaviour of voids in silicone rubber under applied ac electric fields," in *2012 Annual Report Conference on Electrical Insulation and Dielectric Phenomena*, Oct. 2012, pp. 589–592. DOI: 10.1109/CEIDP.2012.6378849.

[10] E. Ildstad, *Tet4160 insulating materials for high voltage applications*, Aug. 2015.

[11] H. A. Illias, G. Chen, and P. L. Lewin, "Modelling of temporal temperature and pressure change due to partial discharge events within a spherical cavity in a solid dielectric material using finite element analysis," in *2010 International Conference on High Voltage Engineering and Application*, Oct. 2010, pp. 501–504. DOI: 10.1109/ICHVE.2010.5640716.

[12] P. Keim Olsen, I. Roen Velo, and F. Mauseth, "Experimental challenges when measuring partial discharges under combined dc and high frequency ac voltage," Sep. 2017.

[13] D. Andre, "Conduction and breakdown initiation in dielectric liquids," in *2011 IEEE International Conference on Dielectric Liquids*, Jun. 2011, pp. 1–11. DOI: 10.1109/ICDL.2011.6015495.

[14] H. Borsi and E. Gockenbach, "Properties of ester liquid midel 7131 as an alternative liquid to mineral oil for transformers," in *IEEE International Conference on Dielectric Liquids, 2005. ICDL 2005.*, Jun. 2005, pp. 377–380. DOI: 10.1109/ICDL.2005.1490104.

[15] R. Schurch, S. M. Rowland, and R. S. Bradley, "Partial discharge energy and electrical tree volume degraded in epoxy resin," in *2015 IEEE Conference on Electrical Insulation and Dielectric Phenomena (CEIDP)*, Oct. 2015, pp. 820–823. DOI: 10.1109/CEIDP.2015.7352053.

[16] L. Lundgaard, "Partielle utladninger. Begreper, måleteknikk og mulige anvendelser for tilstandskontroll," Energiforsyningens Forskningsinstitutt AS, Tech. Rep., Mar. 1996.

[17] *Eksitere*, 2018. [Online]. Available: https://snl.no/eksitere.

[18] *Electron states*, 2015. [Online]. Available: https://www.quora.com/What-is-happening-at-the-electron-level-when-heat-breaks-molecular-bonds.

[19] T. Mizuno, Y.-S. Liu, W. Shionoya, M. Okada, K. Yasuoka, S. Ishii, A. Yokoyama, and H. Miyata, "Electroluminescence from surface layer of insulating polymer under ac voltage application," *IEEE Transactions on Dielectrics and Electrical Insulation*, vol. 5, no. 6, pp. 903–908, Dec. 1998, ISSN: 1070-9878. DOI: 10.1109/94.740774.

[20] *Firing voltage*, 2010. [Online]. Available: https://encyclopedia2.thefreedictionary.com/Firing+Voltage.

[21] *Insulating materials for high voltage applications. breakdown in gases*, 2017. [Online]. Available: https://ntnu.blackboard.com/bbcswebdav/pid-100749-dt-content-rid-1208222_1/courses/194_TET4160_1_2017_H_1/Breakdown%20in%20gases_3.pdf.

[22] D. K. Das-Gupta, "Polyethylene: Structure, morphology, molecular motion and dielectric behavior," *IEEE Electrical Insulation Magazine*, vol. 10, no. 3, pp. 5–15, May 1994, ISSN: 0883-7554. DOI: 10.1109/57.285418.

[23] *Electrical tree*, 2016. [Online]. Available: https://www2.le.ac.uk/departments/engineering/research/electrical-power/images/Electrical%20Tree.jpg/view.

[24] B. X. Du, Z. L. Ma, Y. Gao, and T. Han, "Effect of ambient temperature on electrical treeing characteristics in silicone rubber," *IEEE Transactions on Dielectrics and Electrical Insulation*, vol. 18, no. 2, pp. 401–407, Apr. 2011, ISSN: 1070-9878. DOI: 10.1109/TDEI.2011.5739443.

[25] B. X. Du, T. Han, and J. G. Su, "Electrical tree characteristics in silicone rubber under repetitive pulse voltage," *IEEE Transactions on Dielectrics and Electrical Insulation*, vol. 22, no. 2, pp. 720–727, Apr. 2015, ISSN: 1070-9878. DOI: 10.1109/TDEI.2015.7076767.

[26] Y. Liu and X. Cao, "Electrical tree growth characteristics in xlpe cable insulation under dc voltage conditions," *IEEE Transactions on Dielectrics and Electrical Insulation*, vol. 22, no. 6, pp. 3676–3684, Dec. 2015, ISSN: 1070-9878. DOI: 10.1109/TDEI.2015.005222.

[27] *Diffusjon*, 2016. [Online]. Available: https://snl.no/diffusjon.

[28] *Diffusion*, 2018. [Online]. Available: https://othbiology.wikispaces.com/Diffusion.

[29] R. Gravaune, *Elektrisk trevekst i isolasjonsmaterialer for hfffdfffdyspente ac konnektorer*, Master theses, 2015.

Appendix A

ELASTOSIL A/B

WACKER ELASTOSIL®

Product data

Typical general characteristics	Inspection Method	Value
Hardness Shore A	DIN 53505	60
Appearance		transparent
Density	ISO 1183-1 A	1,13 g/cm³
Viscosity (shear rate 0.9 s^{-1})	DIN 53019	1100000 mPa s
Viscosity (shear rate 10 s^{-1})	DIN 53019	420000 mPa s
Tensile strength	DIN 53504 S 1	9,40 N/mm^2
Elongation at break	DIN 53504 S 1	340 %
Tear strength	ASTM D 624 B	27 N/mm
Rebound resilience	DIN 53512	67 %
Compression set *	DIN ISO 815-B (22 h / 175 °C)	11 %
Dielectric strength (1-mm-sheet)	DIN IEC 243-2	23 kV/mm
Volume resistivity	DIN IEC 93	5 x 10^{15} Ω cm
Dielectric constant at 50 Hz	DIN VDE 0303	2,8 εr
Dissipation factor (50 Hz)	DIN VDE 0303	20 x 10^{-4} tan δ

Cure conditions: 5 min / 165 °C in press; postcuring for 4 h / 200 °C in ventilated air.
* Postcuring for CS: 6 h / 200 °C

These figures are only intended as a guide and should not be used in preparing specifications.

Figure A.1: ELASTOSIL LR 3003&60 A/B data sheet

Appendix B

Platform and SiR sample measurements

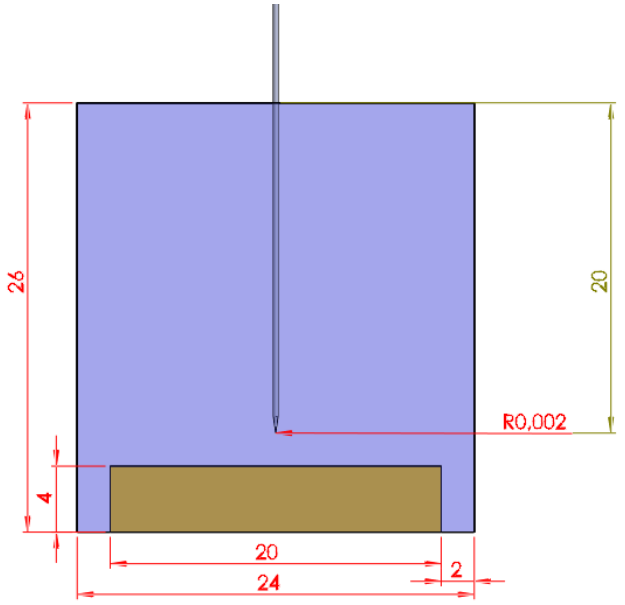

Figure B.1: Front view SiR sample with measurements.

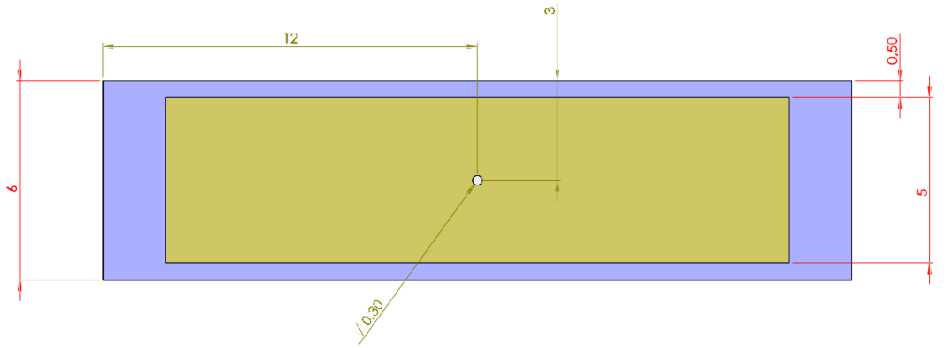

Figure B.2: Top view SiR sample with measurements.

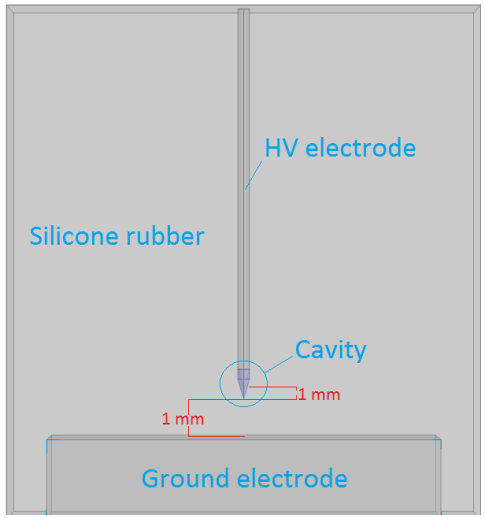

Figure B.3: Front view SiR sample with measurements of needle-cavity and cavity-ground (should be 2mm) distance.

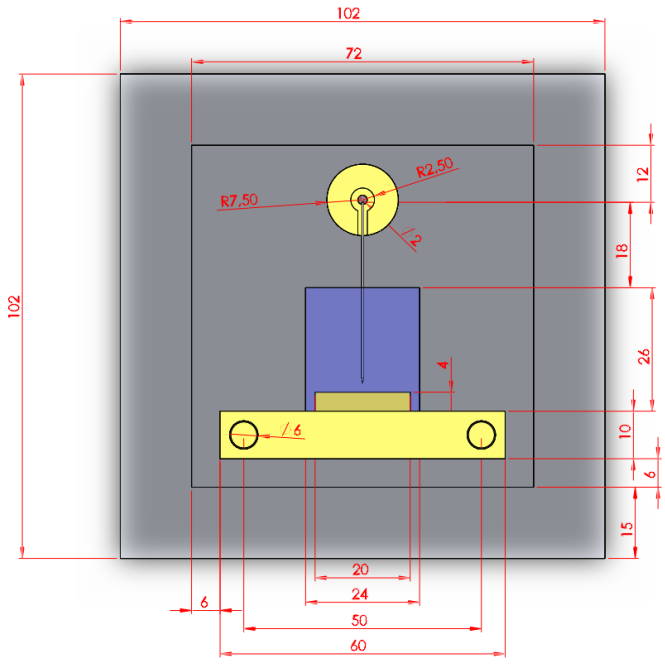

Figure B.4: Top view of test platform with measurements.

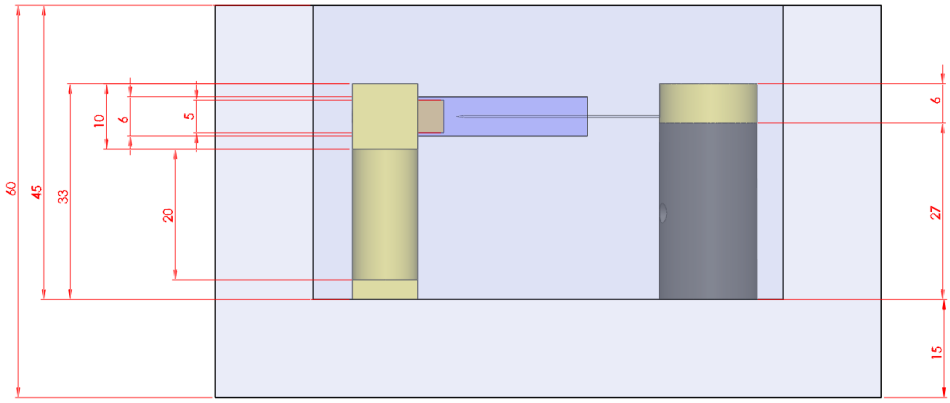

Figure B.5: Side view of test platform with measurements.

Appendix C

Sample events

C.1 Sample 1

C.1.1 Light in whole cavity

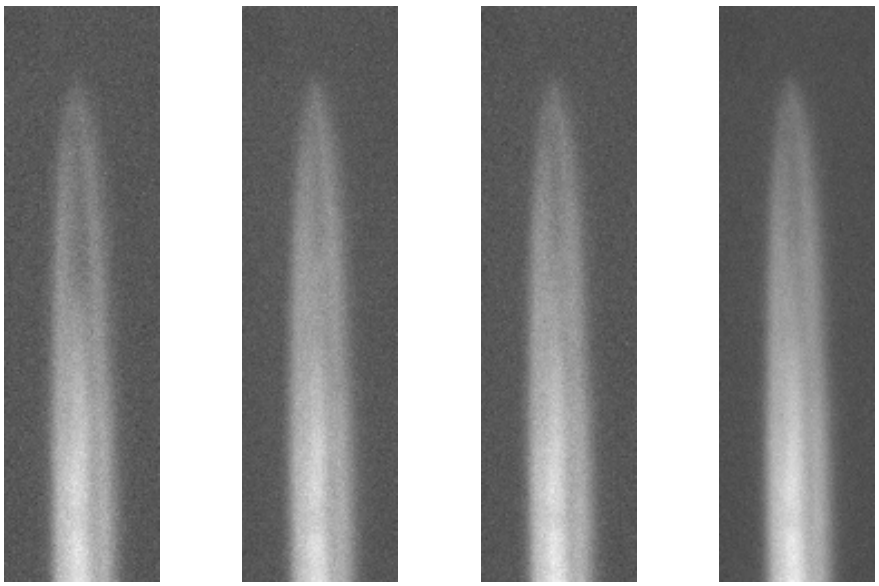

(a) <1 kV **(b)** 2 kV **(c)** 3 kV **(d)** 3 kV

Figure C.1: (a) Reference picture: No PD occurring. (b)(c)(d) Different intensity of light occurring in the cavity: Sample 1

Figure: C.1b with belonging partial discharge pattern. 2kV.

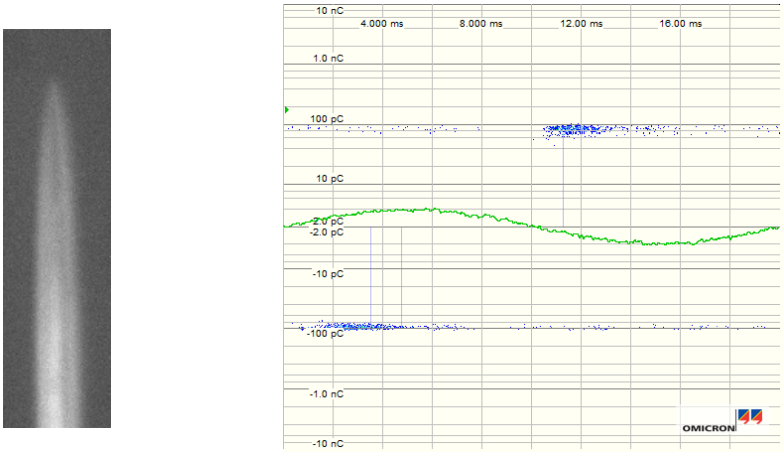

Figure C.2: CCD-camera picture with belonging Omicron measurement for 12 seconds at 2 kV: Sample 1

Figure: C.1c with belonging partial discharge pattern. 3kV.

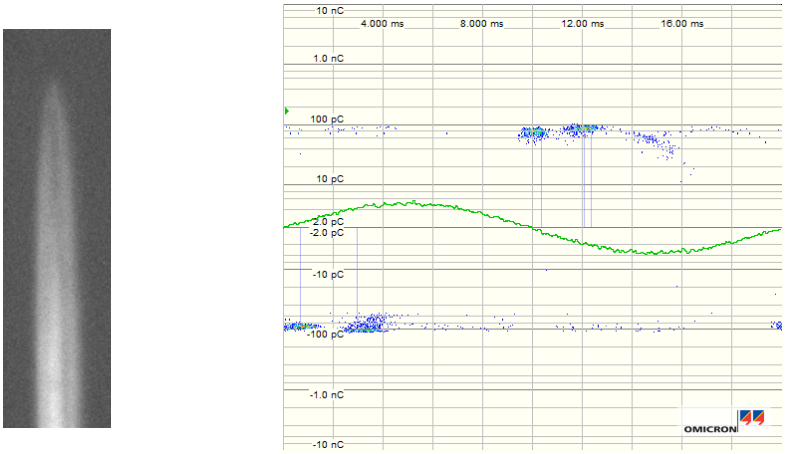

Figure C.3: CCD-camera picture with belonging Omicron measurement for 12 seconds at 3 kV: Sample 1

Figure: C.1d with belonging partial discharge pattern. 3 kV.

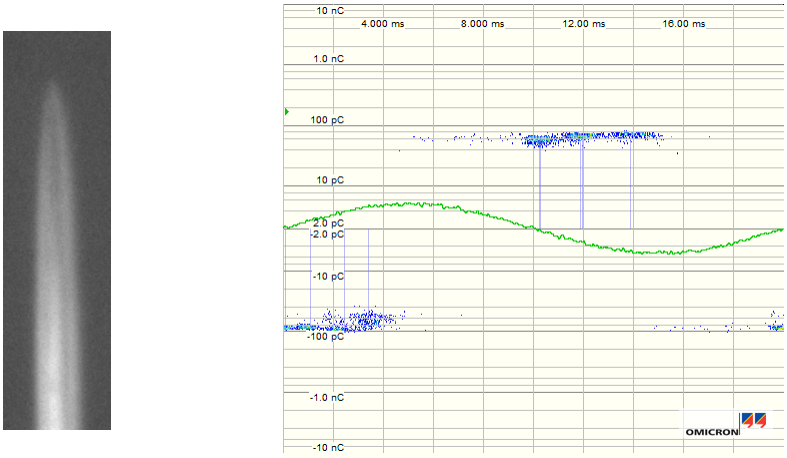

Figure C.4: CCD-camera picture with belonging Omicron measurement for 12 seconds at 3 kV: Sample 1

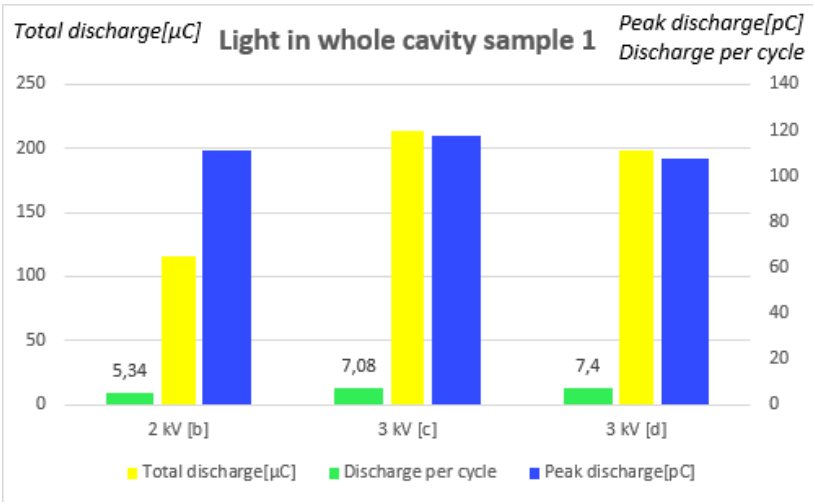

Figure C.5: Bargraph: Total discharge, peak discharge and discharges/cycle for Event 1: Light in whole cavity. Sample 1

C.1.2 Light at needle tip

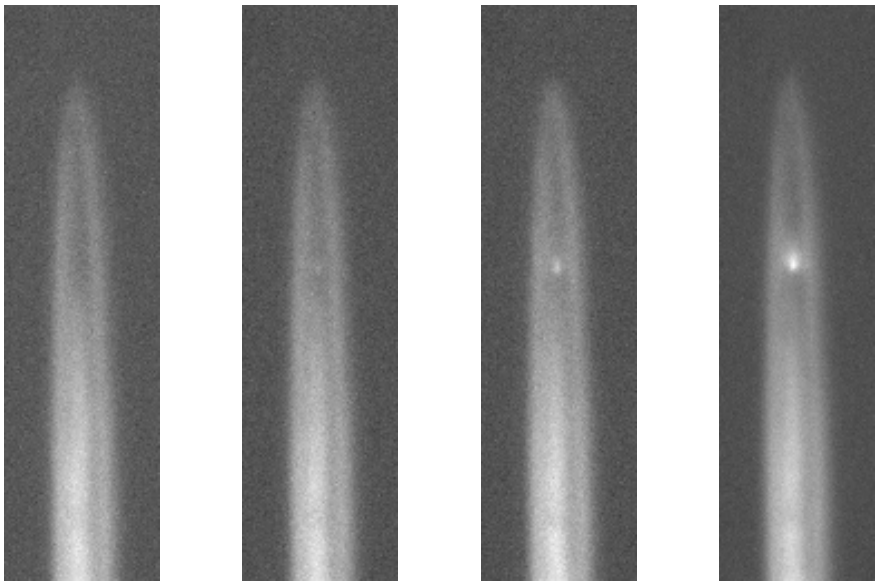

(a) <1 kV **(b)** 2 kV **(c)** 3 kV **(d)** 6 kV

Figure C.6: (a) Reference picture: No PD occurring. (b)(c)(d) Different intensity of light occurring at the needle-tip. Sample 1

Figure: C.6b with belonging partial discharge pattern. 2kV.

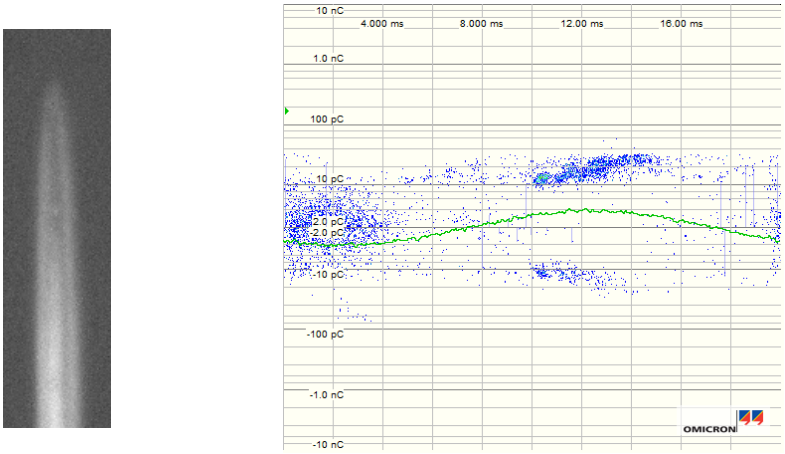

Figure C.7: CCD-camera picture with belonging Omicron measurement for 12 seconds at 2 kV: Sample 1

Figure: C.6c with belonging partial discharge pattern. 3kV.

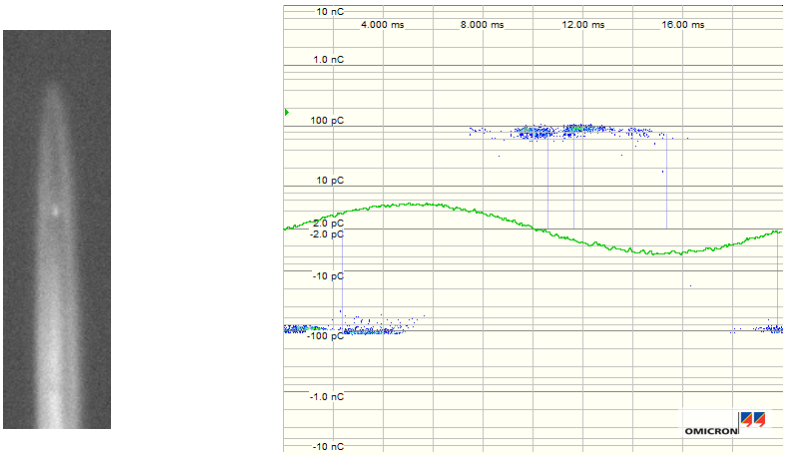

Figure C.8: CCD-camera picture with belonging Omicron measurement for 12 seconds at 3 kV: Sample 1

Figure: C.6d with belonging partial discharge pattern. 6 kV.

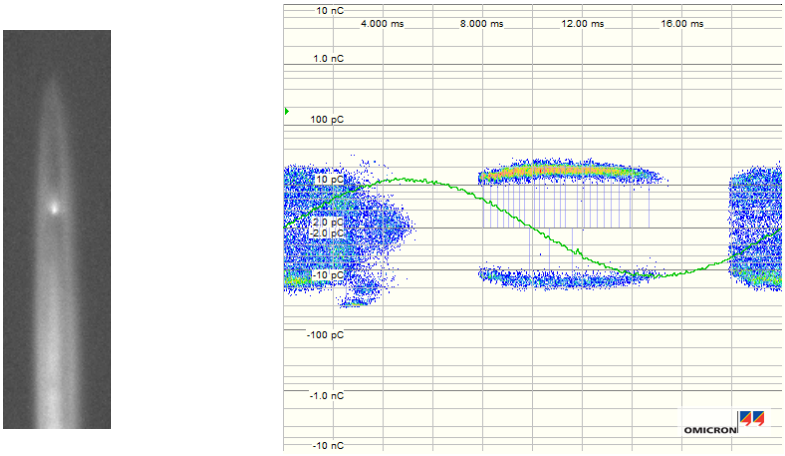

Figure C.9: CCD-camera picture with belonging Omicron measurement for 12 seconds at 6 kV: Sample 1

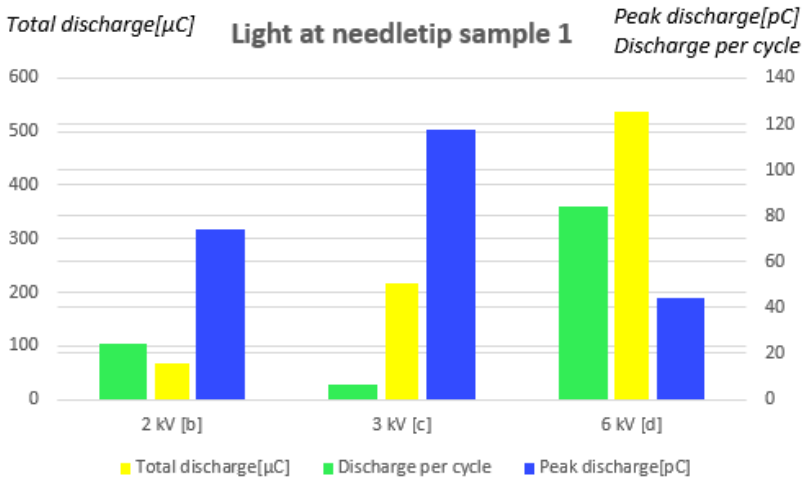

Figure C.10: Bargraph: Total discharge, peak discharge and discharges/cycle for Event 2: Light at needle-tip. Sample 1

C.1.3 Light alongside needle

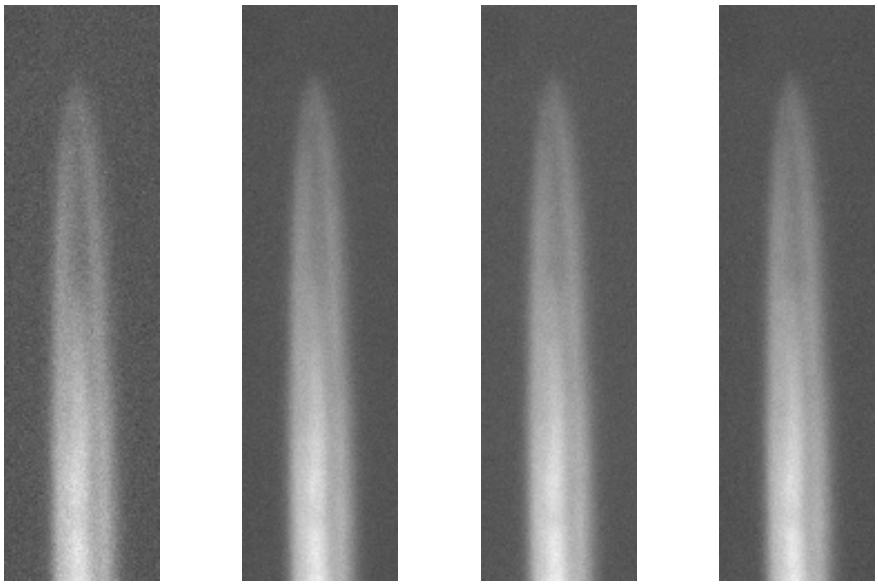

(a) $<$1 kV **(b)** 4 kV **(c)** 4 kV **(d)** 4 kV

Figure C.11: (a) Reference picture: No PD occurring. (b) Picture taken before light alongside needle occurs. (c) Taken when light alongside occurs. (d) Taken during light alongside needle.

Figure: C.11b with belonging partial discharge pattern. 4kV.

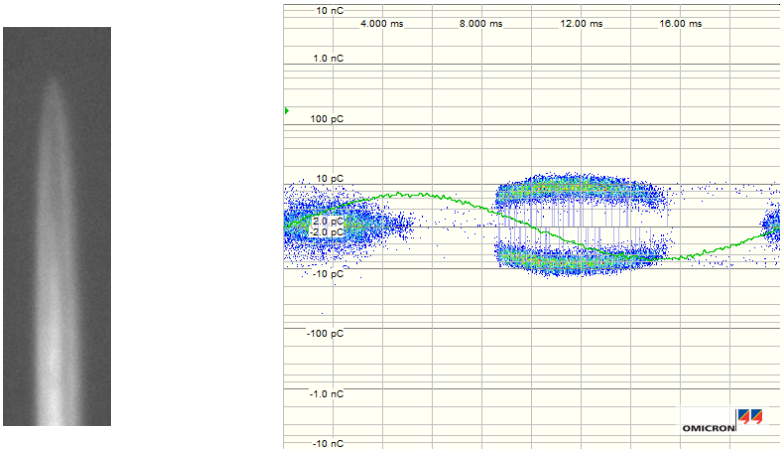

Figure C.12: CCD-camera picture with belonging Omicron measurement for 12 seconds at 4 kV: Sample 1

Figure: C.11c with belonging partial discharge pattern. 4kV.

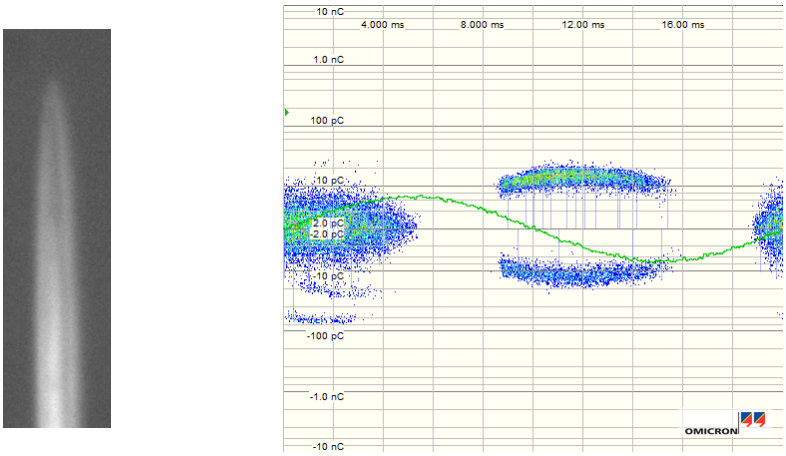

Figure C.13: CCD-camera picture with belonging Omicron measurement for 12 seconds at 4 kV: Sample 1

Figure: C.11d with belonging partial discharge pattern. 4 kV.

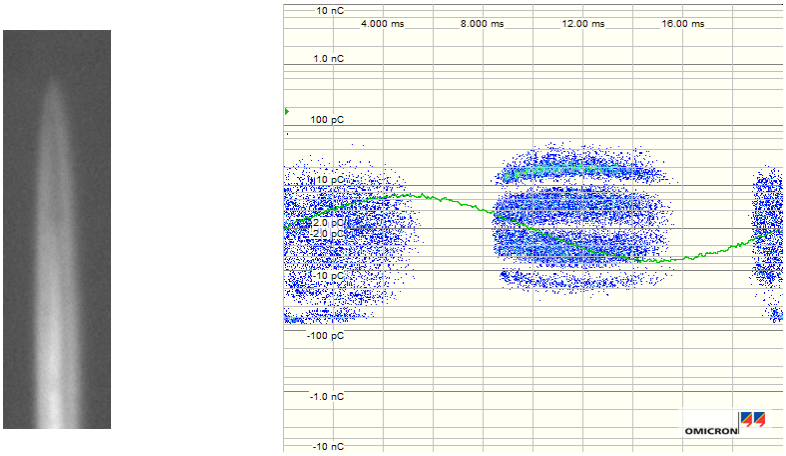

Figure C.14: CCD-camera picture with belonging Omicron measurement for 12 seconds at 4 kV: Sample 1

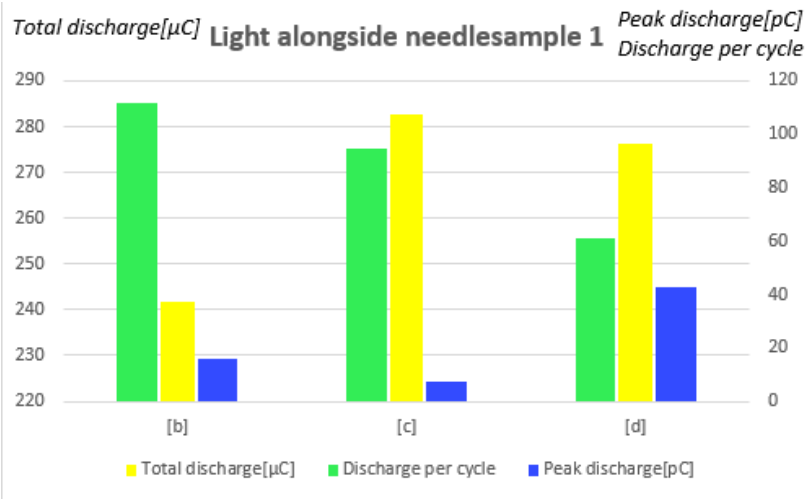

Figure C.15: Bargraph: Total discharge, peak discharge and discharges/cycle for Event 3: Light alongside needle. Sample 1

C.1.4 Tree growth

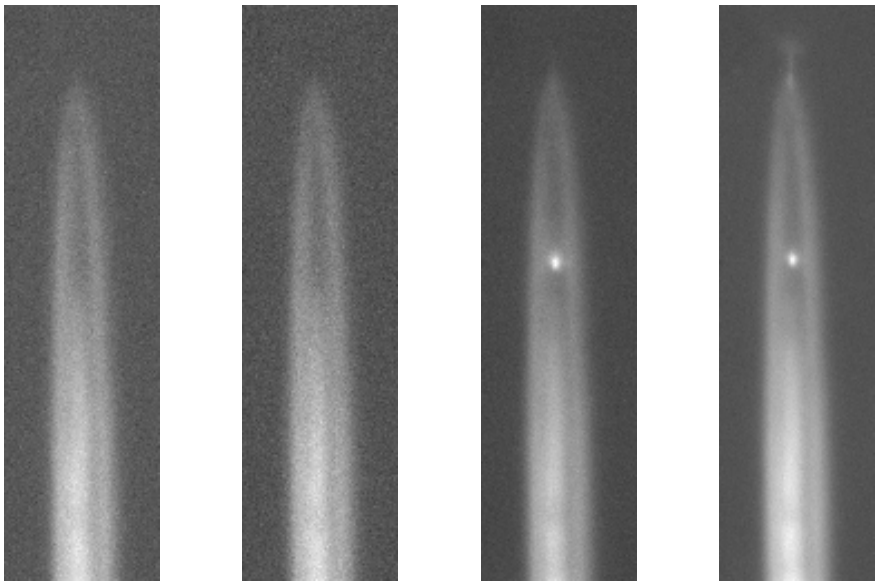

(a) <1 kV **(b)** 1 kV **(c)** 6 kV **(d)** 9 kV

Figure C.16: (a) Reference picture: No PD occurring. (b)(c)(d) Different growth stages of the electrical tree.

Figure: C.16b with belonging partial discharge pattern. 1kV.

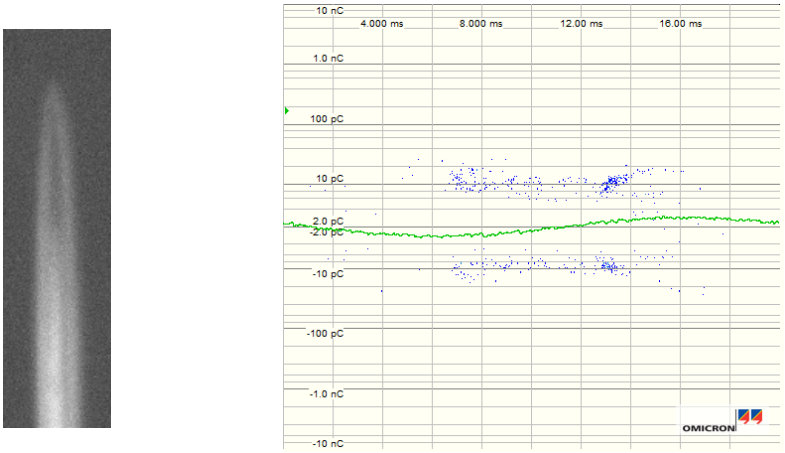

Figure C.17: CCD-camera picture with belonging Omicron measurement for 12 seconds at 1 kV: Sample 1

Figure: C.16c with belonging partial discharge pattern. 6kV.

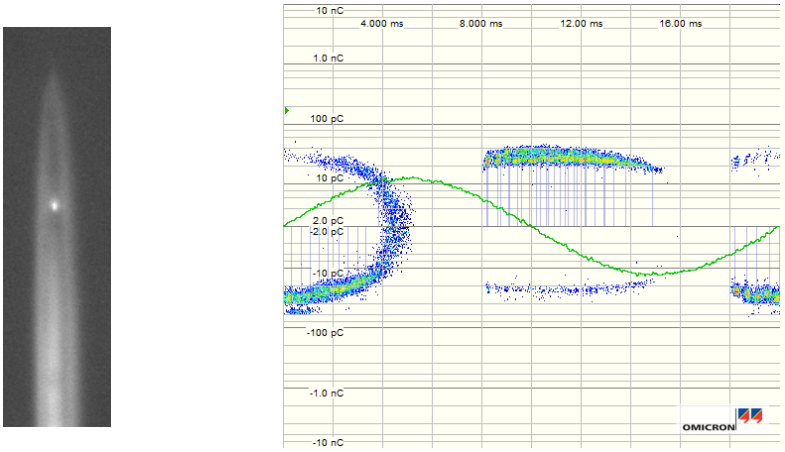

Figure C.18: CCD-camera picture with belonging Omicron measurement for 12 seconds at 6 kV: Sample 1

Figure: C.16d with belonging partial discharge pattern. 9 kV.

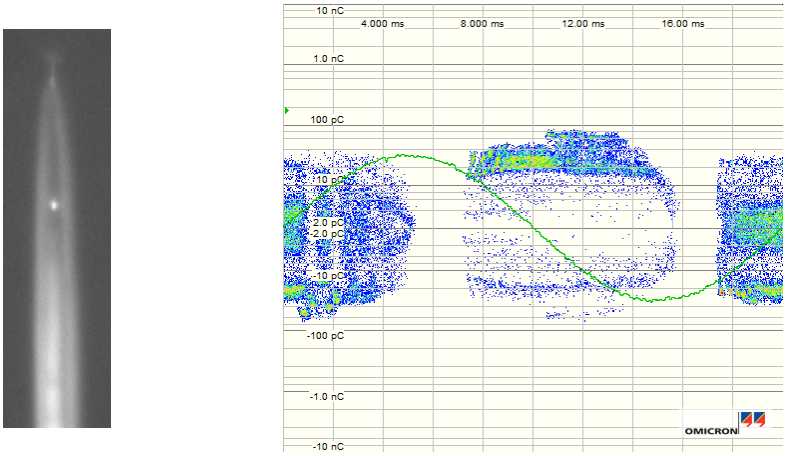

Figure C.19: CCD-camera picture with belonging Omicron measurement for 12 seconds at 9 kV: Sample 1

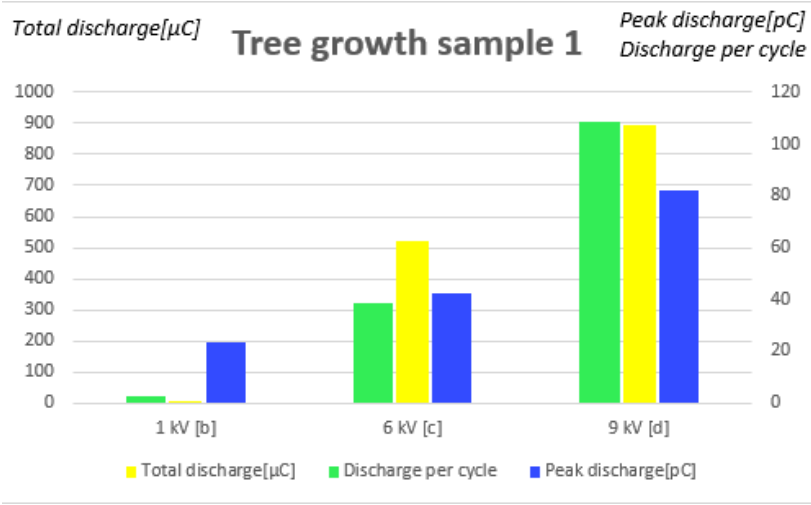

Figure C.20: Bargraph: Total discharge, peak discharge and discharges/cycle for Event 4: Electrical tree growth. Sample 1

C.2 Sample 3

C.2.1 Light in whole cavity

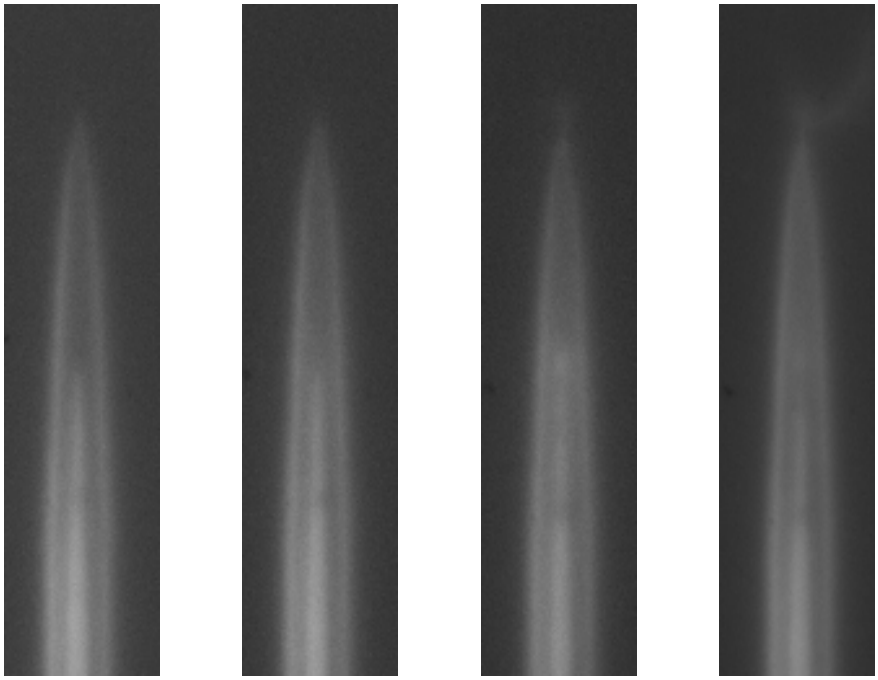

(a) $<$1 kV **(b)** 6 kV **(c)** 11 kV **(d)** 13 kV

Figure C.21: (a) Reference picture: No PD occurring. (a)(b)(c) Different intensity of light occurring in the cavity: Sample 3

Figure: C.21b with belonging partial discharge pattern. 6kV.

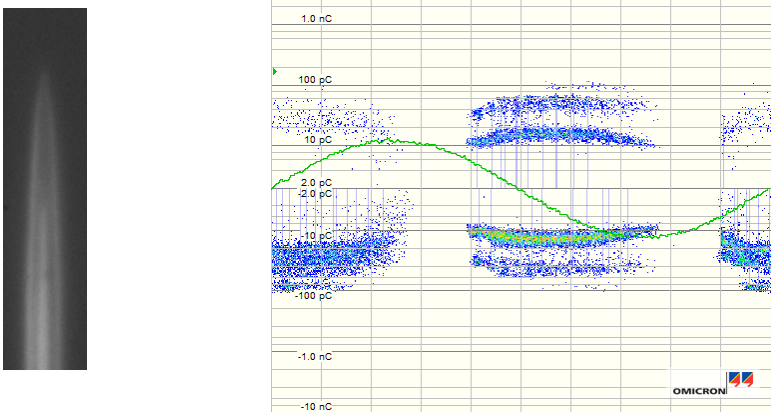

Figure C.22: CCD-camera picture with belonging Omicron measurement for 12 seconds at 6 kV: Sample 3

Figure: C.21c with belonging partial discharge pattern. 11kV.

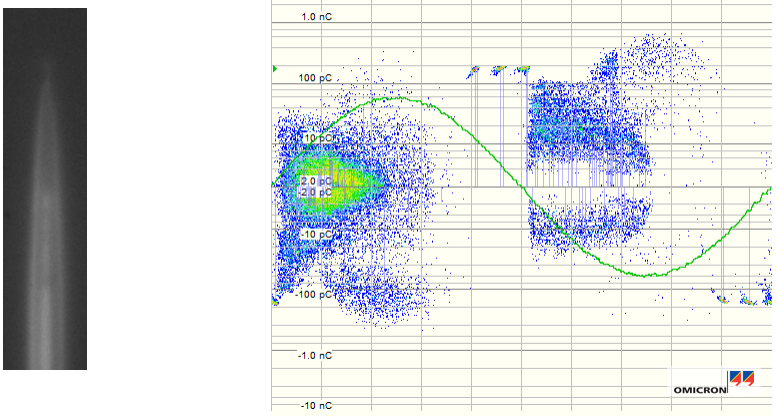

Figure C.23: CCD-camera picture with belonging Omicron measurement for 12 seconds at 11 kV: Sample 3

Figure: C.21d with belonging partial discharge pattern. 13 kV.

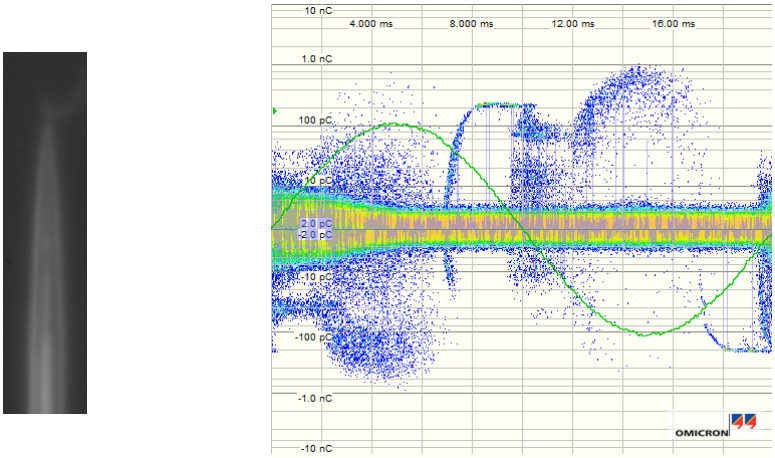

Figure C.24: CCD-camera picture with belonging Omicron measurement for 12 seconds at 13 kV: Sample 3

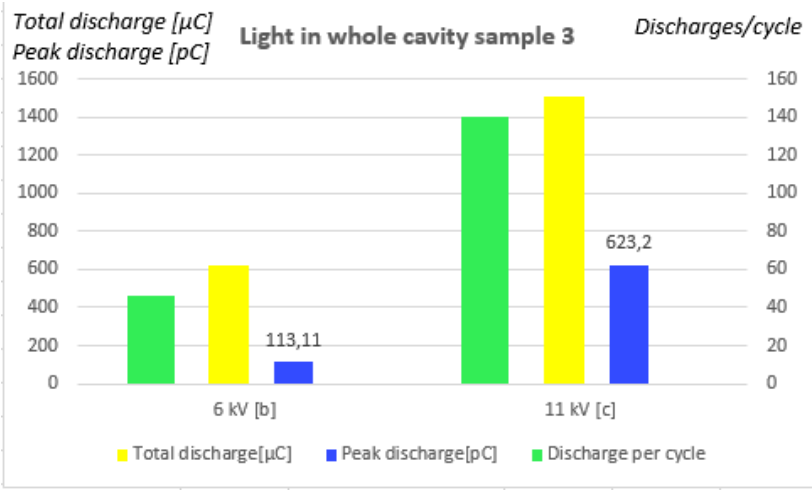

Figure C.25: Bargraph: Total discharge, peak discharge and discharges/cycle for Event 1: Light in whole cavity. Sample 3

C.2.2 Light at needle tip

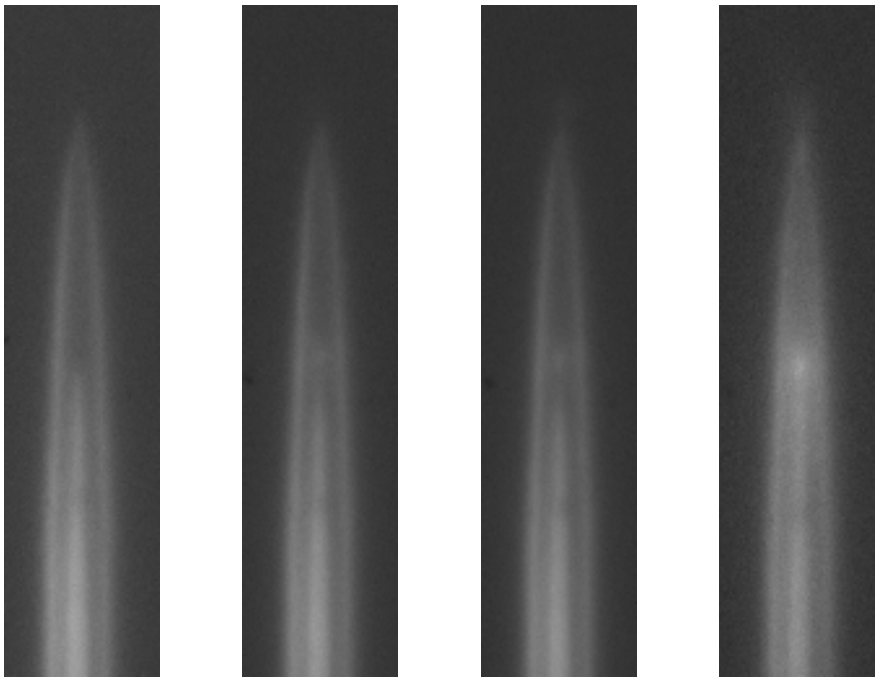

(a) <1 kV **(b)** 8 kV **(c)** 9 kV **(d)** 12 kV

Figure C.26: (a) Reference picture: No PD occurring. (b)(c)(d) Different intensity of light occurring at the needle-tip: Sample 3

Figure: C.26b with belonging partial discharge pattern. 8kV.

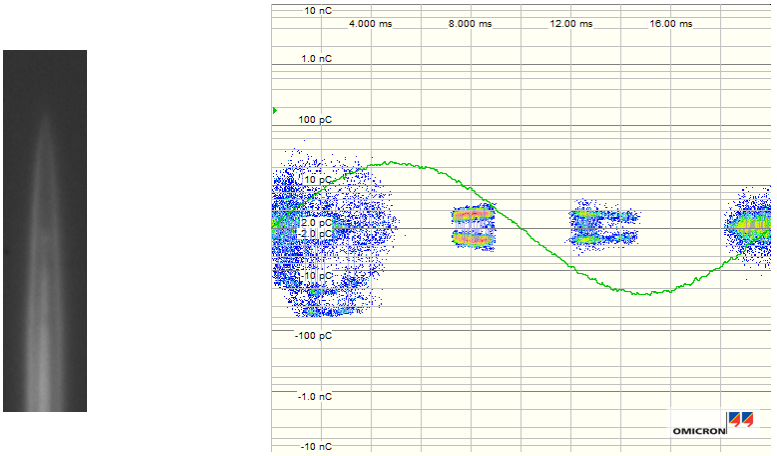

Figure C.27: CCD-camera picture with belonging Omicron measurement for 12 seconds at 8 kV: Sample 3

Figure: C.26c with belonging partial discharge pattern. 9kV.

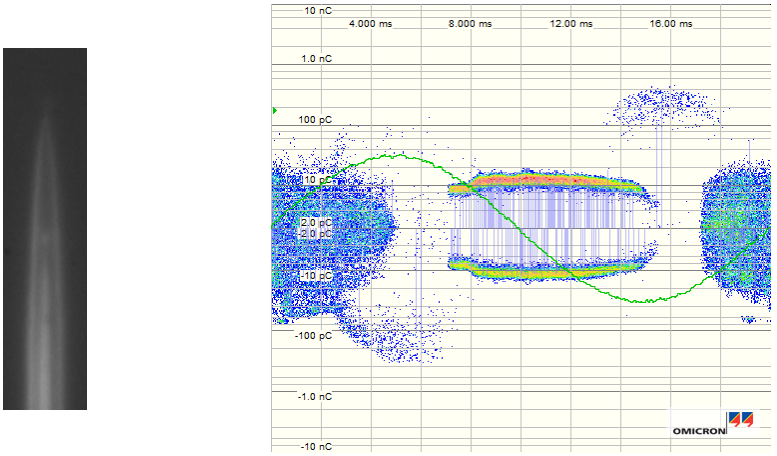

Figure C.28: CCD-camera picture with belonging Omicron measurement for 12 seconds at 9 kV: Sample 3

Figure: C.26d with belonging partial discharge pattern. 12 kV.

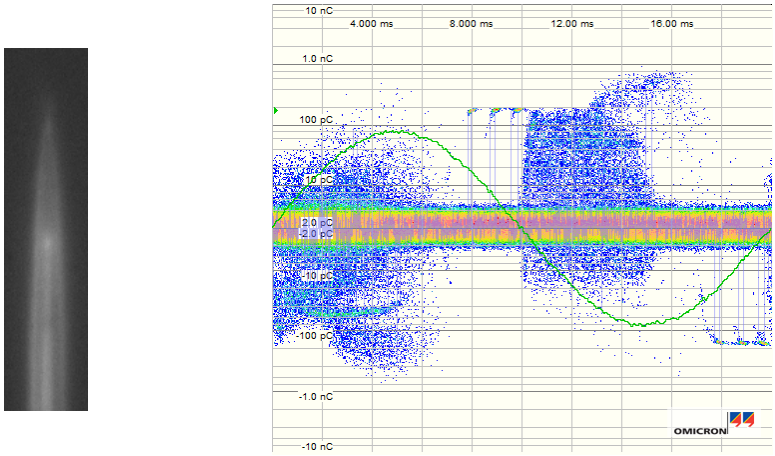

Figure C.29: CCD-camera picture with belonging Omicron measurement for 12 seconds at 12 kV: Sample 3

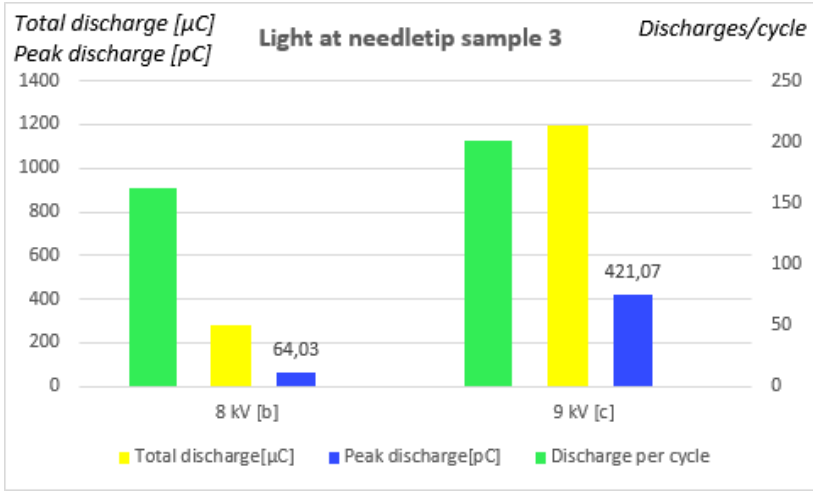

Figure C.30: Bargraph: Total discharge, peak discharge and discharges/cycle for Event 2: Light at needle-tip. Sample 3

C.2.3 Light alongside needle

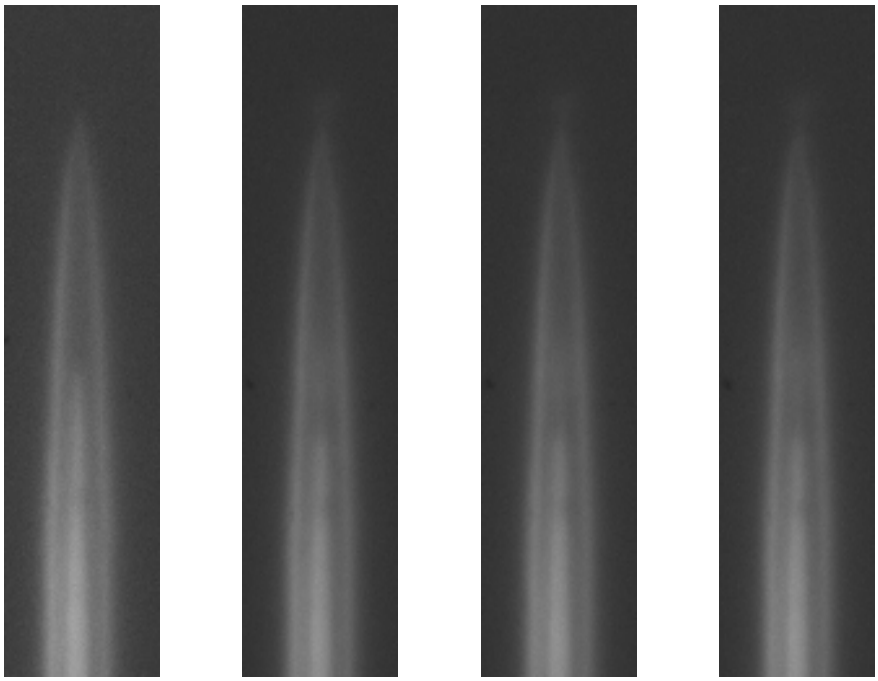

(a) <1 kV **(b)** 10 kV **(c)** 10 kV **(d)** 10 kV

Figure C.31: (a) Reference picture: No PD occurring. (b)Picture taken before light alongside needleoccurs.(c)Taken when light alongside occurs. (d)Taken during light alongside needle.

Figure: C.31b with belonging partial discharge pattern. 10kV.

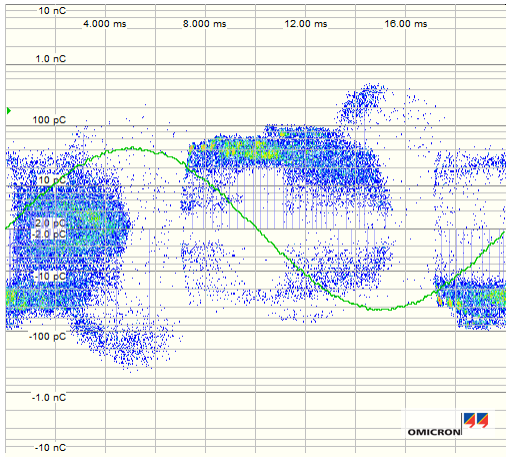

Figure C.32: CCD-camera picture with belonging Omicron measurement for 12 seconds at 10 kV: Sample 3

Figure: C.31c with belonging partial discharge pattern. 10kV.

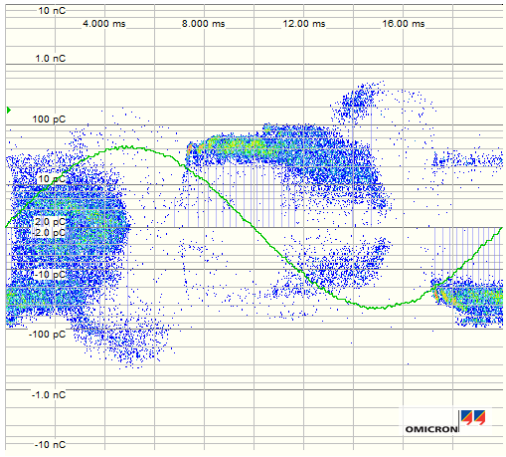

Figure C.33: CCD-camera picture with belonging Omicron measurement for 12 seconds at 10 kV: Sample 3

Figure: C.31d with belonging partial discharge pattern. 10 kV.

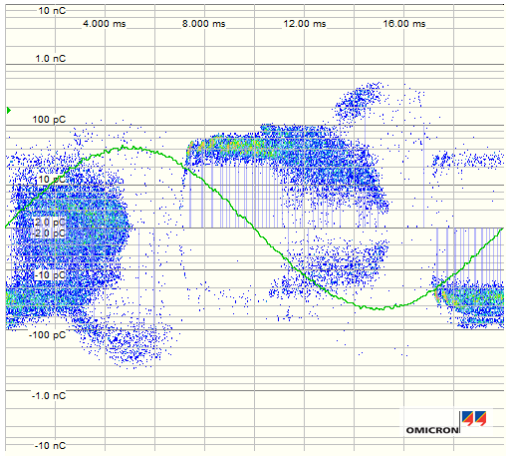

Figure C.34: CCD-camera picture with belonging Omicron measurement for 12 seconds at 10 kV: Sample 3

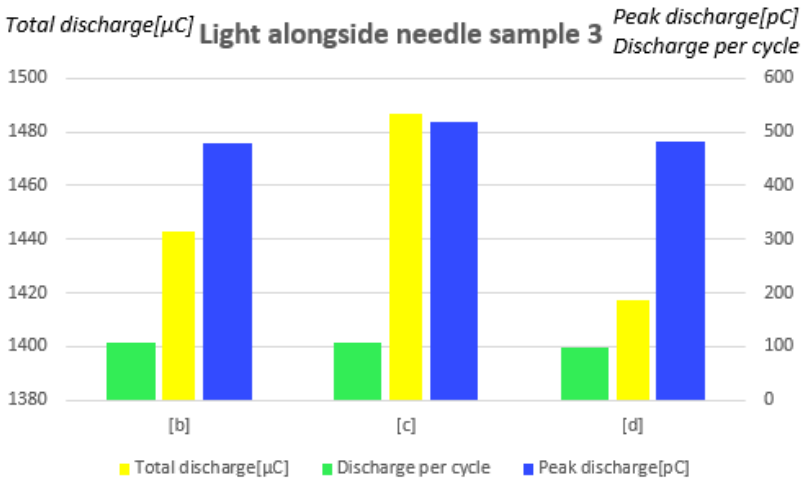

Figure C.35: Bargraph: Total discharge, peak discharge and discharges/cycle for Event 3: Light alongside needle. Sample 3

C.2.4 Tree growth

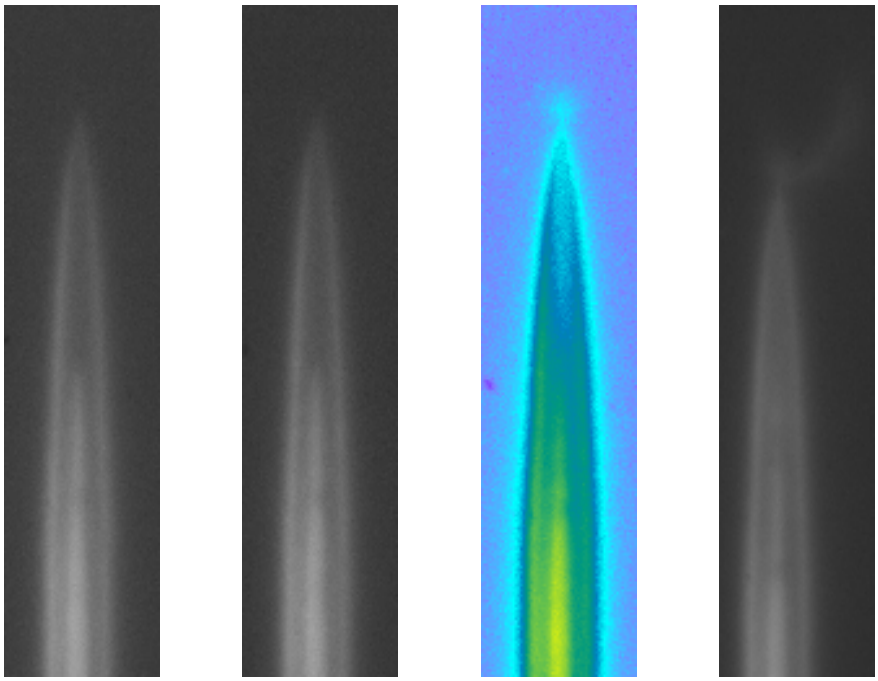

(a) <1 kV **(b)** 2 kV **(c)** 10 kV **(d)** 13 kV

Figure C.36: (a) Reference picture: No PD occurring. (b)(c)(d)Different growth stages of the electrical tree.

Figure: C.36b with belonging partial discharge pattern. 2kV.

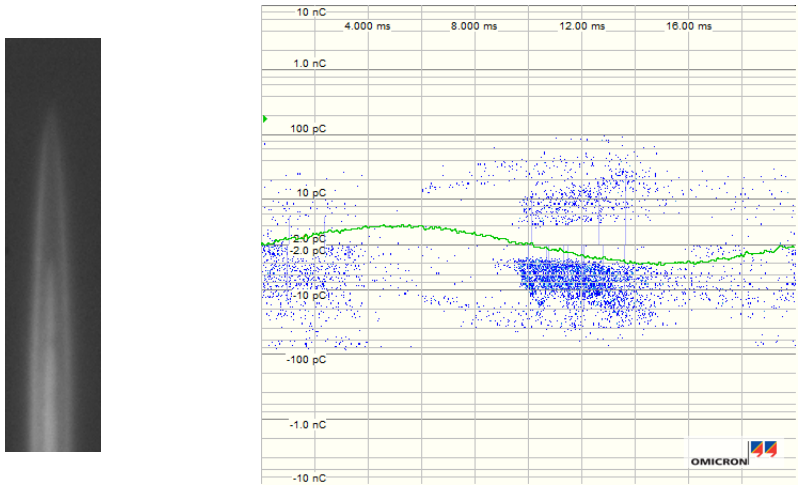

Figure C.37: CCD-camera picture with belonging Omicron measurement for 12 seconds at 2 kV: Sample 3

Figure: C.36c with belonging partial discharge pattern. 10kV.

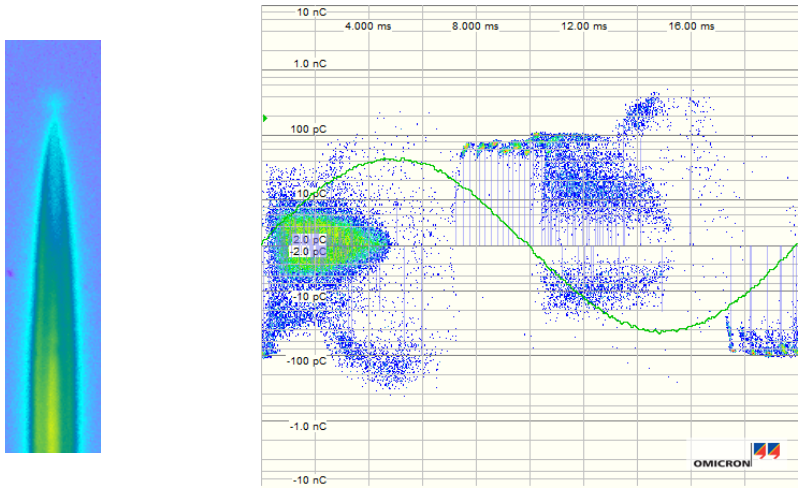

Figure C.38: CCD-camera picture with belonging Omicron measurement for 12 seconds at 10 kV: Sample 3

Figure: C.36d with belonging partial discharge pattern. 13 kV.

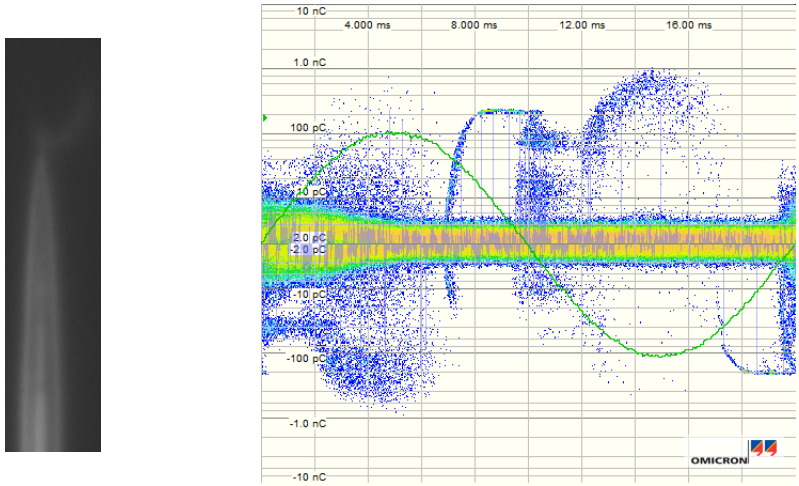

Figure C.39: CCD-camera picture with belonging Omicron measurement for 12 seconds at 13 kV: Sample 3

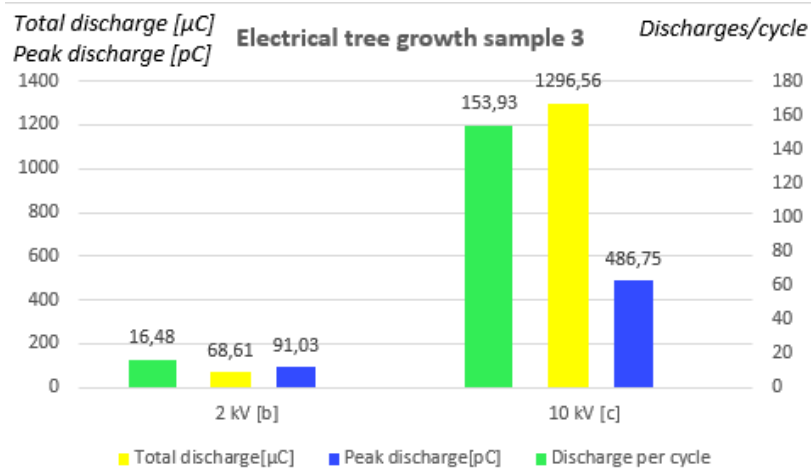

Figure C.40: Bargraph: Total discharge, peak discharge and discharges/cycle for Event 4: Electrical tree growth. Sample 3

C.3 Sample 5

C.3.1 Light in whole cavity

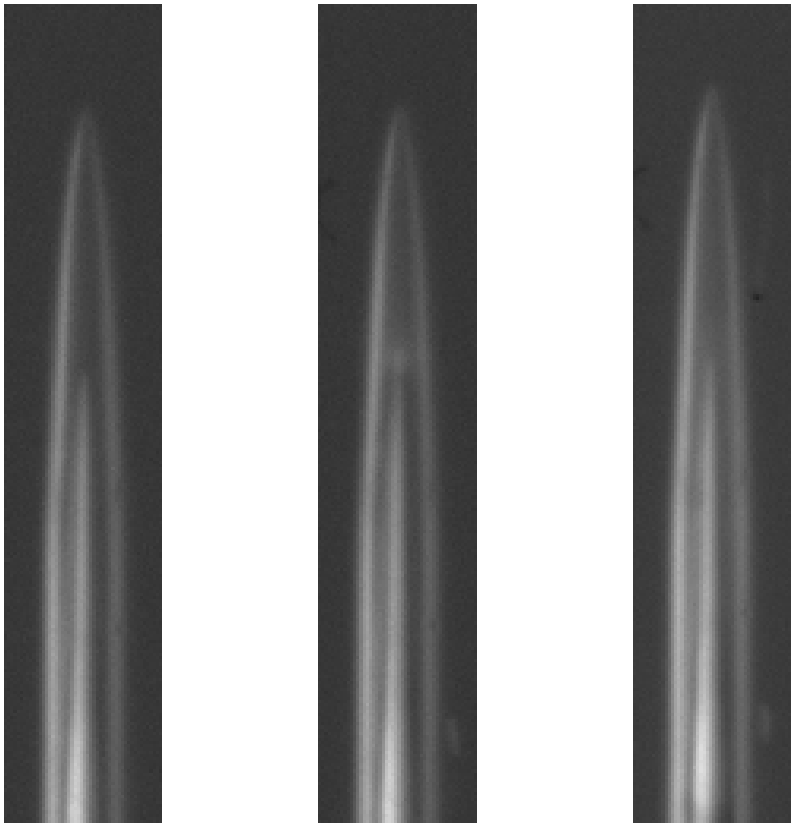

(a) <1 kV **(b)** 5 kV **(c)** 12 kV

Figure C.41: (a) Reference picture: No PD occurring. (b)(c)Different intensity of light occurring in the cavity: Sample 5.

Figure: C.41b with belonging partial discharge pattern. 5kV.

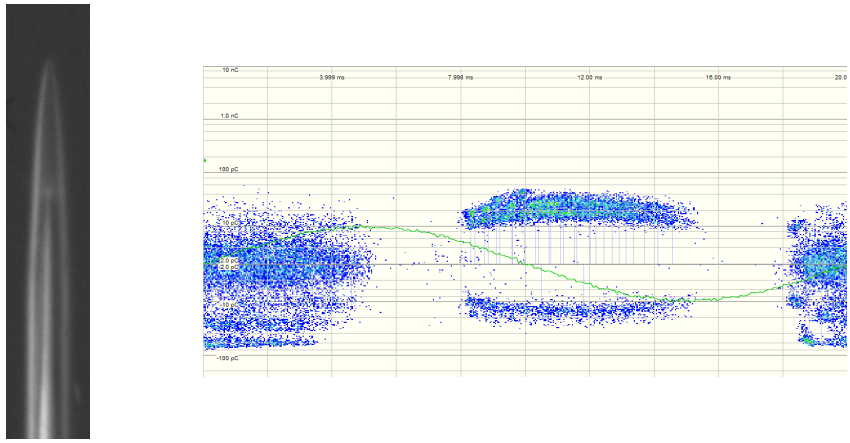

Figure C.42: CCD-camera picture with belonging Omicron measurement for 12 seconds at 5 kV: Sample 5

Figure: C.41c with belonging partial discharge pattern. 12kV.

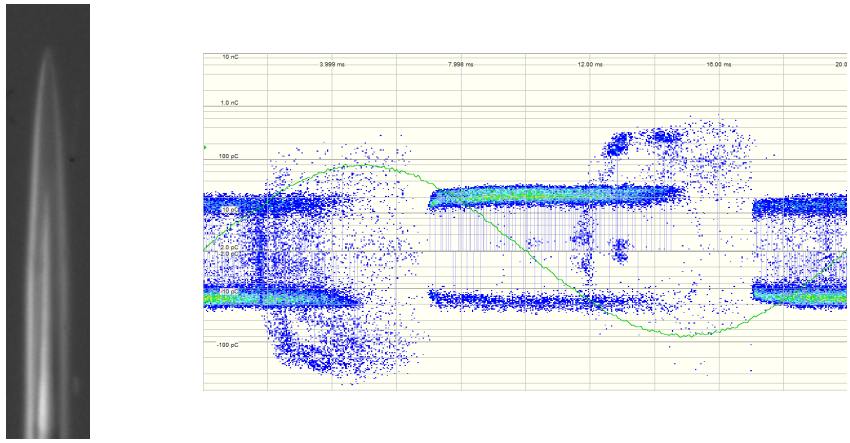

Figure C.43: CCD-camera picture with belonging Omicron measurement for 12 seconds at 12 kV: Sample 5

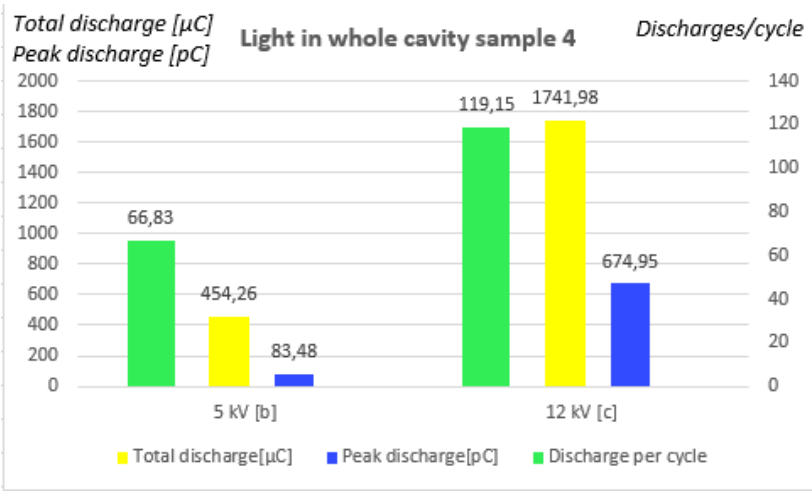

Figure C.44: Bargraph: Total discharge, peak discharge and discharges/cycle for Event 1: Light in whole cavity. Sample 5

C.3.2 Light at needle tip

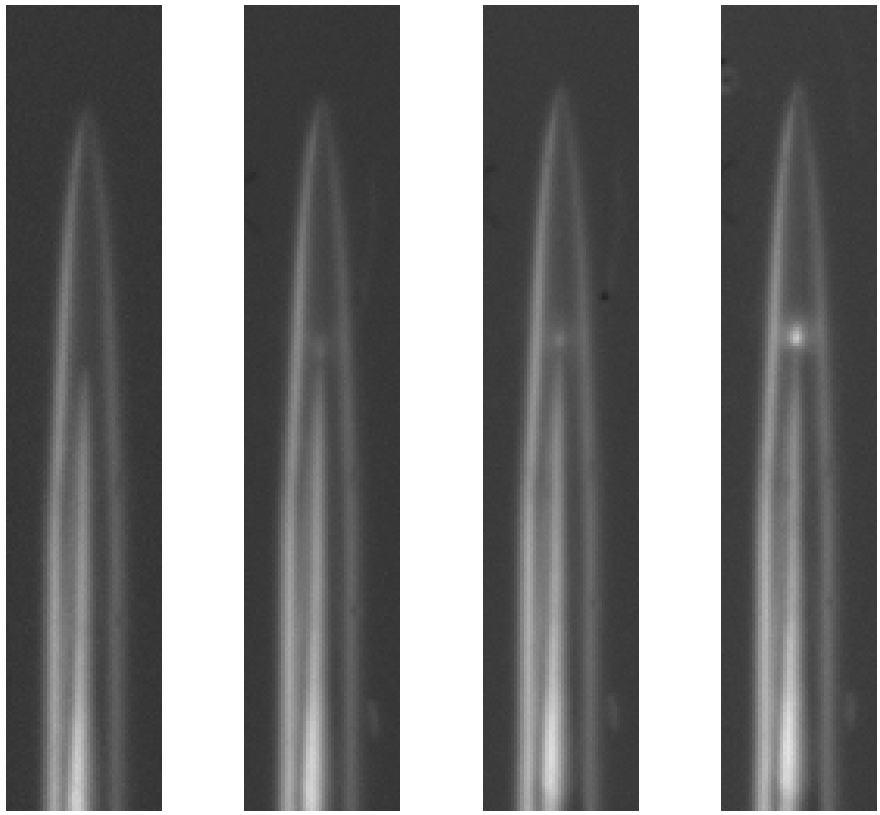

(a) <1 kV **(b)** 7 kV **(c)** 11 kV **(d)** 14 kV

Figure C.45: (a) Reference picture: No PD occurring. (b)(c)(d)Different intensity of light occurring at the needle-tip: Sample 5

Figure: C.45b with belonging partial discharge pattern. 7kV.

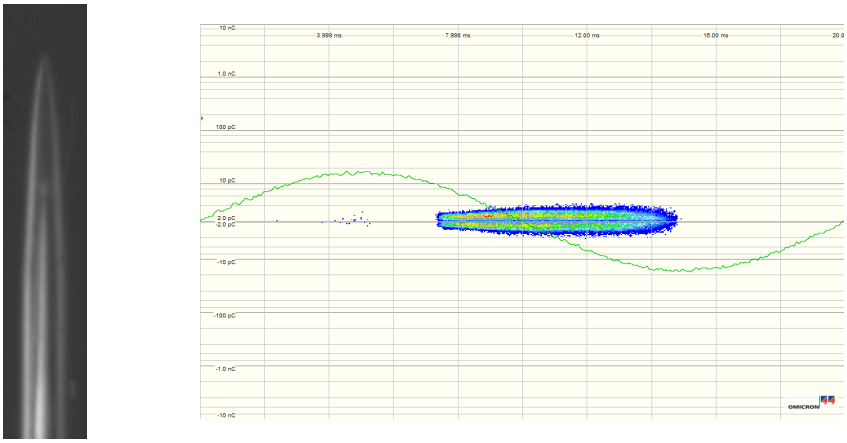

Figure C.46: CCD-camera picture with belonging Omicron measurement for 12 seconds at 7 kV: Sample 5

Figure: C.45c with belonging partial discharge pattern. 11kV.

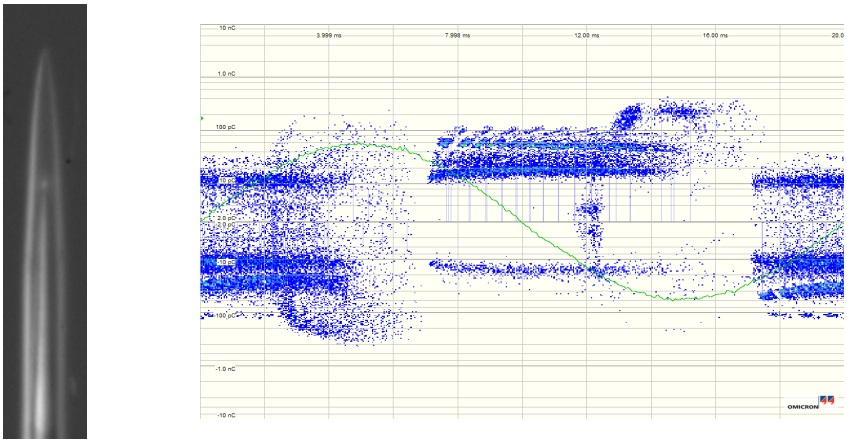

Figure C.47: CCD-camera picture with belonging Omicron measurement for 12 seconds at 11 kV: Sample 5

Figure: C.45d with belonging partial discharge pattern. 14 kV.

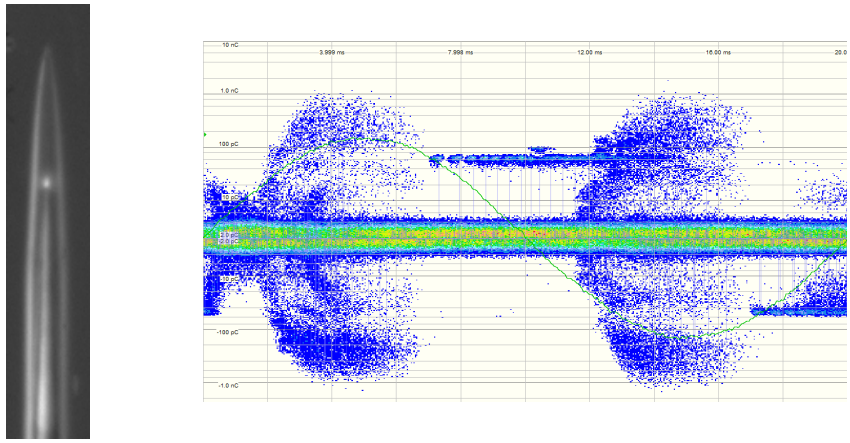

Figure C.48: CCD-camera picture with belonging Omicron measurement for 12 seconds at 14 kV: Sample 5

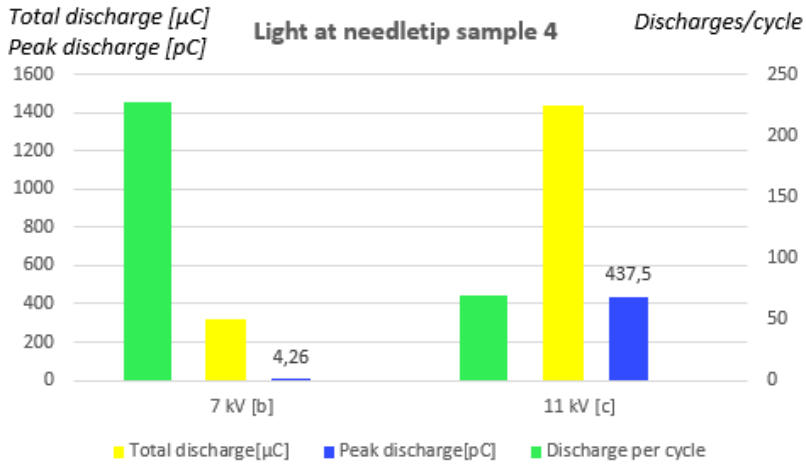

Figure C.49: Bargraph: Total discharge, peak discharge and discharges/cycle for Event 2: Light at needle-tip. Sample 5

C.3.3 Light alongside needle

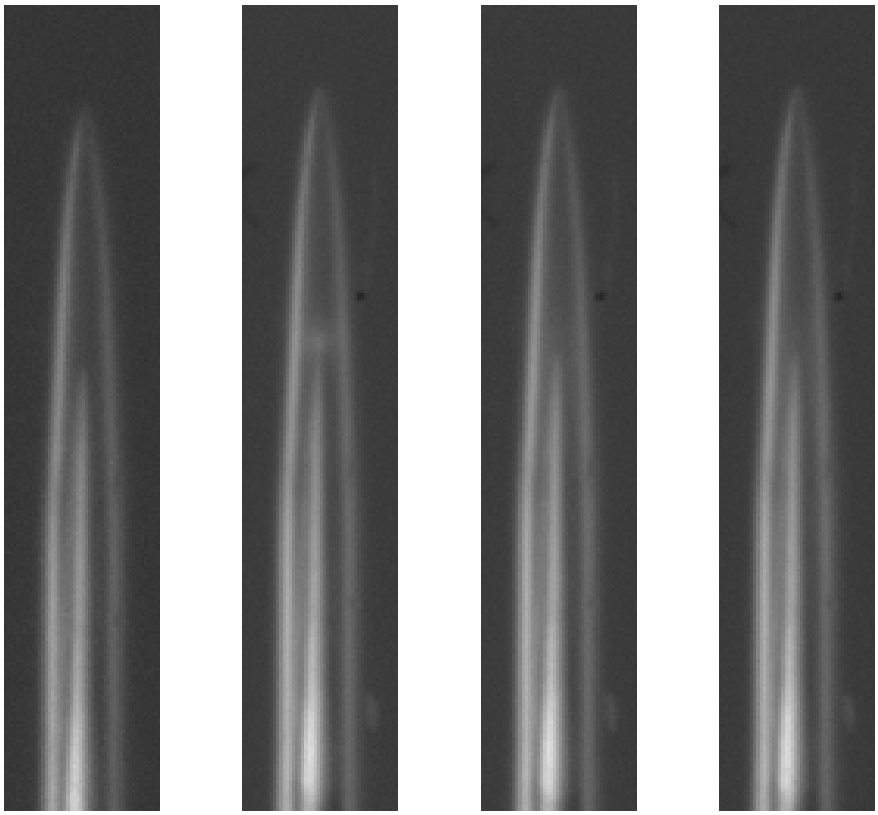

(a) <1 kV **(b)** 11 kV **(c)** 11 kV **(d)** 11 kV

Figure C.50: (a) Reference picture: No PD occurring. (b)Picture taken before light alongside needle occurs. (c)Taken when light alongside occurs.(d) Taken during light alongside needle.

Figure: C.50b with belonging partial discharge pattern. 11kV.

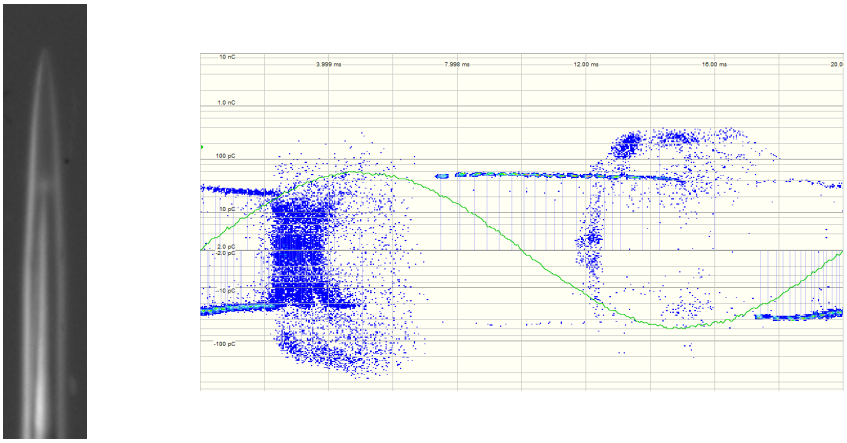

Figure C.51: CCD-camera picture with belonging Omicron measurement for 12 seconds at 11 kV: Sample 5

Figure: C.50c with belonging partial discharge pattern. 11kV.

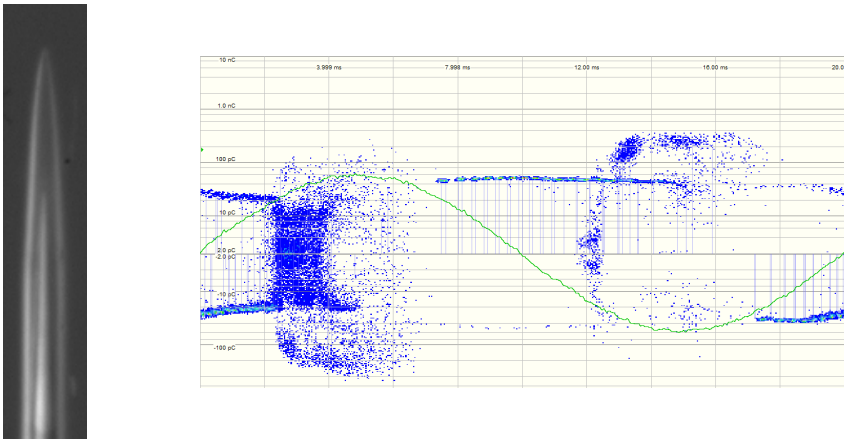

Figure C.52: CCD-camera picture with belonging Omicron measurement for 12 seconds at 11 kV: Sample 5

Figure: C.50d with belonging partial discharge pattern. 11 kV.

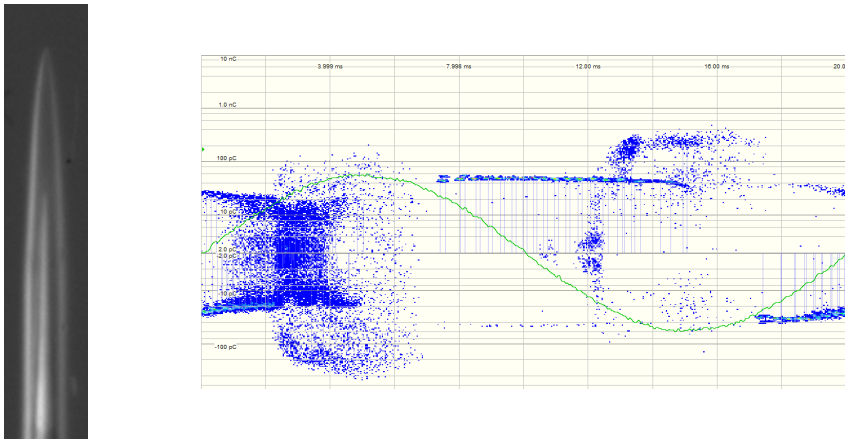

Figure C.53: CCD-camera picture with belonging Omicron measurement for 12 seconds at 11 kV: Sample 5

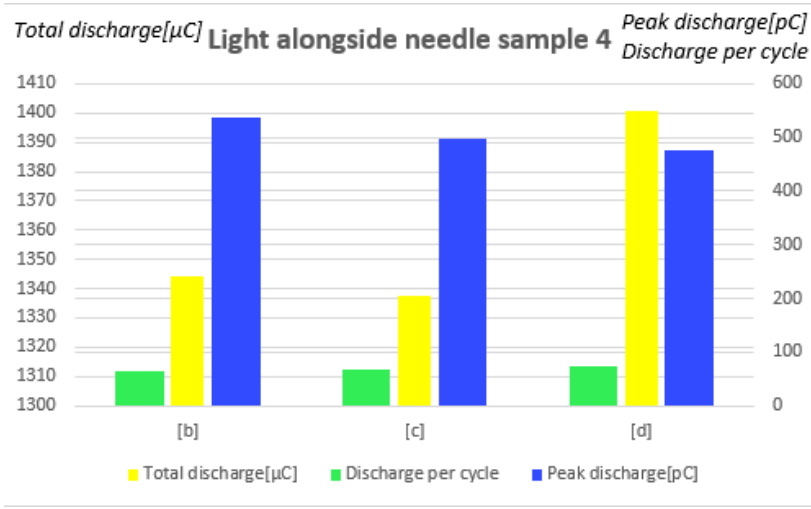

Figure C.54: Bargraph: Total discharge, peak discharge and discharges/cycle for Event 3: Light alongside needle. Sample 5

Appendix D

Matlab script: Calculating partial discharges, peak value and number of discharges

```
% % % % % % % % % % % % % % % % % % % % % % % % % % % % % % % % % % % % %
% % % % % % % % % % % % % % % % % % % % % % % % % % % % % % % %
% % % %Reading of the PD data from OMICRON streaming generated files % % %
%
% % % % % % % % % % % % % % % % % % % % % % % % % % % % % % % % % % % % %
% % % % % % % % % % % % % % % % % % % % % % % % % % % % % % % %


% Clear all variables, windows and the screen before running program
clear all;
clc;
close all;

tic

format long

%% Aquire data from OMICRON

%user define frequency
f=input('Enter the frequency in Hz:');


%user define noise level for raw data
noise=input ('Enter the noise level in pC, (example: 2.5): ');
```

```
%Define replay time from OMICRON

replay_duration = ...
input('Enter the duration of the OMICRON replay in seconds(example: 12): ');

%Import Q data %define de folder number (e.g. 0002)
%Tidspunkt for utladning og strrelse p  utladning
%Gjr om utladning til pC
%Gjr om tid til millisekund

[t_q1_1, q1_1]= importQData('Matlab','unit1.1');
q1_1=q1_1*1e12;
t_q1_1=t_q1_1*1000;

%Import phase data %define de folder number (e.g. 0002)
%En verdi  p  mellom 0 til 1. 0 er nullpunkt, 0.9 er 90 % * 360
%Finner hvor  p  fasen, i grader, utladningen skjer

phase = importPHData('Matlab','unit1.1');
phase=phase*360;

%Import voltage data %define de folder number (e.g. 0002)
%Importerer spenningsdata for hele lpet. Tid for logging (logger
%sepnning hvert 48 microsekund) og tilhrende spenning.
%Gjr om tid til millisekund

[tv1_1, v1_1] = importVData('Matlab','unit1.1');
tv1_1=tv1_1*1000;

% Change the voltage offset in function of the settings in OMICRON
%software (e.g. 17.63)
%Endre voltage offset
%Setter spenning til kV og tar hyde for offset

offset_OMICRON=17.63;
v1_1=(v1_1/1000)+offset_OMICRON;
tv=tv1_1';
i=0;

total_energy = 0;

energy_matrix= [];
time_matrix = [];
voltage_matrix = [];
max_charge = 0;

%% Filter out noise

noiseneg=-noise;

    for i=1:length(q1_1)
        if q1_1(i,1)>noise
            q(i,1)=q1_1(i,1);
            t(i,1)=t_q1_1(i,1);
            ph(i,1)=phase(i,1);
        end
        if q1_1(i,1)<(noiseneg)
```

```
            q(i,1)=q1_1(i,1);
            t(i,1)=t_q1_1(i,1);
            ph(i,1)=phase(i,1);
        end
    end

q_no_noise=q(q~=0);
t_q1_1_no_noise=t(t~=0);
phase_no_noise=ph(ph~=0);
j=0;
i=0;
v=zeros(length(q_no_noise),1);

sum_charge = [];


%Finding absolute peak charge

for i = 1 : length(q_no_noise)

    charge_size = q_no_noise(i);

        if abs(charge_size) > max_charge

            max_charge = abs(charge_size);

        end

end

%Calculating number of discharges per cycle and summing the absolute value
%of the discharges

number_of_discharges = length(q_no_noise);
charges_per_cycle = number_of_discharges/((replay_duration)/0.02);

sum_of_discharges = sum(abs(q_no_noise))*(10^-3); %Sum of charge in microcolomb


%Writing the numbers to Excel.
xlswrite('number_and_charge.xlsx',charges_per_cycle,'Sheet1','D3')
xlswrite('number_and_charge.xlsx',sum_of_discharges,'Sheet1','E3')
xlswrite('number_and_charge.xlsx',max_charge,'Sheet1','F3')

toc
```